

THE COOPER UNION
ALBERT NERKEN SCHOOL OF ENGINEERING

THE USE AND OPTIMIZATION OF THE
HELIX SHAPE AS THE PRIMARY STRUCTURAL ELEMENT
IN THE DESIGN OF A STEEL BRIDGE

by

Jason

Damiano

A thesis submitted in partial fulfillment
of the requirements for the degree of
Master of Engineering

April 13, 2012

Prof. Cosmas Tzavelis

Advisor

THE COOPER UNION FOR THE ADVANCEMENT OF SCIENCE AND ART

ALBERT NERKEN SCHOOL OF ENGINEERING

This thesis was prepared under the direction of the Candidate's Thesis Advisor and has received approval. It was submitted to the Dean of the School of Engineering and the full Faculty, and was approved as partial fulfillment of the requirements for the degree of
Master of Engineering.

Dean, School of Engineering - Date

Prof. Cosmas Tzavelis – April 13, 2012

i. Acknowledgement

I would first like to thank my advisor, Professor Cosmas Tzavelis. His guidance and support were vital in the process of creating this thesis. His knowledge and expertise in the design of bridges was extremely important throughout this process, and his help was greatly appreciated.

I would also like to thank the rest of the Civil Engineering Department, specifically Professor Jameel Ahmad, Professor Vito Guido, Professor Joseph Cataldo and Professor Constantine Yapijakis. I would like to express my gratitude for their support in choosing me as a candidate for the Masters Program.

Next, I would like to thank Dr. Simon Ben-Avi and the rest of the Cooper Union administrative staff. Without their work, the school would not move forward in the way it does.

I would also like to thank Dean Stephen Baker, whose help, support and guidance in my years at The Cooper Union made my experience significantly more enjoyable.

Next, I would like to thank my friends, who have made the entire experience at the Cooper Union so much more memorable. My time spent at The Cooper Union was always positive because of them.

Finally, and most importantly, I would like to thank my family. My mom, dad and sister have supported me throughout my years at The Cooper Union, and without them, this would not have been possible.

ii. Abstract

The helix shape is an aesthetically pleasing one that has rarely been used in structural design. This study contains a complete analysis on the use of the helix shape in the design of a steel bridge with a span length of 2000 feet. The 2000 foot span is longer than that of any other steel non-suspension or cable stayed bridge in the world. The initial trials find the weaknesses in the helix shape, which are the lack of support for the members as they circle about the deck, and this causes excessive deflections, and the other flaw being the excessive thinness of the design near the supports, making it extremely susceptible to shear. An alternative design solution that contains the aesthetic beauty of the helical curve along with the satisfying the structural strength needs is found and recommended. The solution is to combine a “full-helix” shape with that of the “half-helix”, which provides the necessary support and aesthetic qualities that were initially set out to be studied and optimized. The final design passes all necessary code standards that are tested for in the design program during the analysis.

iii. Table of Contents

Acknowledgment	i
Abstract	ii
Table of Contents	iii
List of Figures and Tables	iv
Table of Nomenclature	v
1. Introduction	1
1.1 Statement of Problem	2
1.2 Designing Bridges for Aesthetics: Robert Maillart and Santiago Calatrava	3
2. Structural Background Information	23
2.1 The Simply Supported Beam	24
2.2 Commonly Used Equations in Bridge Design	26
2.3 The Double Helix Shape	29
3. Autodesk Robot Structural Analysis	30
3.1 Modeling a Helix Shaped Bridge in Robot	31
4. Optimizing the Helix Bridge Structure for Live Load Deflections	46
4.1 Radius Size Optimization	49
4.2 Deck Thickness Optimization	57
5. Optimizing the Helix Bridge Structure for Dead Load Deflections	60
5.1 Deck Diagonal Optimization	63
5.2 Layered Helix Optimization	65
5.3 The Use of a Sloped Deck	74

5.4	Bracing the Helix Structure to Reduce Dead Load Deflections	78
6.0	Optimizing the Individual Steel Members	84
6.1	Optimizing the Member Sections	86
6.2	Failure in the Second Order Analysis	90
7.0	Optimizing Alternative Designs to Pass Second and Third Order Analyses	93
7.1	Alternative Design: The Double Helix	94
8.0	Conclusions and Recommendations	101
	Appendices	102
	Bibliography	105

iv. List of Figures and Tables

List of Figures:

Figure 1.2.1 – The Staffacher Bridge	5
Figure 1.2.2 – The Stauffacher Bridge’s three hinges	6
Figure 1.2.3 – Cross-section of the Zuoz Bridge	6
Figure 1.2.4 – A photograph of The Zuoz Bridge	7
Figure 1.2.5 – Cross-section of the bridge over the Rhine River at Tavanasa	8
Figure 1.2.6 – Maillart’s drawings of the bridge over the Rhine River at Tavanasa	8
Figure 1.2.7 – A drawing of the Valtscheilbach Bridge	9
Figure 1.2.8 – A photo graph of the Valtscheilbach Bridge	9
Figure 1.2.9 – A drawing of the Chatelard	10
Figure 1.2.10 – A photograph of the Chatelard	11
Figure 1.2.11 – The bridge over the Grand Fey Viaduct	12
Figure 1.2.12 – A photograph of the Salginatobel Bridge	13
Figure 1.2.13 – A model of the Walenese Bridge	14
Figure 1.2.14 – A model of the Cabelleros Footbridge	15
Figure 1.2.15 – A model of the Cabelleros Footbridge (alternate view)	16
Figure 1.2.16 – A photograph of the Bach de Roda Bridge	17
Figure 1.2.17 – A photograph of the Oudry-Mesly Footbridge	18
Figure 1.2.18 – A photograph of the Alamillo Bridge	19
Figure 1.2.19 – A photograph of the Trinity Footbridge	20
Figure 1.2.20 – A photograph of The Lyre	21
Figure 1.3.1 – The Helix Bridge in Singapore	23
Figure 1.4.1 – The Chaotianmen Bridge	26
Figure 1.4.2 – The Lupu Bridge	27
Figure 1.4.3 – The Pont de Quebec	28
Figure 2.1.1 – Moment and shear diagrams in a simply supported beam	
Figure 2.1.2 – Stress distribution in a beam	
Figure 3.1.1 – The “Load Types” window	
Figure 3.1.2 – The “New Section” window	
Figure 3.1.3 – The “Bars” windows	
Figure 3.1.4 – Helix quarter-circle cross-section	
Figure 3.1.5 – The “Translation” window	
Figure 3.1.6 – Cross-section of the quarter helix with deck connections	
Figure 3.1.7 - Cross-section of the quarter helix with deck connections	
Figure 3.1.8 – Cross-sections after the horizontal and vertical mirrors	
Figure 3.1.9 – Isometric view of half of the helix bridge	
Figure 3.1.10 – The “Rotation” window	
Figure 3.1.11 – Isometric view showing the pinned end supports, cladding and live load.	
Figure 3.1.12 Isometric view showing the completed model.	

Figure 3.2.1 – The “Results” drop-down list	52
Figure 3.2.2 – Side-view of the live load deflected shape	53
Figure 3.2.3 – The “Analysis Type” window	54
Figure 3.2.4 – The “Nonlinear Analysis Parameters” window	55
Figure 3.2.5 – Non-linear analysis failure notifications	56
Figure 3.2.6 – The steel member design “Calculations” window	57
Figure 3.2.7 – The final steel member design “Calculations” window	58
Figure 3.2.8 – Steel member calculation results for the first order dead load case	59
Figure 4.0.1 – Cross section in the X-Z plane with a 65 foot radius.	
Figure 4.0.2 – Isometric view.	
Figure 4.0.3 – Side view in the Y-Z plane with a 2000 foot length	
Figure 4.0.4 – Side view of the exaggerated deflected shape in the Y-Z plane.	
Figure 4.1.1 – Cross-sections of the best performing radius optimization designs.	
Figure 4.1.2 – Maximum live load deflections for 65 foot width models of varying height	52
Figure 4.1.3 – Maximum dead load deflections for 65 foot width models of varying height	53
Figure 4.1.4 – The exaggerated deflected dead load shape of the cross-section of the 65 by 130 foot radius model.	54
Figure 4.1.5 – The exaggerated deflected dead load shape of the side-view of the 65 by 130 foot radius model.	55
Figure 4.1.6 – The exaggerated deflected dead load shape of the isometric view of the 65 by 130 foot radius model.	55
Figure 4.2.1 – Helix bridge model cross-sections with decks.	58
Figure 4.2.1 – Helix bridge model side-views with decks.	59
Figure 5.0.1 – Cross-section of the 65 by 130 foot radius model with the compression helix highlighted in red.	61
Figure 5.0.2 – Isometric view of the 65 by 130 foot radius model with the compression helix highlighted in red.	61
Figure 5.1.1 – Deck diagonal variations listed from top to bottom	64
Figure 5.2.1 – Cross-section of the 100 by 100 foot model with no inner helix layers and a ½ inner helix layer.	68
Figure 5.2.2 – Cross-section of the 100 by 100 foot model with ½ & ¾ inner helix layers and ¼, ½ & ¾ inner helix layers.	68
Figure 5.2.5 – Side views of the 100 by 100 foot models, listed from top	69
Figure 5.2.4 – Cross-section of the 65 by 130 foot model with no inner helix layers and a ¾ inner helix layer.	70
Figure 5.2.5 – Cross-section of the 65 by 130 foot model with ¾ & ⅞ inner helix layers and ⅜, ¾ & ⅞ inner helix layers.	70
Figure 5.2.6 – Side views of the 65 by 130 foot models, listed from top	71
Figure 5.2.7 – Exaggerated deflected cross-section of 65 by 130 foot model with ¾ and ⅞ inner helix layers.	72
Figure 5.2.8 – Exaggerated deflected side view of the 65 by 130 foot model with ¾ and ⅞ inner helix layers.	73
Figure 5.3.1 – Cross-section of the 65 by 130 foot radius model with the	

sloped deck.	75
Figure 5.3.2 – Side view of the 65 by 130 foot radius model with the sloped deck	75
Figure 5.3.3 – Cross-section of the 100 by 100 foot radius model with the sloped deck.	76
Figure 5.3.4 – Cross-section of the 100 by 100 foot radius model with the sloped deck	76
Figure 5.4.1 – Exaggerated deflected shape of sections 8 through 18 of the 100 by 100 foot radius model	77
Figure 5.4.2 – Various bracing types, listed from top left to bottom right	79
Figure 5.4.3 – Cross-sections of the 65 by 130 foot models with top & bottom bracing and center deck bracing.	81
Figure 5.4.4 – Cross-sections of the 100 by 100 foot models with top & bottom bracing (left) and center deck bracing (right).	81
Figure 5.4.5- Isometric view of the most efficient helix bridge shape with bracing.	83
Figure 6.1.1 – The member with the lowest axial force	85
Figure 6.1.2 – The members with the highest axial forces	85
Figure 6.2.1 – Cross-section of the exaggerated deflected shape that passes the first order analysis, but fails the second order analysis	91
Figure 6.2.2 – Side view of the exaggerated deflected shape that passes the first order analysis, but fails the second order analysis	91
Figure 7.1.1 – Cross-section of the 100 by 100 foot radius double helix model	96
Figure 7.1.2 – Side view of the 100 by 100 foot radius double helix model	96
Figure 7.1.3 – Top view of the 100 by 100 foot radius double helix model	96
Figure 7.1.4 – Isometric view of the 100 by 100 foot radius double helix model	96
Figure 7.1.5 – Side view of the exaggerated deflected shape of the 100 by 100 foot radius double helix model	97
Figure 7.1.6 – Cross-section of the modified 100 by 100 foot radius double helix model	98
Figure 7.1.7 – Side view of the modified 100 by 100 foot radius double helix model	98
Figure 7.1.8 – Top view of the modified 100 by 100 foot radius double helix Model	98
Figure 7.1.9 – Isometric view of the modified 100 by 100 foot radius double helix model	98
Figure 7.1.10 – Side view of the exaggerated deflected shape of the modified 100 by 100 foot radius double helix model	99
Figure A.1 – Sample steel section calculation output by Robot	102
Figure A.2 – Isometric view of the 60 by 120 double helix bridge showing the member sections.	103
Figure A.3 – Isometric view of the 60 by 120 double helix bridge showing the member sections (2).	104

List of Tables:

Table 3.1.1 – Helix Bridge: Node Points	33
Table 4.1.1 – Maximum Live Load Deflections for Various Radii	50
Table 4.1.2 – Maximum Dead Load Deflections for Various Radii	50
Table 4.1.3 – Maximum Deflections for 65 foot Radius (Width) Models of Varying Height	52
Table 4.2.1 – Maximum deflections for various deck thicknesses	58
Table 5.1.1 – Maximum deflections for various deck diagonal types	63
Table 5.2.1 – Maximum deflections for various layered helix types (100 by 100)	66
Table 5.2.2 – Maximum deflections for various layered helix types (65 by 130)	66
Table 5.3.1 – Maximum deflections for models with and without sloped decks	74
Table 5.3.1 – Maximum deflections for various bracing types for sections 8 through 18	78
Table 5.4.1 – Maximum deflections for various bracing types	80
Table 6.1.1 – Maximum deflections for various circular section types	84
Table 6.1.2 – Maximum deflections for various square section types	84
Table 7.1.1 – Maximum deflections for modified circular cross-section double helix variations	99
Table 7.1.2 – Maximum deflections for modified oval cross-section double helix variations	100

v. Table of Nomenclature

X-axis: The direction perpendicular to the travel of traffic across the bridge. The width of the bridge can be measured along the x-axis.

Y-axis: The direction parallel to the travel of traffic across the bridge. The bridge span starts at $y = 0$ feet and ends at $y = 2000$ feet.

Z-axis: The direction perpendicular to the road surface. The maximum bridge height is given as the highest point reached along the z-axis.

Half Helix: A helix that starts at one end on the span, reaches its peak at the center of the span, and ends at the other. A half helix starts and ends at $z = 0$, without ever changing signs in that direction. The x value negates over the length of the span.

Full Helix: A helix that starts at one end on the span, reaches its peak at the $\frac{1}{4}$ and $\frac{3}{4}$ points along the span (one peak is positive, the other negative), starting at $z = 0$ and reaching it again at the midpoint of the span. The x and z value of the full helix are the same at the start and the end of the helix on both sides of the span.

Helix Radius or Radii and Maximum Height: The radius of the helix is defined as the maximum x value and the maximum z value when viewing a cross-section of the bridge in the x-z plane. For example, the helix models will often be referred to as the 100 by 120 radius helix model, which means it starts at a maximum x value of 100 feet, while the maximum z value (or maximum height of the bridge at the center) is 120 feet.

Outer Helix Structure: This refers to the helix furthest above and below the bridge deck. There are 2 outer helices above the deck and 2 below the deck which intersect and the center point that make up the outer helix structure

Member Sections: The cross section of a steel member.

1. Introduction

Bridges are structures that span over things like valleys, bodies of water or other man-made creations. They have been created throughout history to transport people and the things they carry with them from one side of a gap to the other. Bridges have clearly had a major impact on the development of society as it is known today.

A bridge is unique in the fact that it has long spans without support directly under the structure, unlike most buildings and other large structures. Depending on the design requirements, one of many different types of bridges can be chosen for a project. Suspension bridges and cable-stayed bridges use cables to distribute the load from the roadway surface to the support structures. Arch bridges use the arc shape to distribute the loads into columns at the ends of spans. Another common type of bridge is made using steel trusses, and trusses are also often used in the other types of bridges for structural purposes, especially in roadway decks. A bridge needs to be designed to take the loads at the center of its span and distribute them to its ends or support columns.

This study will perform a complete analysis on the use of the helix shape as the primary support element in a bridge made up of entirely steel members, spanning a gap of 2000 feet, which would make it the longest steel span bridge in the world without suspension or cable-stays. A thorough amount of necessary background information can be found enclosed within, along with a complete guide for using the appropriate computer programs and finally, an analysis on how the helix shaped bridge structural system performs, and how it can be optimized to maximize the structural integrity of the design, while preserving its aesthetic appeal.

1.1 Statement of Problem

The helix shape is a visually intriguing one that has rarely been used in structural design. The appeal comes from the curved shape, but due to its symmetry and the fact that the full helix is a circle in cross-section, it clearly has structural strength that has not been tapped into.

The main purpose of this study is to explore the use of helix shape as the primary structural element in bridge design, and optimize the design of the shape in order to maximize its structural strength.

The fusion of an aesthetically pleasing design with one that is structurally strong and feasible is truly the goal of this study. The helix shape has structural strength that can be used, and its curved shape gives it a unique look that makes it worth exploring.

While maintaining the aesthetic appeal of the helix shape, the bridge must be designed in order to have maximum live load deflections that are under code standards, and have all individual members pass the first, second and third order tests for the dead load (self-weight) case.

1.2 Designing Bridges for Aesthetics: Robert Maillart and Santiago Calatrava

Throughout history, structures have served a specific purpose. They are designed and constructed with the purpose of making the lives of humans better in one way or another. Whether it is for shelter, travel or financial profit, structures obviously play a major part in the development of human civilization as it seen today.

The most notable structural device used for transportation purposes is the bridge. Bridges have become recognizable landmarks across the world, sometimes becoming the structure that defines a city or town. Although the purpose of a bridge is simply to carry people and their goods across a gap, whether it be over water or a gap of another kind, it is clear that bridges are much more than just transportation structures.

There are, of course, bridges with the simplest of designs; that do little more for the eye than the roadway/railway surface they carry. Bridges of this nature our often older, as they were built purely for practical purposes: getting people and goods from one side to the other. It seems as if that simple design thought process has become a thing of the past, and the design of a bridge is so much more than a simple structure that serves physical needs.

Two men have been at the forefront of this change in thought. The first is Robert Maillart, who spent much of his career innovating new ways in which one could make designs normally considered outrageous technically feasible. Technical feasibility is the obvious obstacle that must be overcome in order to make unique bridges, and this was Rober Maillart's life's work: designing beautiful bridges that were once thought to be technically infeasible. In doing this, he set a precedent for architects and structural engineers alike. Bridges today are designed with a much higher emphasis on aesthetics

than they ever have been before, and it has become the norm, they are often considered works of art. Works of art: with an extremely practical and important primary function.

Robert Maillart was born in Berne, Switzerland in February of 1872. As a student, he was frustrated by the overemphasis often put on mathematics in structural design, and rather “pioneered innovative research and design in direct opposition to authorities and peer groups that had been seduced by the applied science view” [1]. Maillart believed that the emphasis on applied science in structural engineering discouraged real innovation, and he thought that studying real life structures was a significantly more effective way to come up with innovative bridge design. Maillart studied the ways in which geometric shapes distributed forces, and he found “that elegant appearance could arise from the patterns traced by these forces. Elegance arose from the structure itself and not from an extraneous idea of beauty.” [1] It is this thought for which Robert Maillart will truly be remembered.

In his attempts to create bridges not from classical applied science methods, but from untraditional alternatives, he innovated many major design features that had never before been seen in structural design. These included the concrete hollow box, the concrete flat-slab floor, the concrete deck-stiffened arch, and the idea of shear center.

In the late 1800's, iron was the main structural element being used in construction projects. In his first opportunity to design a bridge in Switzerland, Maillart instead designed a concrete single-arch bridge over the Sihl River in Zurich, known as the Stauffacher Bridge.

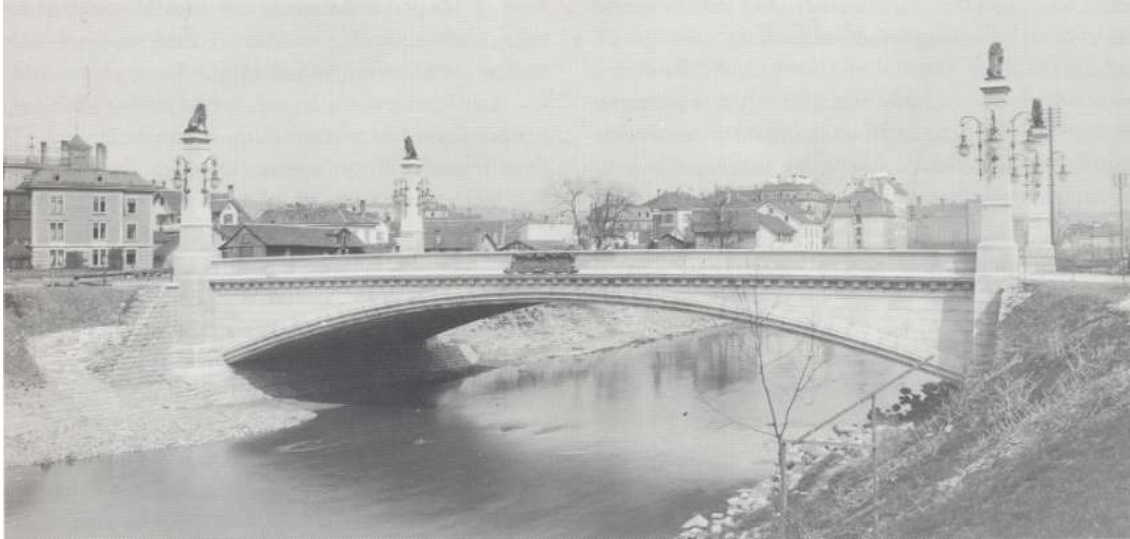


Figure 1.2.1 – The Staffacher Bridge [1]

It was significantly more cost effective than the iron alternatives, and it used concrete arch that did not contain reinforcement. The bridge was submitted against 3 other designs, 2 of which were steel, the other concrete, and Maillart's bridge was chosen as the victor. The use of concrete was vitally important, as it was more aesthetically pleasing than metal designs, and it was more lightweight and cost effective than commonly-used stone designs. Maillart used 3 hinges, as shown in the figure on the following page, one in the center of the arch and one on each end, and that allowed for unreinforced concrete to be used without the stresses in the arch becoming unbearable.

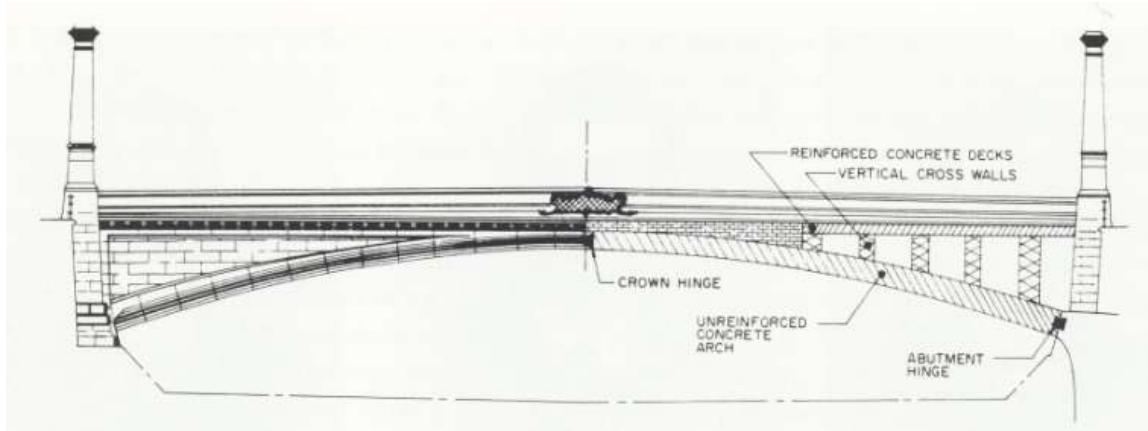


Figure 1.2.2 – The Stauffacher Bridge’s three hinges [1]

It was at the turn of the century when the use of reinforced concrete had started to become popular in design and construction. Maillart used reinforced concrete in his first major innovation, the Zuoz Bridge. In this design, Maillart used an arch that was made up of 2 hollow concrete boxes (connected by a vertical center wall), and his design was unique in the fact that it allowed for the arch, walls and deck to carry the load, rather than just the arch, as was done with more traditional designs.

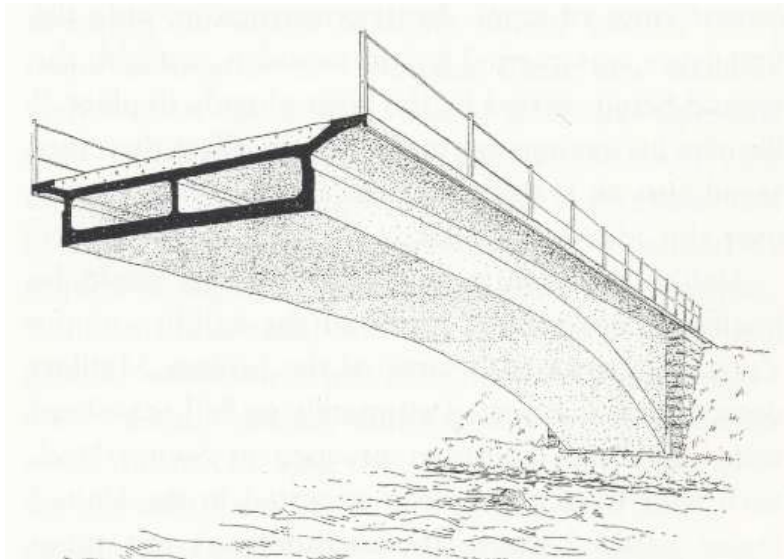


Figure 1.2.3 – Cross-section of the Zuoz Bridge [1]

“Maillart stressed that the structure would have all of the virtues of stone but without its great weight for, like steel, the concrete sections are reduced to a minimum” [1].



Figure 1.2.4 – A photograph of The Zuoz Bridge [2]

Maillart’s next major innovation was the use of the three-hinged arch, which he popularized at the Rhine River Bridge at Tavanasa. The three-hinged arch was used in other designs of his, but at Tavanasa, it was the main focus in this particular model. The design allowed for the bridge to be extremely thin, which was both unprecedented and visually appealing. “He created that innovation by expressing the three hinges as places where the arch has minimum thickness, and between hinges, the arch fuses with the horizontal deck to provide the necessary stiffening” [1]. Though completed in 1905, the Maillart’s bridge over the Rhine River at Tavanasa has an extremely modern feel to it, even by today’s standards.



Figure 1.2.5 – Cross-section of the bridge over the Rhine River at Tavanasa [1]

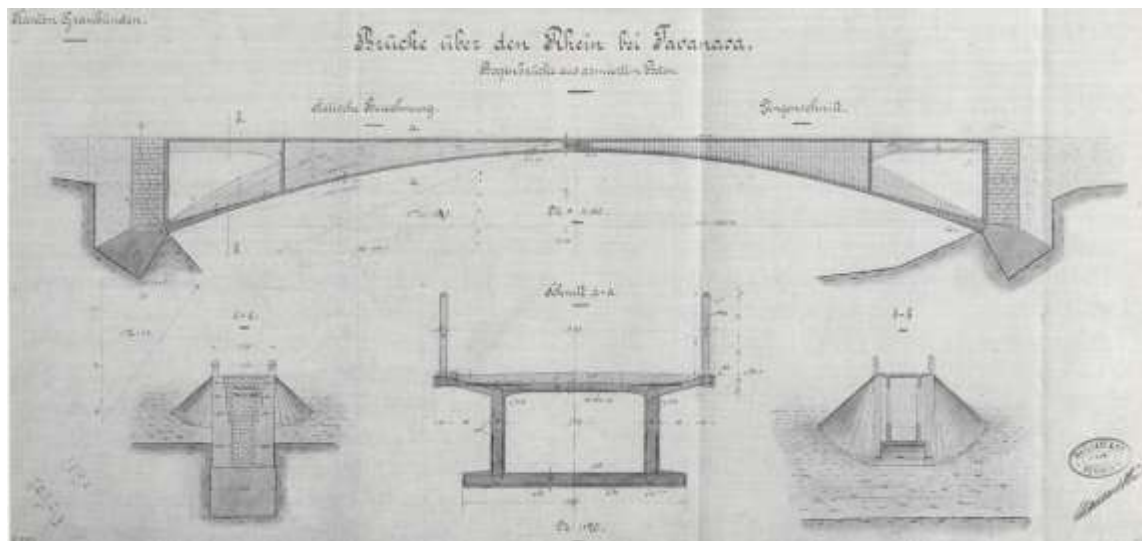


Figure 1.2.6 – Maillart's drawings of the bridge over the Rhine River at Tavanasa [1]

Maillart's technological breakthroughs in bridge design allowed him to fuse together beauty with practicality and function. Without making any further major engineering innovations, Maillart designed 3 bridges known primarily for their beauty in the mid-1920's. The first of these designs was the Valterscheilbach Bridge, which is best known for having the thinnest arch of its time.

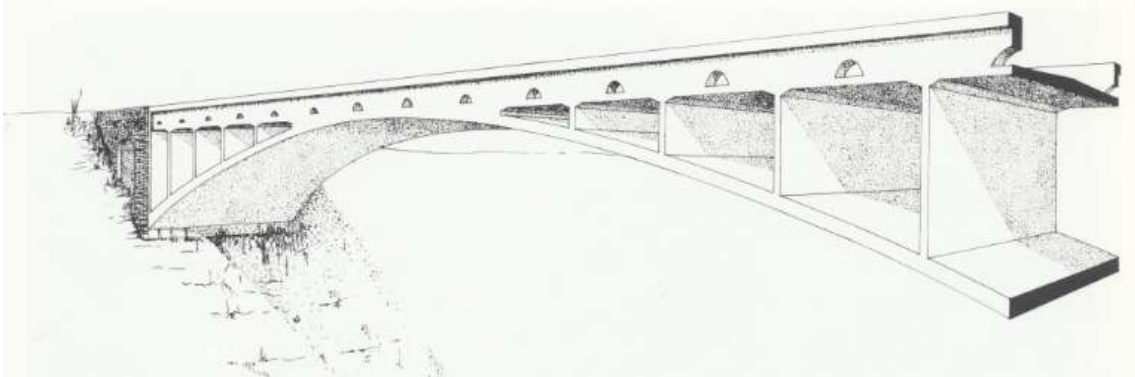


Figure 1.2.7 – A drawing of the Valterscheilbach Bridge [1]

“Its lyrical contrast of a light arch with a stout deck remains its primary delight” [1]. In the past, Maillart's designs had unique and relatively cheap to build, but they weren't necessarily known for their aesthetic appeal. The Valtshielback Bridge changed that thought, as its thinness was not only financially practical, but undeniably beautiful.



Figure 1.2.8 – A photograph of the Valterscheilbach Bridge [1]

His next achievement in style came with the Chatelard, with which he insisted on symmetry, despite what the landscape called for. Dealing with an asymmetrical ravine, Maillart designed a symmetrical frame that would need a stone pedestal for one half of the legs, while the other half set directly into the earth. “Maillart’s symmetrical frame reflects his concern for a trouble-free structure more than for visual conformity to a given landscape” [1].

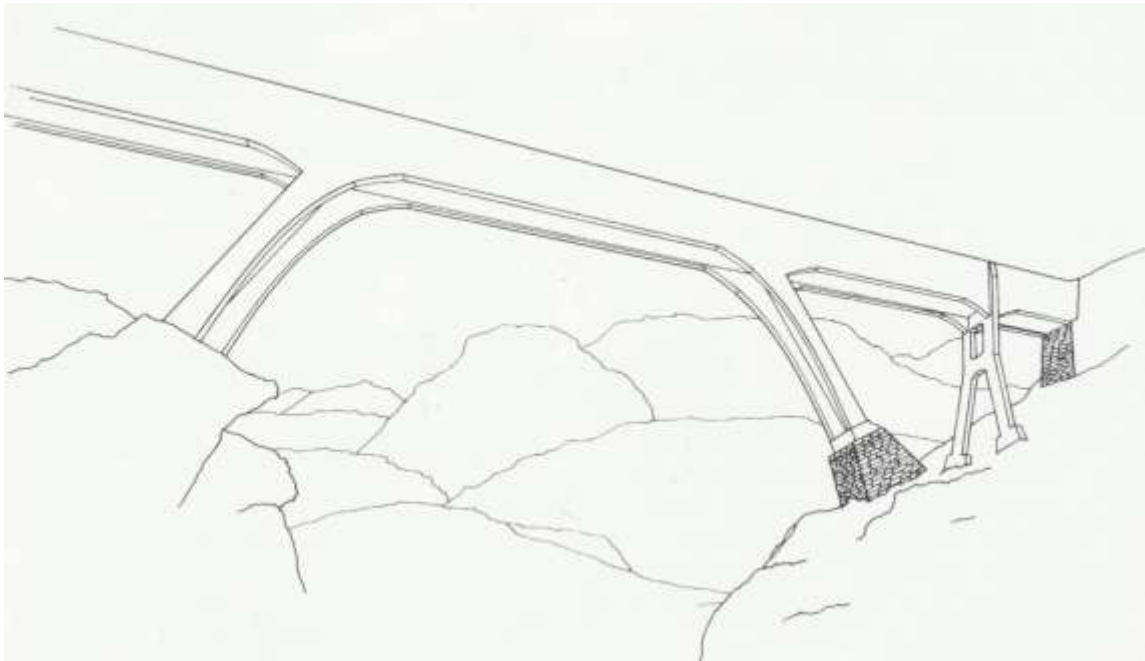


Figure 1.2.9 – A drawing of the Chatelard [1]



Figure 1.2.10 – A photograph of the Chatelard [1]

The final bridge in the stretch was designed to carry the Swiss national railway across the Grand Fey Viaduct. This massive undertaking was far larger than the other bridges he had designed and constructed, and it posed a great technical challenge for Maillart, as he was known for designing his concrete arches for unprecedented thinness. “The arches and other vertical members are so light by comparison to the pillars that in profile there is the same feeling of surprise as at Valterschielbach” [1]. Though massive, Maillart was able to design a bridge that resonates with the eye just as his sleekest design does, despite the fact that it has 6 arches to the Valterschielbach’s single arch, and covers a much longer span.

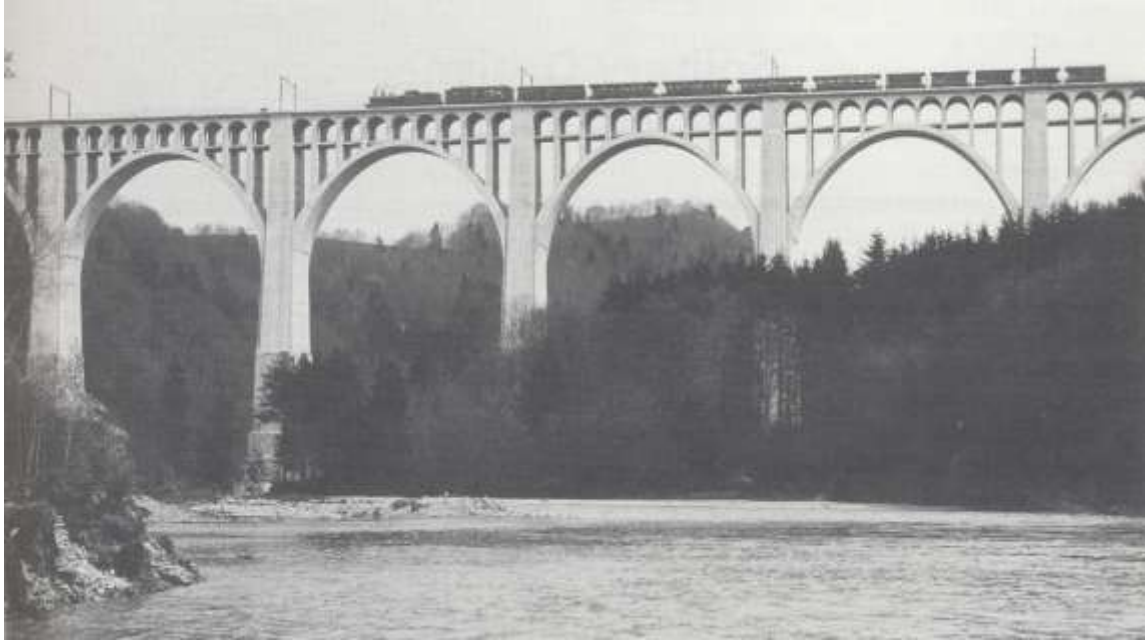


Figure 1.2.11 – The bridge over the Grand Fey Viaduct [1]

Robert Maillart was finally given the recognition he deserved by others for his artistic form with the Salginatobel Bridge. His designs had been critiqued in the past for being too focused on technical progression, rather than pure beauty. When Maillart designed bridges, he made them thin and sleek because it was cost effective and physically practical, as he had an engineer's viewpoint on such matters. His critics wanted more of an architect's touch to his designs, and they finally got what they wanted with the Salginatobel. "It was the beauty of the bridge that engaged other artists, architects and engineers and has put Maillart's design in the center of more art museum exhibitions than any other comparable structure" [1]. Though not necessarily his sole intent, he clearly made an intentional move towards physical allure, and he gained the recognition of his peers for it.



Figure 1.2.12 – A photograph of the Salginatobel Bridge [3]

The second designer that has revolutionized the way bridge design is looked at in the modern world is Santiago Calatrava. Born in Spain and educated in both architecture and civil engineering, he has been able to fuse technical triumphs with breathtaking visuals in bridge design like no other before him. His feats in the bridge design world go virtually unmatched, and it is clear that his background as both an architect and a structural engineer have had a huge impact on his designs.

“Calatrava has long maintained that bridges, as design objects, could combine technological intelligence with poetry to enhance the sense of identity and cultural significance of a particular place” [4]. Bridges throughout history have generally had one singular focus: stability. Designers like Calatrava have made aesthetics equal in importance to stability, without sacrificing anything from the latter. This achievement has gone from a trivial pursuit for beauty, to a seemingly necessary part of the design process, since the time Calatrava started designing bridges.

In his early career as a designer in the late 1970's, Santiago Calatrava often drew inspiration from real life forms in his bridge designs. He was influenced in his tubular design for the Walensee Bridge in Switzerland by “the tubular limbs of birds, insects and crustaceans” [4]. His next design, for the Aclata Alpine Motor Bridge in Disentis, Switzerland, came about from, “In Calatrava’s own words, the ‘form of a bird’” [4]. He went through multiple iterations in this particular design, constantly removing unnecessary redundancies, and through them “the structure became even more transparent, even more articulated, demonstrating more clearly the way forces traveled through matter” [4]. It is clear through Calatrava’s early work that his form is beginning to emerge, and it is a beautiful fusion of grace and stability.

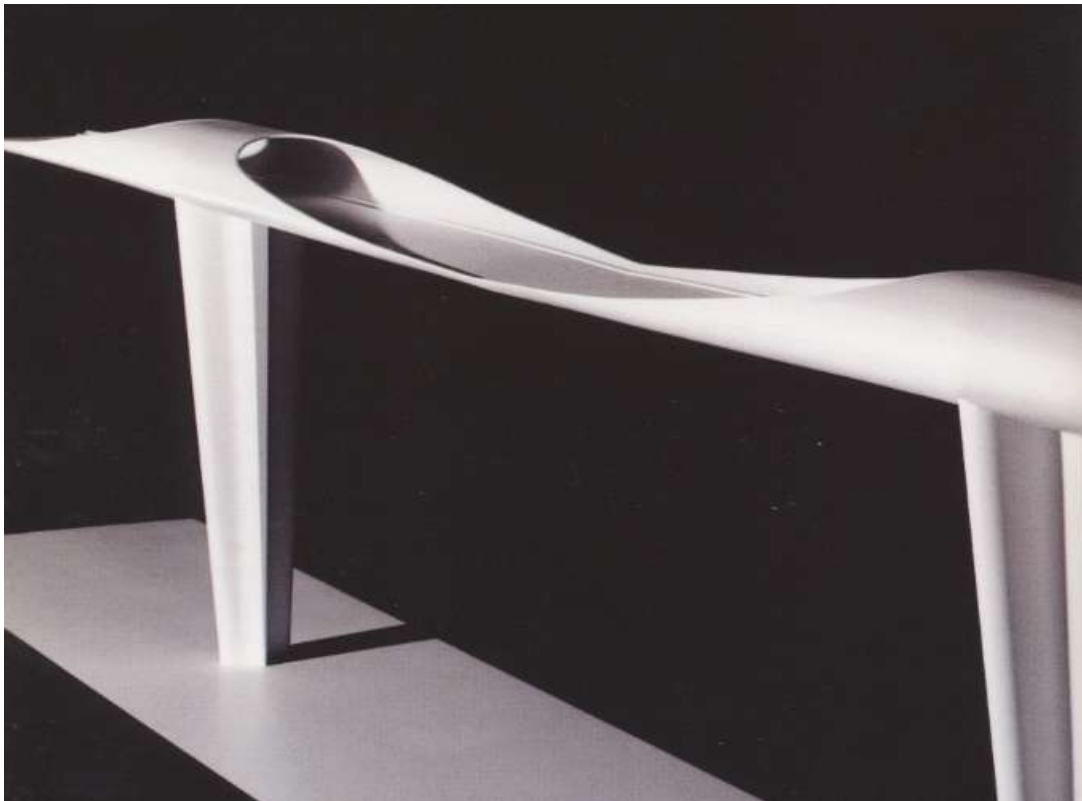


Figure 1.2.13 – A model of the Walensee Bridge [2]

Calatrava's first design that ventured into his trademark asymmetrical pylon motif was the Caballeros Footbridge in Lerida, Spain. Due to uneven topographical conditions, Calatrava designed an asymmetrical bridge that would be supported by an angled pylon from only one side, with cables stretching from it that would hold up the cantilevered deck that came from the base of the pylon. "Its components are differentiated, each assigned the specialized tasks of compression and tension, and the materials were chosen and allocated to these components to carry out tasks specifically fitting their nature" [4]. In summary, each member of the bridge serves a very specific structural purpose, but when assembled as a whole, the members make up a shape that is extremely pleasing to the eye.



Figure 1.2.14 – A model of the Caballeros Footbridge [4]



Figure 1.2.15 – A model of the Cabelleros Footbridge (alternate view) [4]

Calatrava's next two famous designs were constructed in Europe in the late 1980's. The first was the Bach de Roda Bridge in Barcelona. Though designing a rigid structure that is literally built to stay still, Calatrava's main focus in this design was movement. When referring to his design, Calatrava said "Mobility is implicit in the concept of strength ... strength is crystallized movement" [4]. This simply shows the unique thought process that went into his bridges, and he also considered the actual movement of people in vehicles in his design. Rather than make a pedestrian walkway that would force people across in a thin straight line, Calatrava designed pedestrian platforms on each side of the bridge (that jut out as half ovals from the sides) and stairs leading up to them. This made this design more than just a bridge for transportation purposes, which is clearly always on the forefront of his mind.



Figure 1.2.16 – A photograph of the Bach de Roda Bridge [5]

The second design of his constructed in the late '80's was the Oudry-Mesly Footbridge in Creteil-Paris, France. The arch spans above the bridge, clearly reminiscent of a spinal column or back of an animal, giving it the previously mentioned life form that Calatrava so often designed for.



Figure 1.2.17 – A photograph of the Oudry-Mesly Footbridge [6]

Arguably the most famous bridge Santiago Calatrava has designed is the Alamillo Bridge in Seville, Spain. “No other Bridge by Calatrava manifests more powerfully and in a more succinct and lucid manner the leaning pylon motif and the general spirit of the poetics of movement than the Alamillo Bridge in Seville” [4]. In this design, Calatrava was able to use the angle pylon without counterstays, a first for him. He was able to do this because the deck weighed enough to counteract the forces from the pylon. The Alamillo Bridge in Seville is both a feat in architectural design and engineering feasibility. Santiago Calatrava proves that neither of those factors need be ignored when designing a bridge, and in fact, they can be considered equally important.



Figure 1.2.18 – A photograph of the Alamillo Bridge [7]

Calatrava's next aesthetic marvel was the Trinity Footbridge, which was constructed in Salford, England in the mid-1990's. Calatrava's design needed to account for the large differences in the heights of the riverbanks on either side of the bridge, and that is why he chose to use the asymmetrical mast design, as the angle made up for the change in elevation. This design is a perfect example of how the engineering criteria for a project allowed for it to become visually pleasing, as the angled pylon stands out, while the uneven river banks were the primary reason for necessity of the design.



Figure 1.2.19 – A photograph of the Trinity Footbridge [8]

Calatrava also took his beautiful pylon motif to the Netherlands, where he designed 3 angled mast bridges in the town of Hoofddorp, known as The Lyre, The Lute and The Harp. “As part of its infrastructure planning, the regional government resolved to create bridges that would not only serve transportation needs but also function as landmarks at main crossings over the Hoofdvaart to reflect the economic and social changes affecting the region” [4]. The project was started in 1999, and it was clear that at this point in time that the aesthetics of larger bridge projects had become equally important to the engineering behind them. The tallest mast for this set of bridges is over 200 feet tall, which is almost twice as tall as the one for Calatrava’s Trinity Footbridge.



Figure 1.2.20 – A photograph of The Lyre [4]

One can now argue that the look and feel of a bridge has become more important than its primary function as a structure for transportation. No longer can a bridge be designed purely for function, it is a necessity to include the look of a bridge in every phase of the design process. With advances in technology, the structural strength of a bridge has become almost a given, and the aesthetic aspects of the bridge have become the main focus of bridge design.

1.3 The Helix Bridge: Singapore

The first bridge in the world to use the helix shape as part of its structural design was constructed in Singapore, and it is known simply as “The Helix” [9]. The 280 meter long pedestrian bridge spans the Marina Bay, but requires multiple supports to cross the gap, as can be seen in the figure below.



Figure 1.3.1 – The Helix Bridge in Singapore [9]

Although the main element supporting the bridge is the supports below, the helix is vital to taking the load. The two repeating helical rings that make up the double helix structure act together as a tubular truss, which allows the bridge to use 5 times less steel than a conventional box girder bridge [9]. Although the helix shape is used as structural element in the design of this bridge, it is clear that it is not the primary load bearing element across the entire span, as the supports are needed. This is due to the fact that the outer helical structure was not designed to distribute the loads across the entire span, only to the supports, which are less than 100 meters apart. The helix shape is used primarily

as an architectural element with aesthetics as its primary function, but clearly has structural strength.

1.4 Longest Steel Bridge Spans

The longest bridge spans in the world are cable-stayed or suspension bridge types, as these designs are extremely strong while also having a significantly lower dead weight than a steel girder bridge of similar length. The efficiency of the suspension bridge allows for bridges to span distances of thousands of feet, with the longest in the world being the Akashi Kaikyo Bridge in Japan, which spans a maximum distance of 6,532 feet [10]. Due to the efficiency of these bridge types, they have become the primary choice for long span bridges, and are the only bridge types that have spanned gaps of more than 1900 feet. The longest steel non-suspension or cable-stayed span bridges in the world are the Chaotianmen and Lupu bridges in China, which are both steel arch bridges [11].

The Chaotianmen Bridge is located in Chongqing, China and was completed in 2009. With a span of 1,811 feet, it is the longest steel non-suspension or cable-stayed bridge in the world. It uses two curved steel truss tied arches, which span the gap while distributing the loads into the supports [12]. The deck is suspended from the arches, and the bridge carries both vehicular traffic and rail traffic. The curved trusses also give the bridge a look that is extremely appealing to the eye. When looking at the side view of the bridge, one can clearly see how the bridge distributes the load from the center into the supports at either end, as seen in the figure on the following page. It is also clear how a steel span bridge must be designed, the maximum height above the supports is found at the center, while the arches drive into the supports at the ends. This bridge only has compression support on the top, as there is no need for tension support below the deck because the bases of the supports are much lower than the deck that is being supported.



Figure 1.4.1 – The Chaotianmen Bridge [13]

The next longest steel arch bridge is the Lupu Bridge in Shanghai, China, and it spans a maximum distance of 1,804 feet. This bridge was completed in 2002, and was the longest bridge of its kind upon its completion, until the aforementioned Chaotianmen Bridge was completed in 2009. The arches meet at the center of the bridge at the highest point, and drive directly into the ground at either end of the span. The steel arches, as pictured on the following page, are over 29 feet thick and 15 feet wide in cross section, which are unprecedentedly large when it comes to steel bridge design [14].



Figure 1.4.2 – The Lupu Bridge [15]

The Pont de Quebec, or the Quebec Bridge, has the longest steel truss cantilevered bridge span in the world, with a distance of 1,800 feet. It is currently only used only for rail and pedestrian traffic, though it once carried vehicular traffic as well. This bridge shows how designs can vary while still using similar materials, as the cantilevered design technique allows for the suspended span at the center to be supported by the cantilevers on the opposite sides of the supports at either ends. This is why the bridge, which was completed in 1917, does not reach its maximum height at the center, as pictured on the following page. This particular bridge is still considered an engineering marvel, and due to a serious accident during construction, it has had a huge impact on the evolution of bridge design and construction [16].



Figure 1.4.3 – The Pont de Quebec [17]

Although the precedent for a steel bridge with a main span of more than 1800 feet is apparent, designing one with a span of 2000 feet adds over 10 percent to the overall length. The choice of the 2000 foot span length for the helix bridge in this study will provide the challenge of designing the world’s longest steel bridge, while also using and optimizing the helix shape.

2. Structural Background Information

A bridge is unique from other large structures due to the fact that it is made to span distances without supports over a given distance. This makes the design of a bridge significantly different from that of a building or other large structure. The following sections cover the theory behind long span bridge design, the commonly used equations in the field and information specific to the geometry of the helix shape.

2.1 The Simply Supported Beam

If a bridge is simplified to its most basic elements, it can be modeled as a beam with pin supports at one end and roller supports at the other. This is also known as a simply supported beam.

As is the case for a simply supported beam, the moment for a bridge span is highest at the center, and this is the primary element that must be designed for when designing a long span bridge. The moment and shear diagrams for a uniformly loaded simply supported beam can be found in the figure on the following page, and they are extremely similar to those experienced over a bridge span. The highest amount of shear occurs at the ends of the bridge, at the supports, while the moment is equal to zero at these same locations. The stress distribution in a simply supported beam is also very similar to the way that forces are distributed at the center of the span of a bridge, and that is shown on the lower figure on the following page. The top members above the road at the center of the bridge span will be in the highest compression, while the members under the roadway at the center of the bridge will experience the highest tension. The force, moment and stress distribution in a simply supported beam shows why most long span bridges look the way they do, the bridge members increase in height above the supports (not necessarily the roadway) as they get closer to the center of the span.

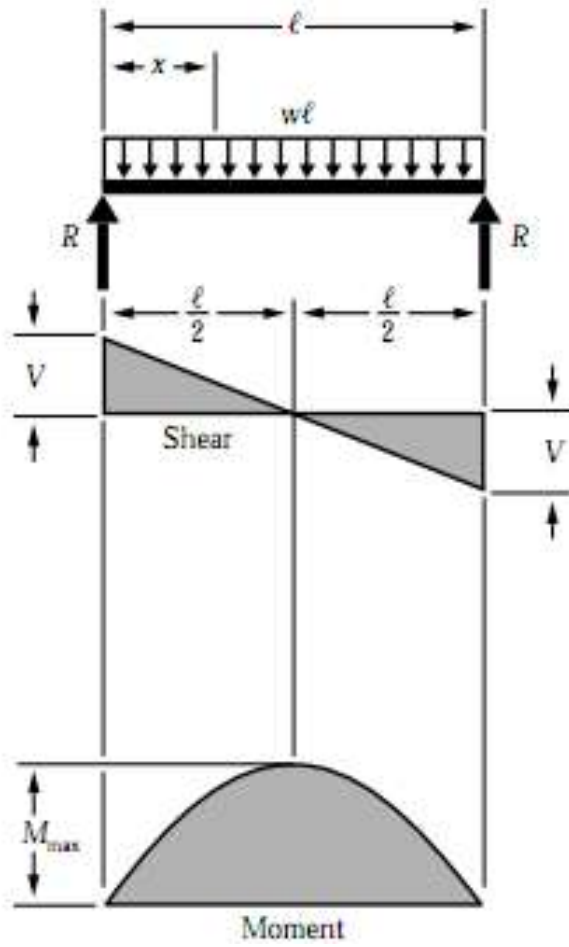


Figure 2.1.1 – Moment and shear diagrams in a simply supported beam [18]

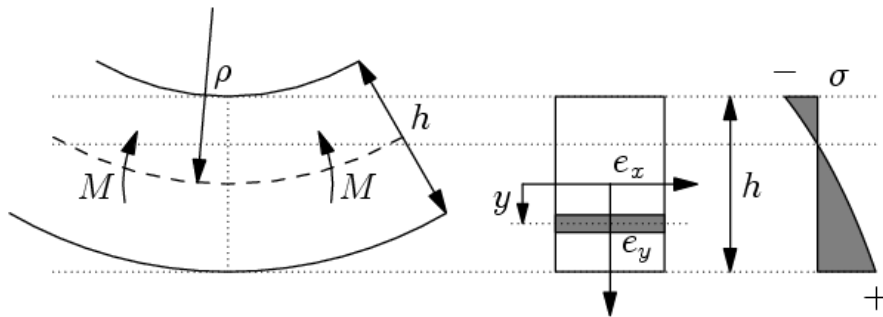


Figure 2.1.2 – Stress distribution in a beam [19]

2.2 Commonly Used Equations in Bridge Design

As shown in the previous section, a long span bridge can be modeled as a simply supported beam. The equation for the moment in a uniformly loaded simply supported beam is shown below [18]:

$$M_x = \frac{wx}{2}(l - x)$$

Where l is the length of the beam, w is the uniformly distributed load and x is the distance from one end. This shape is also the optimum shape of an arch that can be used in bridge design. If the arch follows the exact shape of the moment distribution curve, it will provide the most efficient distribution of the force possible. This means that the highest members above the supports at any point along the span of bridge that is perfectly designed in this sense will follow the equation above, so that the bridge arch will make the out the moment equation when viewed from the side of the span. For a bridge with 2000 foot span and a center height of 100 feet above the support, the equation for the height above the support of the top-most member should be as follows for optimal performance:

$$Z = \frac{x}{C * 2}(l - x)$$

$$C = f(l, h)$$

Where Z is the height in feet, x is the distance from the end support, 2000 is the span length in feet and C is a coefficient that converts for the maximum height (h) desired at the center of the bridge from the from the fact that the actual moment equation is based in units for a uniformly distributed load, which includes units containing forces.

The next important equations to be discussed are for axial loads applied to individual steel members in bridges. There are two main ways a member can fail, reaching its yield strength and buckling. Buckling is more common and more worrisome when dealing with the long members typically used in steel bridge design. The equation for stress in a member is as follows:

$$\sigma = \frac{P}{A}$$

Where P is the axial force and A is the cross-sectional area of the member [20]. If the stress, σ , reaches the yield strength for the material, the member will begin to fail. The yield strength for steel can vary, but the standard is 36ksi. It is more common for a steel member to fail due to reaching its yield strength from a tensile axial force, because a member under compression will typically buckle first. The buckling equation, known as Euler's equation, is shown below [20]:

$$P_{cr} = \frac{\pi^2 EI}{\left(\frac{L}{r}\right)^2}$$

Where P_{cr} is the critical force that causes buckling in a member with given values of length (L), modulus of elasticity (E), radius of gyration (r) and moment of inertia (I). This particular buckling equation is used for members connected by pins at both ends. The equation for members with fixed ends uses the effective length of the members as they are not as free to buckle, which is found to be approximately L/2.

The next equations important to bridge design are those for the maximum allowable live load deflections. A bridge must be designed so that it can handle the live load without deflecting considerably, according to code standards. If the bridge deflects

too much, it will be noticeable to the traffic crossing the bridge, which is not allowable.

The equations for the maximum allowable live load deflections are found below [21].

For standard bridges:

$$\Delta_{LL} \leq \frac{1}{800} (L)$$

For bridges with pedestrian traffic:

$$\Delta_{LL} \leq \frac{1}{1000} (L)$$

Where L is the length of the bridge and Δ_{LL} is the maximum allowable live load deflection. The maximum allowable live load deflection is based purely on the length of the bridge, and a 2000 foot span has a maximum allowable live load deflection of 2.5 feet (30 inches) for standard bridges, and a maximum allowable live load deflection of 2 feet (24 inches) for a bridge with pedestrian traffic.

2.3 The Helix Shape

A helix is essentially a spiral shape, which is a circle dragged out in a third dimension. The “double-helix” shape is best known for being the shape of DNA, which was discovered by James Watson and Francis Crick in 1953 [22]. In theory, the helix is a smooth shape, but for design purposes, the helix must be divided into straight line segments. These straight line segments still give the look and structural integrity of the helix, while also making construction technically feasible. Parametric equations are used in order to determine the points for which a helix intersects. These parametric equations are shown below [22]:

$$x(t) = a \cos(t)$$

$$y(t) = bt$$

$$z(t) = a \sin(t)$$

The t value that is used is the angle (in radians), about the origin. The x and z coordinates make the shape of a circle with constant radius a . The y coordinate is determined using the pitch, or length, of the helix, where the pitch is defined as $2\pi b$, where b is the length. The y -coordinate increases as the x and z coordinates circle around the y -axis, giving the desired helix shape. For construction purposes, the helix must be divided into segments. Therefore, for a “half-helix”, the total angle of rotation is π across the span of a bridge, while a “full-helix” has an angle of rotation of 2π across the span of the bridge.

3. Autodesk Robot Structural Analysis

The structural analysis program used in the analyses for the design and optimization of the helix bridge is Autodesk Robot Structural Analysis Professional 2012 (Robot). The following section is a step-by-step guide on how to construct a helix shaped bridge in Robot, and how to go about analyzing it for live and dead load (self-weight) cases for first, second and third order tests. The most helpful tool for learning to use Autodesk Robot is the User's Guide [23], and any user is encouraged to supplement the guide in this section with the User's Guide provided by Autodesk. All of the figures found in the following sections are taken directly from the program.

3.1 Modeling a Helix Shaped Bridge in Robot

The focus of this section will be to guide a user through the process of constructing a helix shape bridge in Autodesk Robot Structural Analysis Professional 2012. The user will learn to model the helix shape based on a set on pre-defined parameters, and analyze the dead and live load deflections using Robot.

The first step is to define the parameters that the bridge must be designed for. In this example, a 2000 ft span will be used. The first step is to choose the radius of the helix. In a view of the bridge from one of its ends down its full length, the helix makes a perfect circle. The radius of this circle needs to be chosen by the designer in order to construct the model. This radius can be optimized, but a starting radius must be chosen in order to start the process.

The helix shape is, in reality, a perfect circle extended in a third dimension. For the purposes of construction feasibility, the helix must be broken into segments, as it cannot be constructed as a perfect helix for the length of the span. For this example, the segments will be 40 feet along the deck of the bridge (40 feet in the y-direction). For the 2000 foot span, this division will create 50 sections. The length of each member of the helix will be slightly longer than 40 feet, due to the fact that it is connecting the 40 feet in the y-direction over an angle. After defining this step, the points of the helix can then be found.

Using Microsoft Excel, the helix equation can be input in order to find the node locations where each member of the helix will connect. The equations are as follows:

$$x = r\cos(t)$$

$$y = \frac{l}{\pi t}$$

$$z = r \sin(t)$$

Where:

t goes from 0 to π over the length of the bridge

r is the radius

l in the length of the bridge

The t values must be calculated by dividing pi into the previously defined 50 sections, as the t value must increase at the same rate for each section. The data can then be input into Excel, and the output table is shown on the following page. Only half of one of the helical shapes is shown (there are 4 in total) because of the mirroring and rotating options in Robot, which greatly reduce the time to create a model, while also decreasing the chance for human error.


Once the helix node points are obtained, construction of the model can begin in Robot. The first step when opening the program is to select “3D Frame Design” under the options for “New Project”. The next step is to define the dead and live load cases. Other load types can be used for analysis, but they can be added at a later time. Select “Load Types” under the “Loads” drop-down list on the menu bar, or select the “Load Types” toolbar button: . This will bring up a window which allows the user to define any load cases that are desired. For this example, the first load case will be a dead load case. Using Robots default naming and numbering system, this case will be load case 1,

Table 3.1.1 – Helix Bridge: Node Points			
Radius =100ft		Length=2000ft	
T	x	Y	z
0	100.00	0	0.00
$\pi/50$	99.80	40	6.28
$2\pi/50$	99.21	80	12.53
$3\pi/50$	98.23	120	18.74
$4\pi/50$	96.86	160	24.87
$5\pi/50$	95.11	200	30.90
$6\pi/50$	92.98	240	36.81
$7\pi/50$	90.48	280	42.58
$8\pi/50$	87.63	320	48.18
$9\pi/50$	84.43	360	53.58
$10\pi/50$	80.90	400	58.78
$11\pi/50$	77.05	440	63.74
$12\pi/50$	72.90	480	68.45
$13\pi/50$	68.45	520	72.90
$14\pi/50$	63.74	560	77.05
$15\pi/50$	58.78	600	80.90
$16\pi/50$	53.58	640	84.43
$17\pi/50$	48.18	680	87.63
$18\pi/50$	42.58	720	90.48
$19\pi/50$	36.81	760	92.98
$20\pi/50$	30.90	800	95.11
$21\pi/50$	24.87	840	96.86
$22\pi/50$	18.74	880	98.23
$23\pi/50$	12.53	920	99.21
$24\pi/50$	6.28	960	99.80
$25\pi/50$	0.00	1000	100.00

and it will be labeled as “DL1”. To add the case, select “dead” under the “Nature” drop-down menu, and then click “Add”, and DL1 will be added to the list of defined cases below. The next load case that needs to be added will be the live load case, and it will be defaulted as case number 2 and labeled “LL1”. To add it, select “live” under the “Nature” drop-down list and click “Add”. The “Load Types” window will look like the figure below once the cases have been defined:

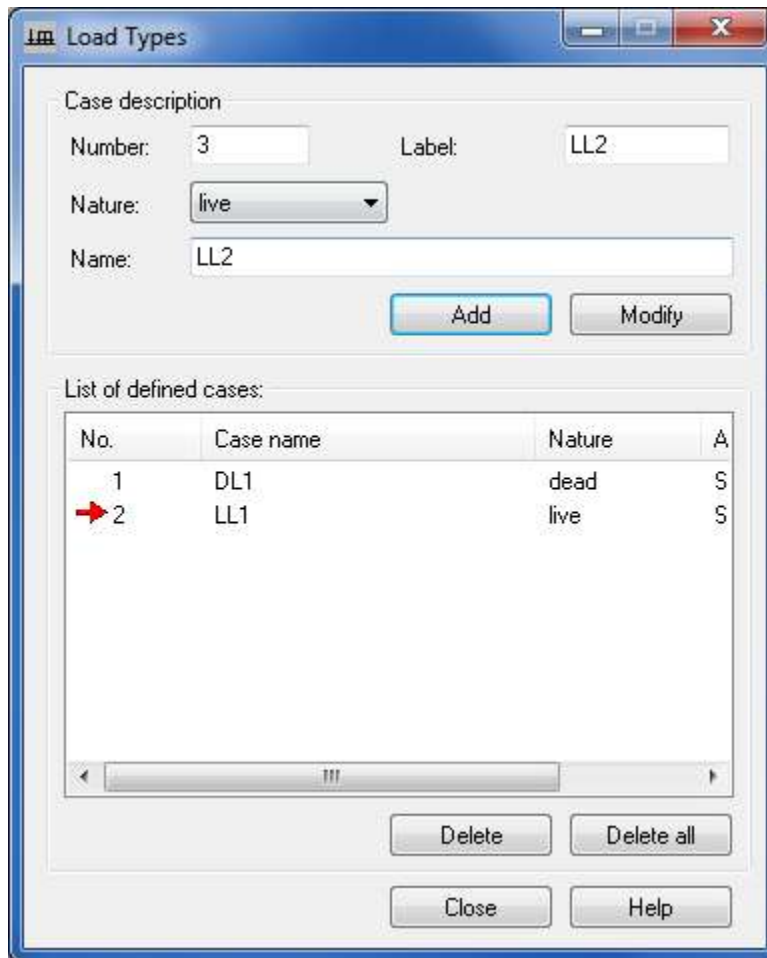




Figure 3.1.1 – The “Load Types” window

The next step is to begin constructing the model. The node points calculated earlier will be used to construct one quarter of the helix, which will be connected to the deck, and then the helix and deck connections will be mirrored and rotated to create the entire helix bridge structure.

To begin the construction of the helix, the user must select the “Bars...” option from the “Geometry” drop-down list on the menu bar, or the “Bars” toolbar button: . Once the window pops up, the user is allowed to select the bar type, section and many other options. The first step must be to define an appropriate bar section by selecting the button next to the “Section” drop-down list. Another window will then open, which will allow for the user to define a new section. The standard section (W16x40) is far too small for a bridge span of 2000 feet, so a new section must be defined. The selected sections will have to be redefined after an analysis is done on the individual members, but having a reasonable starting point will help with that process once the bridge is ready to be analyzed. The recommended starting bar will be a 24-inch diameter solid steel bar, which can be created from the “New Section” window by selecting the “Parametric” tab at the top, and then selecting the “Tube” button: . The user can then input the diameter (in inches) and then select the “Solid” checkbox to make the section a solid, rather than a tube. The desired name (“Label”) can also be input, and then clicking “Add” will add the section to the list of bar sections, while also selecting it as the current bar for modeling. The final “New Section” window is shown in the figure on the following page:

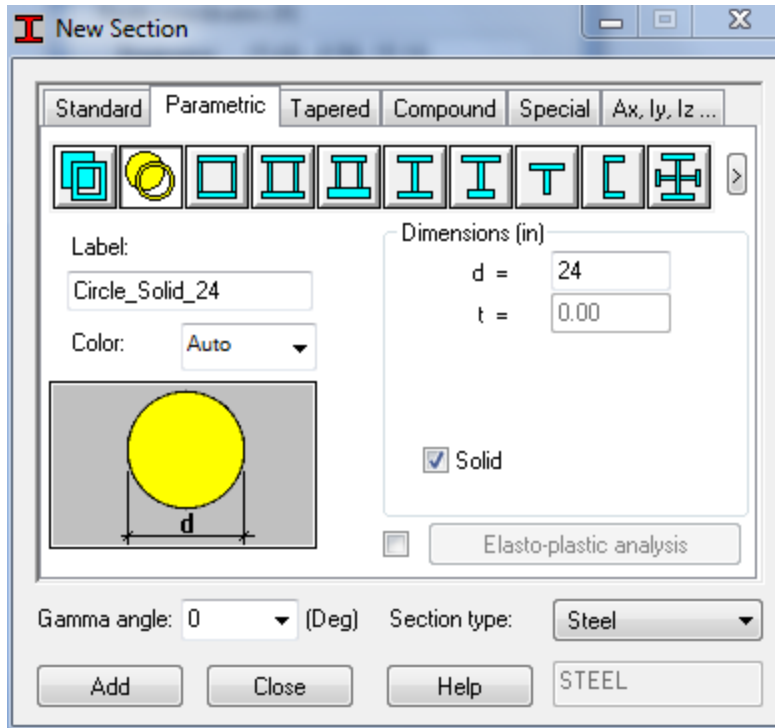


Figure 3.1.2 – The “New Section” window

The helix will be constructed directly from the “Bars” window, by typing in the previously calculated node points as the “Beginning” and “End” of each bar. By checking the “Drag” checkbox, each node will only need to be input once, and after the bar is added to the model, the previously input endpoint will automatically become the next bar’s start point, as shown in the figure on the following page:

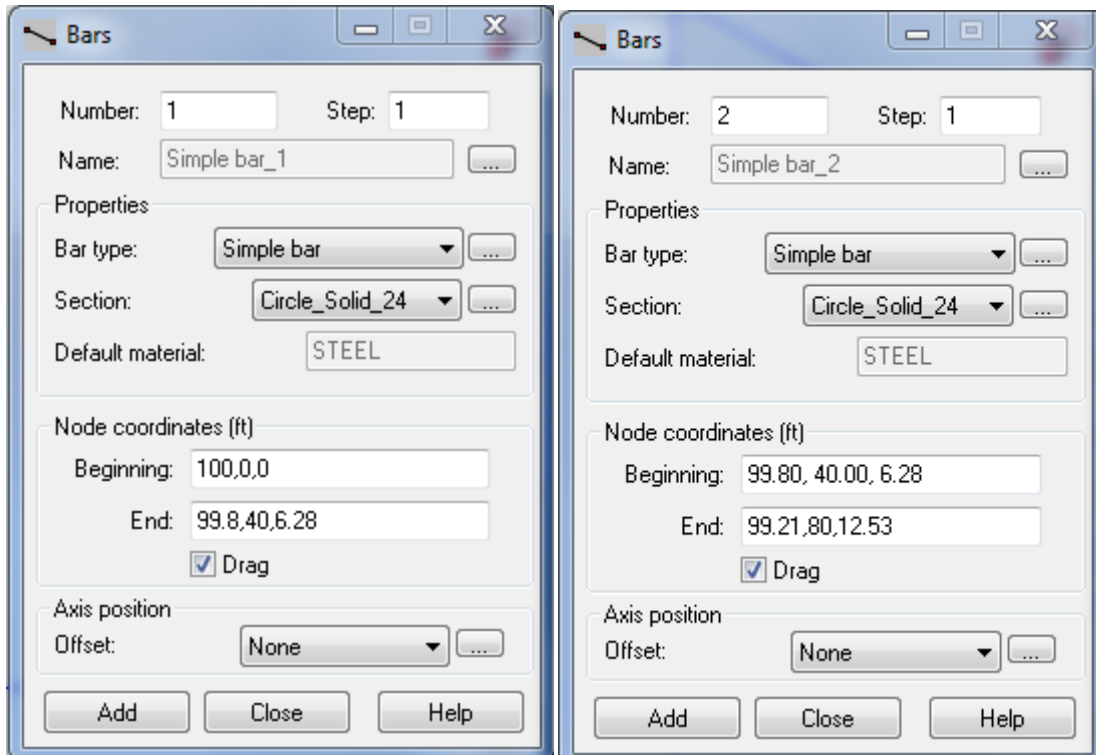


Figure 3.1.3 – The “Bars” windows. The first bar created in the helix is shown on the left, while the second is on the right.

Once the first half is complete ($y=1000\text{ft}$), the bridge should look as it does below from the “Front” view on the 3D view cube (The cross section looking down the bridge should be a perfect quarter-circle):

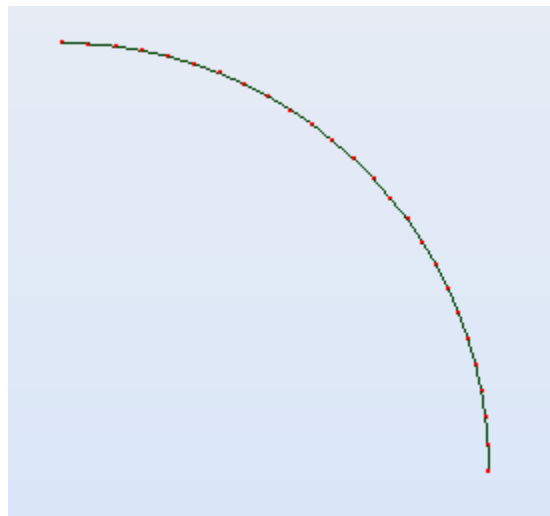



Figure 3.1.4 – Helix quarter-circle cross-section

To view the bridge in this way, the "Dynamic View" option must be selected from the "View" drop-down list on Menu Bar, which will make the model viewable in 3D space. The next step is to create the deck. The deck will be created before the rest of the helix members are copied, as the connections can be copied as well.

In this example, the deck will be a simple, flat deck with 40-foot sections. The same procedure can be used to create a deck of any thickness, and a thicker deck will give better results, but for the purposes of this model, the flat deck will be created. To start, a bar must be drawn and then copied for the length of the bridge. The user can select the "Bars" button and then type in the start and end points of the first bar of the deck. In this example, the deck will be 50 feet wide, with four 10-foot lanes, and space for pedestrian walkways. To create this, a bar must be created with a beginning point of (-25,0,0) and an end point of (25,0,0). The user must then select the bar, and then select the "Move/Copy..."  option from the "Edit" pull-out list, which is found under the "Edit" drop-down list on the menu bar. The "Translation" window will open, and the input for the copy should be (0,40,0) in the "Translation vector" box, and the "Number of repetitions" should be input as 25 (window shown below), which will create half of the bridge deck sections.

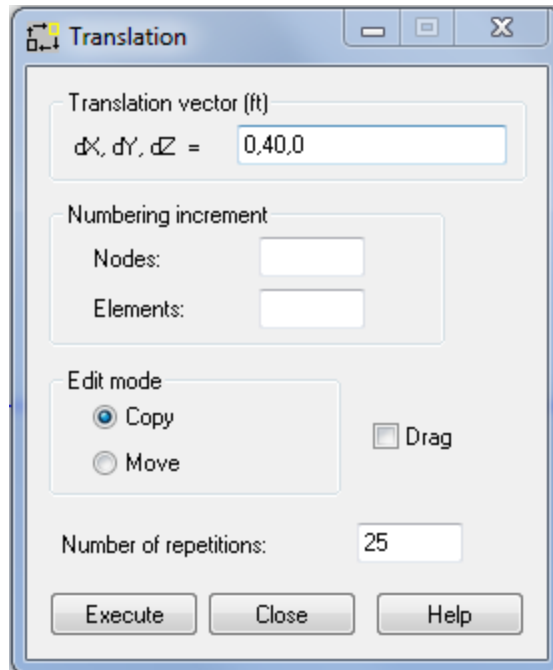



Figure 3.1.5 – The “Translation” window

The deck sections will be created once the translation is executed. If the deck has multiple levels or a thickness, the user can create the deck by selecting all of the members that need to be copied. Only the first section needs to be drawn. After the deck sections are visible, the deck members should be connected. This can be done by selecting the “Bars” button, and then physically selecting the start and end points of the bar to be inserted, rather than typing in the start and end points in the window. A single bar can be input to connect the end of the first section to the end of the last on each side of the deck. The 1000-foot long member that is created can then be divided into 40-foot sections by selecting the “Intersect”  button from the “Edit” drop-down list, which will automatically create bar endpoints at every intersection for the entire structure. The endpoint of each deck section should then be connected to the corresponding endpoint of each helix section, so that each deck section connects to a helix section, and the y-value

of the connection bar should remain constant. Once all of the connections are input, the cross-section and side view of the bridge should look as pictured below:

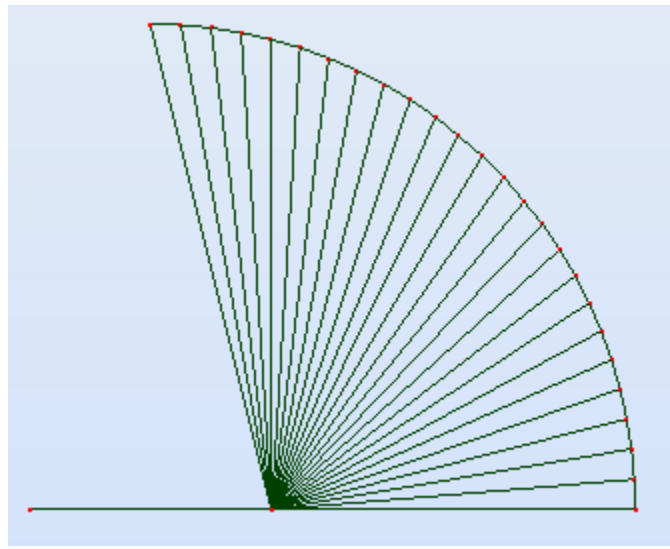


Figure 3.1.6 – Cross-section of the quarter helix with deck connections

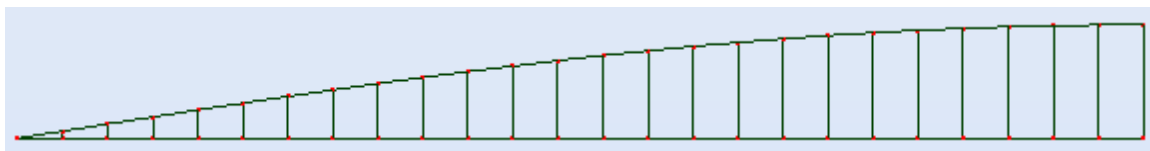




Figure 3.1.7 - Cross-section of the quarter helix with deck connections

The next step is to mirror the helix and connection bars (not the deck), in 2 planes. First, the user must select all of the non-deck members, and then mirror them over the horizontal plane. Once the members are selected, the “Horizontal Mirror...”  option must be selected from the “Edit” pull-out list on the “Edit” drop-down list on the menu bar. The user must then select any point on the x-y plane, and the bars will be mirrored over the plane. The next step is to again select all of the non-deck members, and then use the “Vertical Mirror...”  option, which is found next to the “Horizontal Mirror” option. The user must select a point on the y-z plane, and the members will be mirrored across it. The result of each mirroring is shown in the figures on the following page:

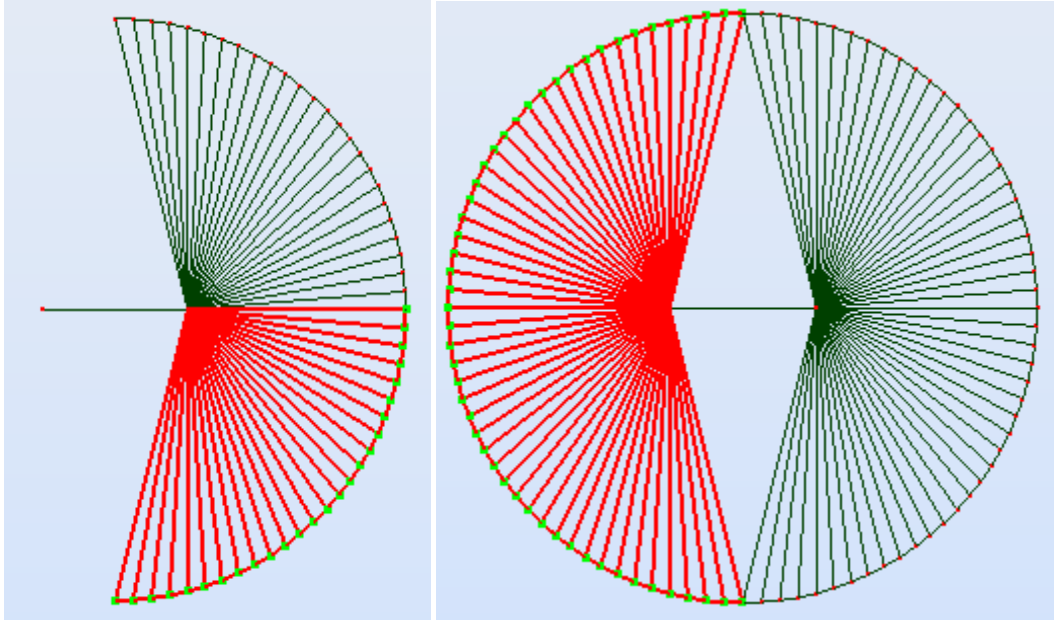


Figure 3.1.8 – Cross-sections after the horizontal (left) and vertical (right) mirrors

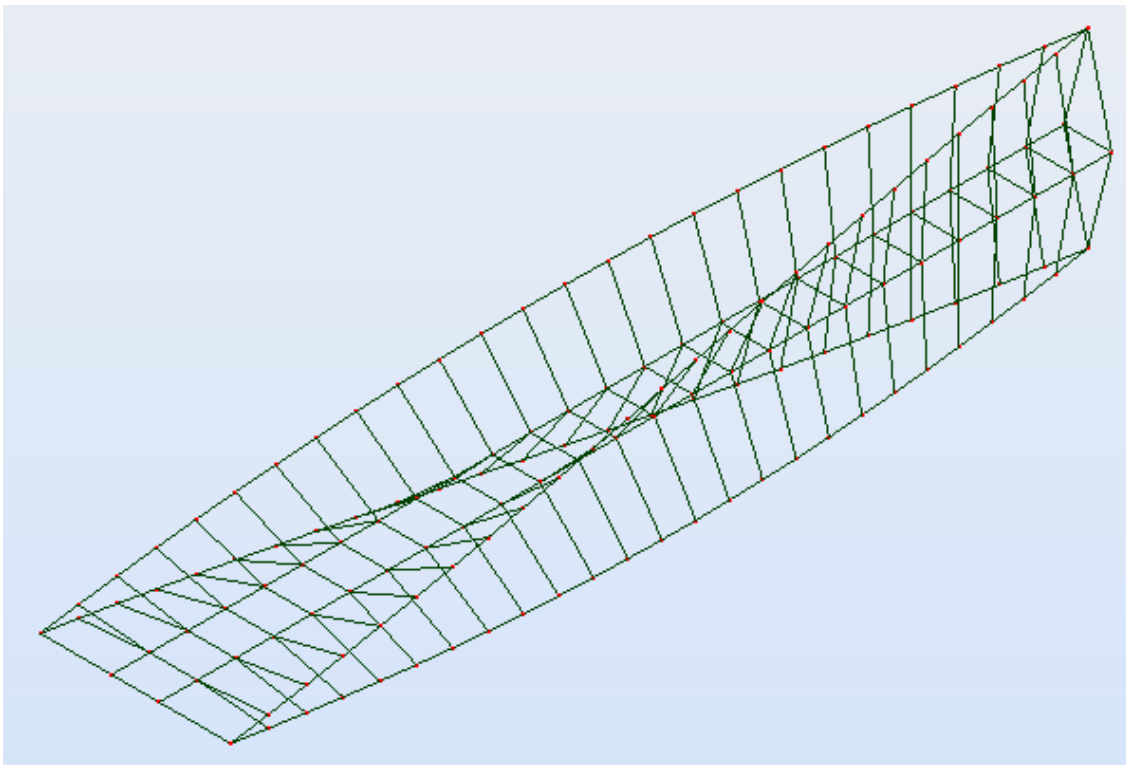



Figure 3.1.9 – Isometric view of half of the helix bridge

The half bridge will then be rotated about itself, and the entire bridge will be created. This is done by selecting all of the members, and then using the “Rotate...”  option, which is found next to the horizontal and vertical mirror options. The user must then change the “Axis end” to the X-Y plane by selecting the “Plane” circle. Then, the point that the bridge will be rotated about must be selected (select any point where $x = 0$ and $y = 1000$). The “Angle” must be input as 180 degrees, and the full bridge will be created when the “Execute” button is clicked. The final inputs are shown in the figure below:

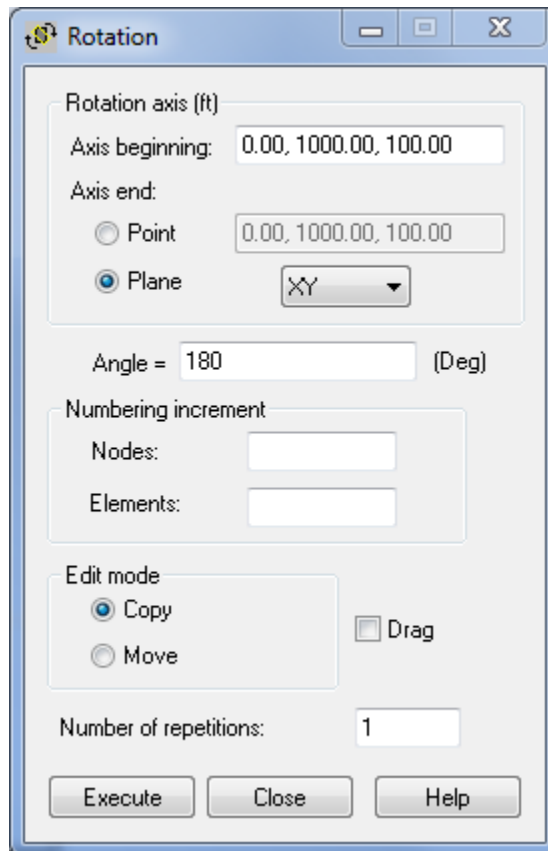






Figure 3.1.10 – The “Rotation” window

The full bridge should be visible after the rotation step is complete. The next steps are to add the end supports and the live load, which will complete the basic model.

The bridge end supports should be pinned on one end with rollers on the other. The pinned end support is a standard Robot support (along with fixed), but the roller end support must be created. To do this, the user must select the “Supports...” option from the “Geometry” drop-down list on the menu bar, or the “Supports”  button on the toolbar. The window that opens will have an option to create a new support, and selecting this will open the “Support Definition” window. For the roller support, the “Fixed directions” that should be checked are UX and UZ (under the “Rigid” tab). UY should not be selected so that the end is free to roll in that direction. The pinned and roller supports can then be added to the ends of the bridge by selecting the appropriate support, and then selecting the node on the model where the support is wanted. 8 total supports should be put on the model, four pinned supports at the four nodes at $y = 0'$, and four roller supports at the four nodes where $y = 2000'$.

In order to load the bridge with a live load from the traffic, an area must be created that the load will be distributed over. A cladding must be created, and it will act as the roadway for the purposes of distributing the load. The user must select the “Claddings...”  option from the Geometry drop-down list, and a window will open prompting the user to enter the cladding definition. The load distribution should be selected as “Two-way”, and the definition method should be “Rectangle”. Selecting the “Geometry” button will open an option to input three points, and the three points input should create a cladding that is 40 feet wide (four 10-foot lanes), 2000 feet long and is centered on the deck. The user must then load the created cladding with the live load.

The “Load Definition”  button should be selected (from the “Loads” drop-down list) in order to load the cladding. The model must be in load case 2, LL1, in order to input the live loading. The “Uniform Planar Load”  should be selected from the “Surface” tab, as this will distribute the load throughout the cladding evenly, which is the desired result. The input load should be 64psf (standard live load for bridges) in the negative Z-direction. The input must be -0.064 kips/ft² in the “Z” box, and by clicking “Add”, the user can select the cladding, and the load will be distributed on it. The load can be viewed on the cladding if the “Load symbols” option is on (this option is on a bar at the bottom of the model space, next to the right-left scroll bar), and the red arrows will be visible.

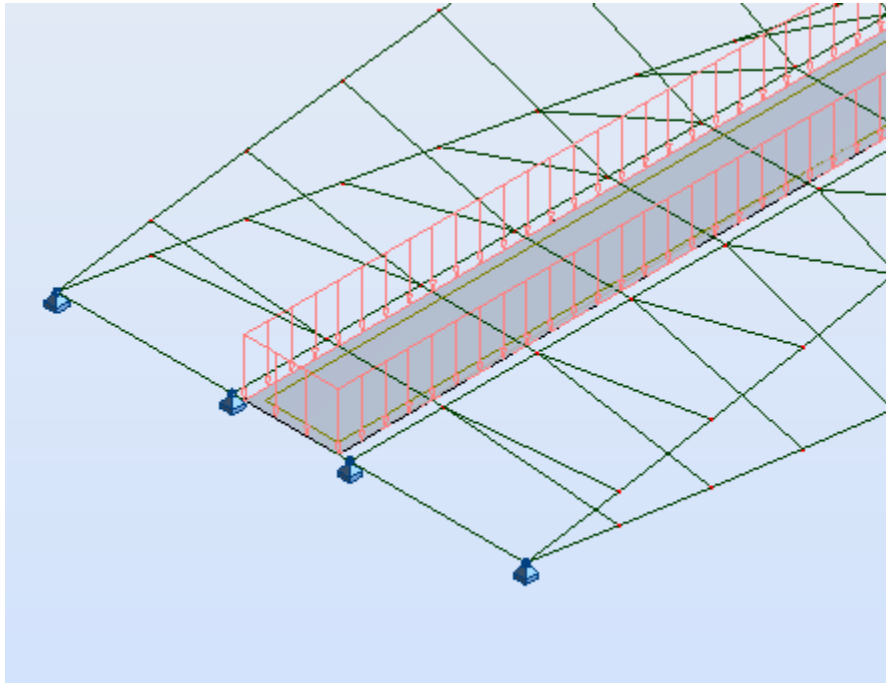



Figure 3.1.11 – Isometric view showing the pinned end supports, cladding and live load.

To analyze the model, the user must select the “Calculations”  option in the “Analysis” drop-down list on the menu bar. The program will then analyze the bridge, and the results will become available. A full guide on how to analyze this model is shown in the following section. For this particular model, the deflections will be too high for the bridge to pass inspection. The model must be optimized through an analysis of the shape, and the various member sections must also be optimized to ensure strength while minimizing the dead weight. This process for this analysis is shown throughout the coming sections of this paper, and it can be used as a guideline for optimizing the bridge for a given set of parameters.

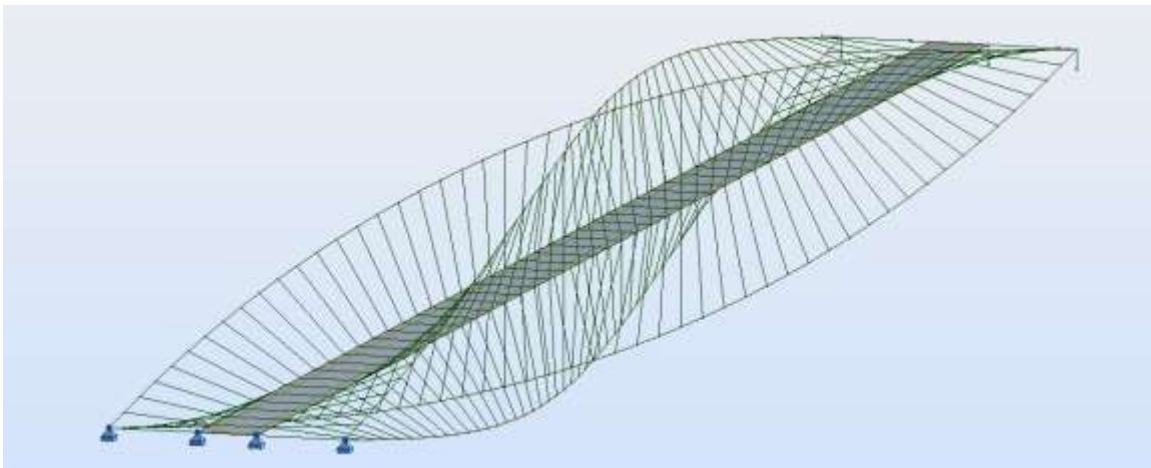



Figure 3.1.12 Isometric view showing the completed model.

3.2 Analyzing a Helix Shaped Bridge in Robot

After completing a model in robot, the next step in the process is to analyze it. When the model is analyzed, the problems and flaws can be found, which are needed in order to optimize the design of the bridge. In this section, the bridge will be analyzed for live and dead load cases for both first and second (non-linear) order analyses using Autodesk Robot Structural Analysis Professional 2012. This section is only a guide on how to perform the analysis using Robot, the actual optimization of the helix bridge begins in the next section.

Using the bridge model created in the previous section, the first step is to run a basic first order analysis for both the dead and live load cases. To analyze the model, the user must select the “Calculations”  option in the “Analysis” drop-down list on the menu bar. Once this is complete, the results will be available. Click the “Results” drop-down list on the menu bar and a wide array of options will appear, as shown below:

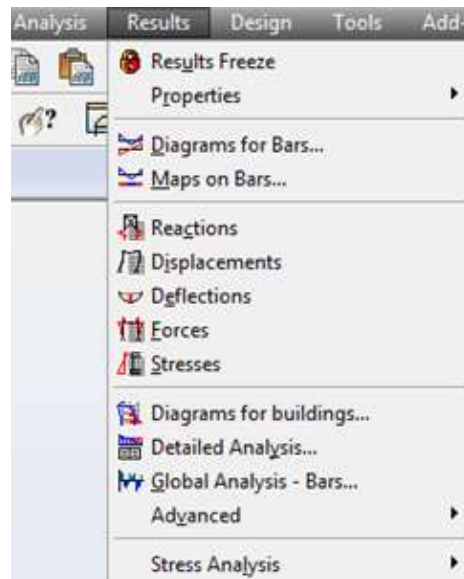



Figure 3.2.1 – The “Results” drop-down list

The options on this menu are numerous and are all important to the overall design of a bridge, but the main focus in this experiment is the maximum deflections of the bridge. The deflections referred to in the results list are actually for individual bars, which are not desired for this section. The desired values for this study are referred to in Robot as displacements, which is how much each node displaces from its original starting point. The maximum any node displaces on the bridge is the maximum deflection of the bridge.

Please note that whenever there is trouble with viewing options, select the “View” drop-down list on the main menu bar, and then select “Structure View” (which is only available if not already in Structure View), next select “Zoom” and “Zoom All”, and the model should reappear at the center of the window.

To quickly find the maximum displacement of the bridge, the “Displacements (deformation)”  button should be selected. It is found in the lower right corner of the model screen. Selecting this option will show the deflected shape of the bridge and give the maximum deflection for each load case. To select the live load case, click the “Cases” drop-down arrow (on the toolbar with the “Nodes” and “Bars” drop-downs) and select “2: LL1”. The deformed shape should look like the figure below:

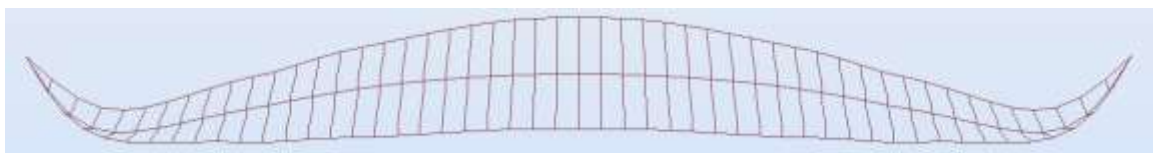




Figure 3.2.2 – Side-view of the live load deflected shape

If all of the steps followed in the previous section were followed exactly, the maximum displacement should be approximately 61.4 inches. This is far too high, as the maximum allowable displacement (or overall bridge deflection) is 30 inches, but the techniques used to lower the maximum bridge deflections are shown in the following

sections. The maximum first order dead load deflection can also be viewed by selecting the dead load case (1: DL1), from the “Cases” drop-down arrow (on the toolbar with the “Nodes” and “Bars” drop-downs). The deformed shape will appear if the “Displacements (deformation)”  button is selected, and the maximum dead load displacement should read approximately 455.0 inches (an extremely high value that will be reduced in the following sections).

The next type of analysis is for second and third order types. There are two ways to access the analysis types window, the first of which is to click the “Analysis Parameters”  button on the main toolbar (next to the calculations button). The other way is to click the “Analysis” drop-down list on the main menu bar, and select “Analysis Types”. The Analysis Types window will appear, as shown in the figure below:

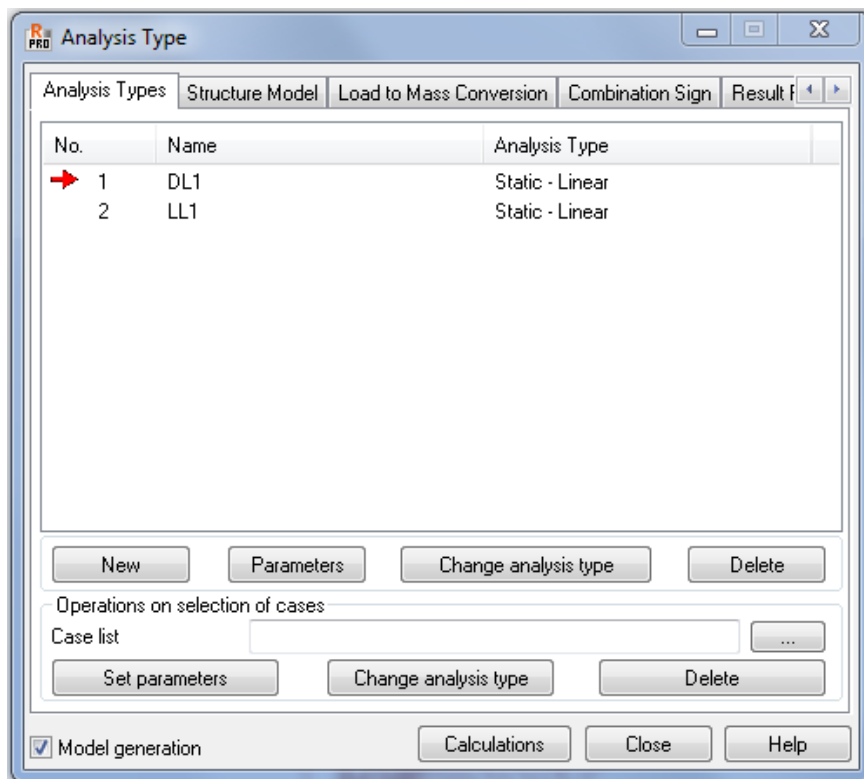


Figure 3.2.3 – The “Analysis Type” window

In order to change the analysis type, select the desired load case and click the “Parameters” button, which will bring up the “Nonlinear Analysis Parameters” window, as shown below:

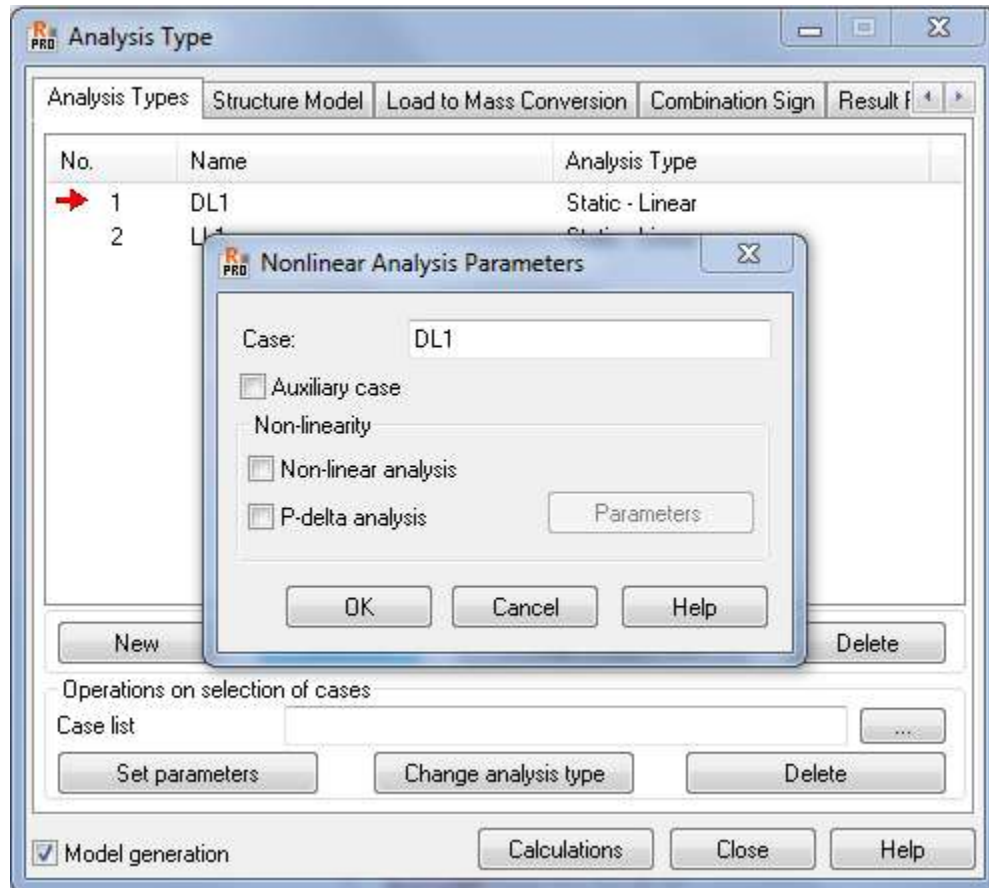


Figure 3.2.4 – The “Nonlinear Analysis Parameters” window

To select a second order analysis, check off the “Non-linear analysis” box, then click “OK”, and the analysis type for the load case will change (note that if the model has current analysis results, a warning will appear any time a change is made to it, just click “Yes” to continue). If a third order analysis is desired, check off the “P-delta analysis” box (which will auto select the non-linear case as well). If done correctly, the “Analysis Type” should change to read “Static - Nonlin” for a second order analysis or “Static -

Nonlin.PD.” for a third order analysis.

Once the analysis type is change to second (or third) order, the calculations should be run again. A different analysis window will appear, and the analysis will be run. This is a more time consuming calculation as it requires multiple iterations, and there are two common errors that will be viewed if there is failure, both of which are pictured below:

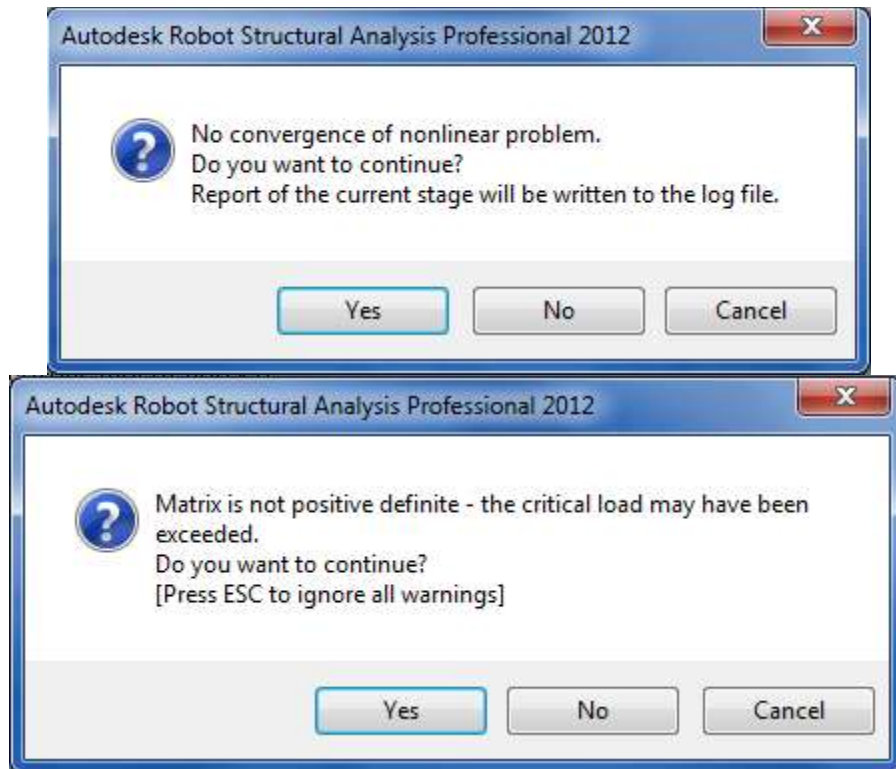


Figure 3.2.5 – Non-linear analysis failure notifications

If either of these two dialogue boxes appears, the bridge model has failed the second order analysis. The first dialogue box means that the members in the model are bending and displacing so much the non-linear analysis is not converging, meaning the shape is deforming so badly that the bridge cannot pass the second order tests. The second dialogue box implies that a member or, most likely, multiple members are buckling due to the axial forces applied to them. Either of these notifications implies failure of the

analysis, and that the bridge model must be strengthened.

The next step is to analyze which members are failing. When the failure is due to a non-convergence of the nonlinear problem, the program does not allow for the user to view which members are the failing ones. The best way to figure out which members are performing the worst is to go back to the linear first order analysis type, as the members are still experiencing the same proportion of forces to the other members as in the higher order analyses. Using the live load case under a first order analysis, running the calculations again will produce the same results as found earlier. To analyze the individual members, select the “Design” drop-down list on the main menu bar, and then select “Steel Members Design – Options”, followed by “Calculations”, and the following window will appear:

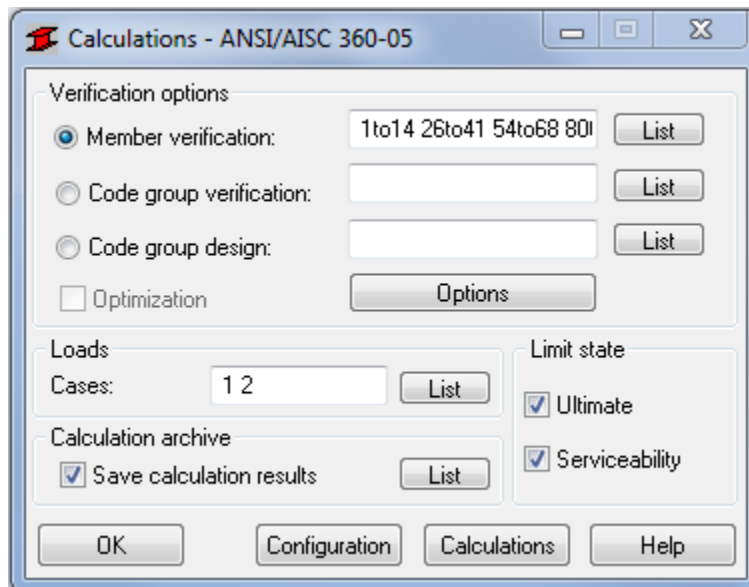


Figure 3.2.6 – The steel member design “Calculations” window

The next step is to make a couple of changes to the settings. First, make sure every member is actually selected to be analyzed by clicking the top “List” button and then selecting “All” at the top. Next, change the load cases to just Case 2 (the live load case)

by selecting it after clicking the “List” button in the “Loads/Cases” area of the window. Also uncheck the “Save calculation results” and the “Serviceability” boxes, as these are not needed, but each has a corresponding warning/dialogue box. Note: If the design parameters call for non-custom sections (meaning standard I-beams like W4x16 will suffice), the optimization options can be used, and the program will automatically select the optimal beams, but that is not possible for a bridge with all custom members. The final window with the appropriate setting should look as below:

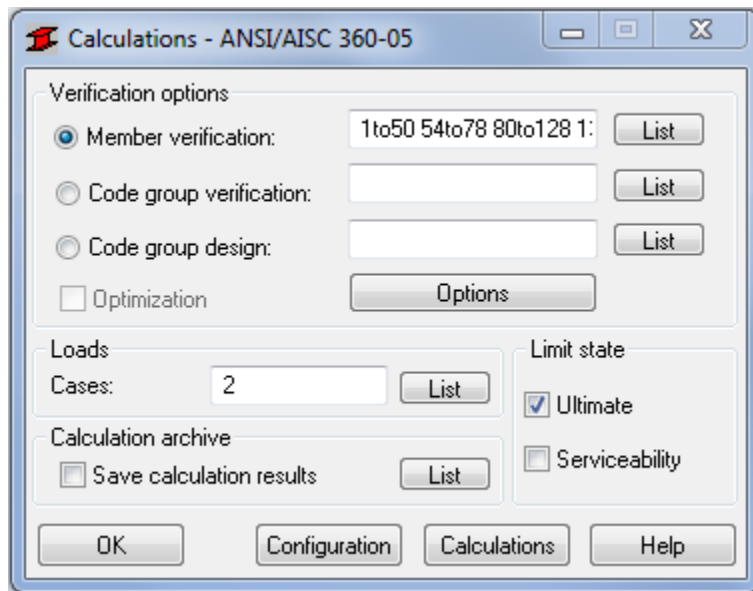


Figure 3.2.7 – The final steel member design “Calculations” window

Next, click “Calculations” at the bottom, and another window will appear. These are the calculation results for each individual members based on the standards in ANSI/AISC 360-05 (the code parameters can also be changed). The code calculations produce an efficiency ratio, which needs to be less than 1.00 to pass the tests. If the ratio is greater than 1, the member is failing. The higher the efficiency ratio, the greater the need to strengthen that member, as any member that has an efficiency ratio near or above one will fail the second order tests. In this case, the live load members all pass, with some

members coming back with instabilities, which is normally due to excessive length.

Running the calculations again with the dead load case shows that most of the members are failing; and therefore, they must be strengthened. The figure below shows some passing (green) and failing (red) members due to the first order dead load analysis:

Member	Section	Material	Lay	Laz	Ratio	Case
811 Simple bar_	Circle_Solid_	STEEL	80.00	80.00	0.84	1 DL1
810 Simple bar_	Circle_Solid_	STEEL	80.00	80.00	1.50	1 DL1
809 Simple bar_	Circle_Solid_	STEEL	80.00	80.00	1.83	1 DL1
808 Simple bar_	Circle_Solid_	STEEL	80.00	80.00	1.71	1 DL1
807 Simple bar_	Circle_Solid_	STEEL	80.00	80.00	1.56	1 DL1
806 Simple bar_	Circle_Solid_	STEEL	80.00	80.00	1.49	1 DL1
805 Simple bar_	Circle_Solid_	STEEL	80.00	80.00	1.51	1 DL1
804 Simple bar_	Circle_Solid_	STEEL	80.00	80.00	1.67	1 DL1
803 Simple bar_	Circle_Solid_	STEEL	80.00	80.00	1.74	1 DL1
802 Simple bar_	Circle_Solid_	STEEL	80.00	80.00	1.87	1 DL1
801 Simple bar_	Circle_Solid_	STEEL	80.00	80.00	1.29	1 DL1
800 Simple bar_	Circle_Solid_	STEEL	80.00	80.00	2.16	1 DL1
799 Simple bar_	Circle_Solid_	STEEL	80.00	80.00	1.69	1 DL1
798 Simple bar_	Circle_Solid_	STEEL	80.00	80.00	1.32	1 DL1
797 Simple bar_	Circle_Solid_	STEEL	80.00	80.00	1.72	1 DL1
796 Simple bar_	Circle_Solid_	STEEL	80.00	80.00	1.38	1 DL1
795 Simple bar_	Circle_Solid_	STEEL	80.00	80.00	1.23	1 DL1
794 Simple bar_	Circle_Solid_	STEEL	80.00	80.00	1.08	1 DL1
793 Simple bar_	Circle_Solid_	STEEL	80.00	80.00	0.95	1 DL1
792 Simple bar_	Circle_Solid_	STEEL	80.00	80.00	0.81	1 DL1
791 Simple bar_	Circle_Solid_	STEEL	80.00	80.00	0.66	1 DL1
790 Simple bar_	Circle_Solid_	STEEL	80.00	80.00	0.52	1 DL1
789 Simple bar_	Circle_Solid_	STEEL	80.00	80.00	0.39	1 DL1
788 Simple bar_	Circle_Solid_	STEEL	80.00	80.00	0.31	1 DL1
787 Simple bar_	Circle_Solid_	STEEL	80.00	80.00	0.31	1 DL1
786 Simple bar_	Circle_Solid_	STEEL	80.00	80.00	0.39	1 DL1
785 Simple bar_	Circle_Solid_	STEEL	80.00	80.00	0.52	1 DL1
784 Simple bar_	Circle_Solid_	STEEL	80.00	80.00	0.66	1 DL1
783 Simple bar_	Circle_Solid_	STEEL	80.00	80.00	0.81	1 DL1
782 Simple bar_	Circle_Solid_	STEEL	80.00	80.00	0.95	1 DL1
781 Simple bar_	Circle_Solid_	STEEL	80.00	80.00	1.08	1 DL1

Figure 3.2.8 – Steel member calculation results for the first order dead load case

The techniques on how to reduce the failures and pass the appropriate tests are shown in the following sections. The ability to model and analyze the bridge models in Autodesk Robot Structural Analysis Professional 2012 is vital to proceeding with the optimization of the helix bridge design.

4.0 Optimizing the Helix Bridge Structure for Live Load Deflections

A starting point for the optimization of the helix shape is chosen to be a 65 foot radius in cross-section with a flat 65 foot wide deck. The span length of 2000 feet is divided into 50 sections (40 feet each), with pin supports on one end of the bridge and rollers on the other. The members are chosen to be 22.5 inch thick solid steel circles with a yield strength of 36ksi. The helix is connected to the 65 foot wide bridge deck by connecting one member directly from the helix to the edge of the deck at the intersection of every 40 foot section. The live load is modeled as a 60 foot wide slab with a live load force of 65 psf, while the dead load is from the self-weight of the bridge members. Some images of the initial bridge model can be found on the following pages.

After performing an analysis in Robot using these established initial parameters, it becomes clear that the bridge must be strengthened. The maximum live load deflection of this bridge model is 95.7 inches, which is well over the allowable 30 inches for a 2000 foot span. The dead load deflections are even greater, having a maximum of 473.2 inches. The exaggerated deflected shape can also be seen on the following pages.

Using the results from the initial model, the optimization process can begin. The main problem with this design is shear at the ends of the bridge, as can be clearly seen in the deflected shape. Although the maximum deflection point of the bridge model occurs at the center as expected, it is clear that the weakness in the model is at the ends. As can be seen in the image, the majority of the bridge deflection occurs in the sections near the ends of the bridge, whereas the middle sections do not deflect significantly compared to the rest. In fact, the deflection in the first four forty-foot sections from the live load is 70.9 inches, while the next 21 sections only deflect an additional 24.8 inches to the

maximum at the center of the bridge.

The center of the bridge is strong due to the fact that the helix reaches its highest point at the center, which is certainly where the most strength is needed, but this strength is not distributed efficiently enough to the supports at the ends of the bridge. The flaw in this early design is the thinness of the bridge at its ends near the connections, which are clearly not strong enough to resist the load.

Using the initial results from the 65 foot radius model, the optimization of the helix shaped bridge can begin. There are many variables that can be changed in order to try and strengthen the bridge, which include: increasing the radius of the cross-section of the bridge (or, more importantly, increasing just the height in the Z-plane), increasing the thickness of the deck, adding a slope to the deck, changing the member sections, increasing the yield strength of the steel, changing the shape of the outer support structure and adding bracing or supports where needed.

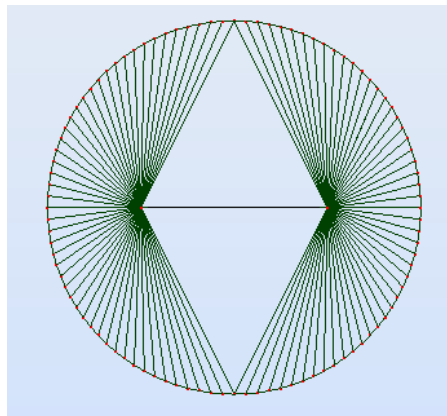


Figure 4.0.1 – Cross section in the X-Z plane with a 65 foot radius.

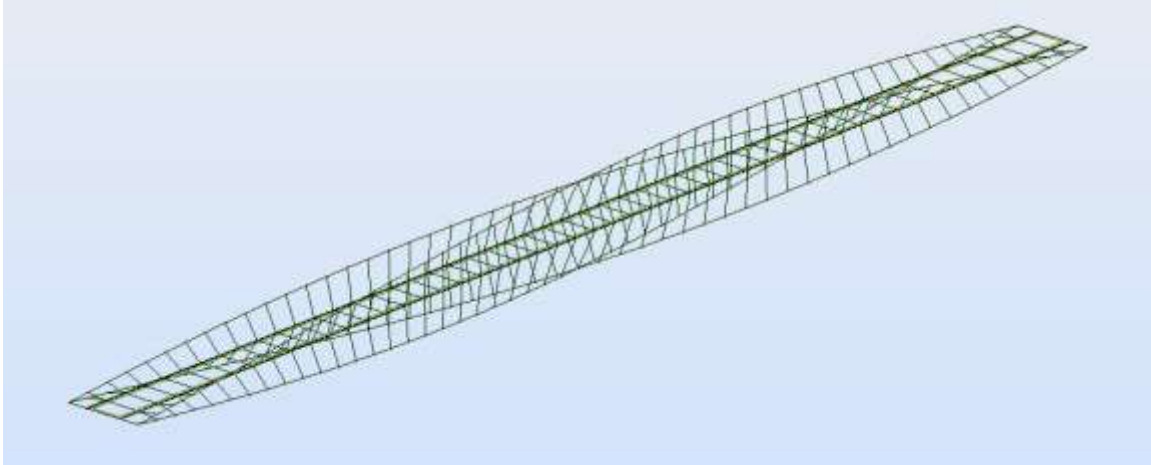


Figure 4.0.2 – Isometric view.

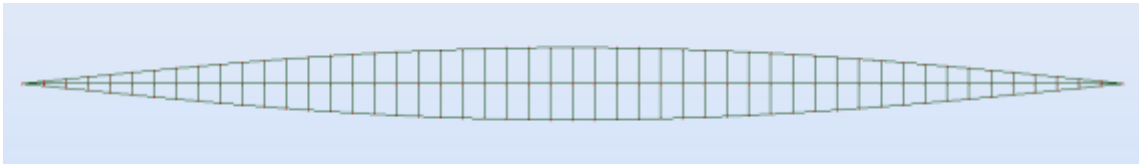


Figure 4.0.3 – Side view in the Y-Z plane with a 2000 foot length

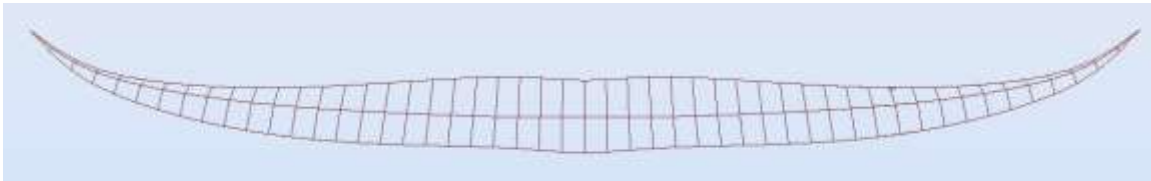


Figure 4.0.4 – Side view of the exaggerated deflected shape in the Y-Z plane. The deflection in the end sections is seen to be greater than in the center sections.

4.1 Radius Size Optimization

The first parameter to be optimized will be the radius (or height) of the bridge, as this is the most important factor when addressing the overall strength of the bridge. The bridge can be braced at the ends and the member sections can be strengthened, but if the height of the bridge at the center is not tall enough, there is no way the models will be able to pass any of the relevant tests and standards, as they will not be strong enough.

To start this process, multiple models are produced with varying radii, and even varying height to width ratios. The first step is to figure out what seem to be the optimal height and width of the bridge cross section. Because of the number of parameters that will change throughout the optimization process, the results from this particular analysis will have to be re-optimized once the other parameters are finalized. This simply means that adding a deck or increasing the area of the member sections might change the optimal radius/height, as the weight of the bridge and the way forces are distributed will change as various parameters are altered throughout the analysis.

To start this portion of the analysis, multiple bridge models will be analyzed using various radii and height to width ratios. For the purposes of aesthetics, the ideal scenario will be a helix shape bridge which forms a perfect circle in cross-section, meaning a bridge with equal height and width. Increasing the height to width ratio will cause the bridge to look like an oval in cross-section. All of the models in this section will cover the 2000 foot span using a 65 foot wide flat deck that connects to the helix structure every 40 feet. The members are all 22.5 inch solid steel circles (in cross-section), with a yield strength of 36 ksi.

Using the aforementioned parameters, the following tables of results were produced. Table 4.1.1 shows the maximum live load deflections for each model, while Table 4.1.2 shows the maximum dead load deflections for each model. Each model follows the helix shape, though only the models where the height equals the width will produce a circle in cross-section, the rest produce ovals. Each variation still follows the sine (height) or cosine (width) equation for the given radii, which produces the aesthetically desired curve.

		Width (Radius) of Bridge Cross-Section			
		48.75 ft	65 ft	80 ft	100 ft
Height (Radius) of Bridge Cross-Section	65 ft	96.3	95.7	-	-
	80 ft	72.8	72.2	74.3	-
	100 ft	59.6	57.2	61.6	82.8
	130 ft	54.5	53.5	54.4	69.3

		Width (Radius) of Bridge Cross-Section			
		48.75 ft	65 ft	80 ft	100 ft
Height (Radius) of Bridge Cross-Section	65 ft	455.5	473.2	-	-
	80 ft	352.4	385.2	421.5	-
	100 ft	323.2	368.6	404.8	474.0
	130 ft	382.0	435.0	487.5	563.4

As can be seen in the tables above, the maximum load deflections can change drastically depending on the height and width of the bridge cross-section. The best performing bridge has radii of 65 feet (width) and 130 feet (height) for live load purposes, while the best for dead load deflections is the model with radii of 48.75 feet for the width and 100 feet for the height. Images of the cross-sections of these two models are shown on the following page.

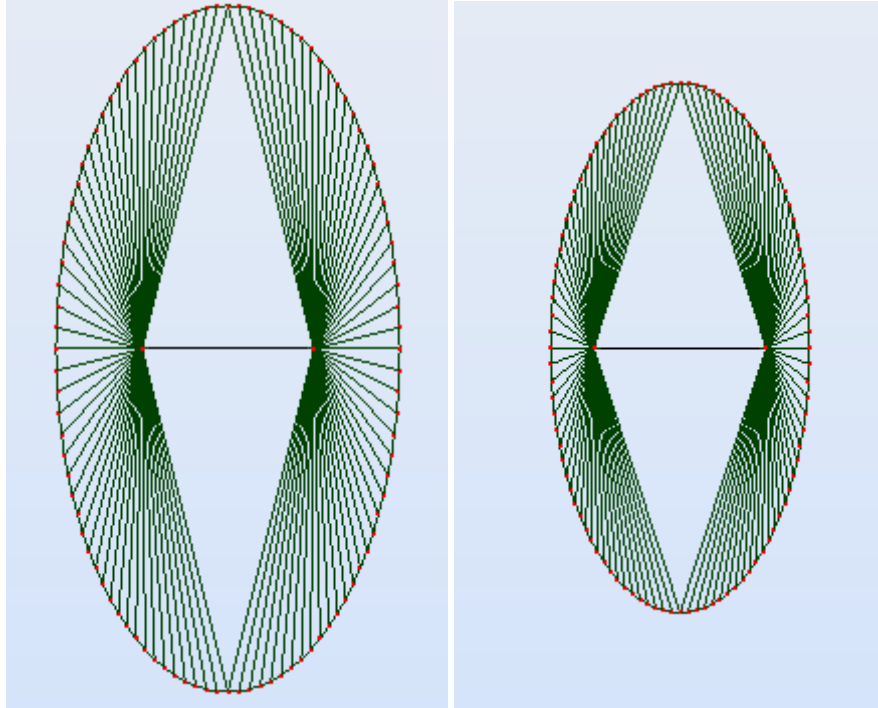


Figure 4.1.1 – Cross-sections of the best performing radius optimization designs. The 65 foot (radius) width by 130 foot (radius) height model is shown on the left, while the 48.75 foot (radius) width by 100 foot (radius) height is shown on the right.

An analysis into the data given produced makes it clear that increasing any parameter will not always add strength to the bridge model. For the dead load cases, this is clearly due to the fact that once the bridge is too large, it has more trouble supporting itself, which causes greater deflections. Because the first priority in the analysis is to get the maximum live load deflections within the allowable standards, the next step is to try and optimize the model that performed best for live load deflections. For each height in the live load analyses, the best performing model was always the one with a 65 foot radius width. The next step is then to take this assumed optimal width, and optimize the height that will produce the overall lowest live load deflections. This will be done by producing multiple models with a 65 foot radius width at varying heights, and again seeing which model has the lowest maximum live load deflections.

Keeping all other parameters the same, the models are analyzed again using Robot, and the table shown below is a summary of the results, while the figure shown the graph of the data. The models were also tested for dead load maximum deflections, as this will become a more important parameter later in the optimization process.

Table 4.1.3 - Maximum Deflections for 65 foot Radius (Width) Models of Varying Height								
Height:	65 ft	80 ft	105 ft	130 ft	150 ft	172.5 ft	215 ft	315 ft
Max. Live Load Deflection (in)	95.7	72.2	59.2	53.5	56.6	62.9	76.9	104.2
Max. Dead Load Deflection (in)	473.2	385.2	372.8	435.0	522.2	644.1	924.6	1635.2

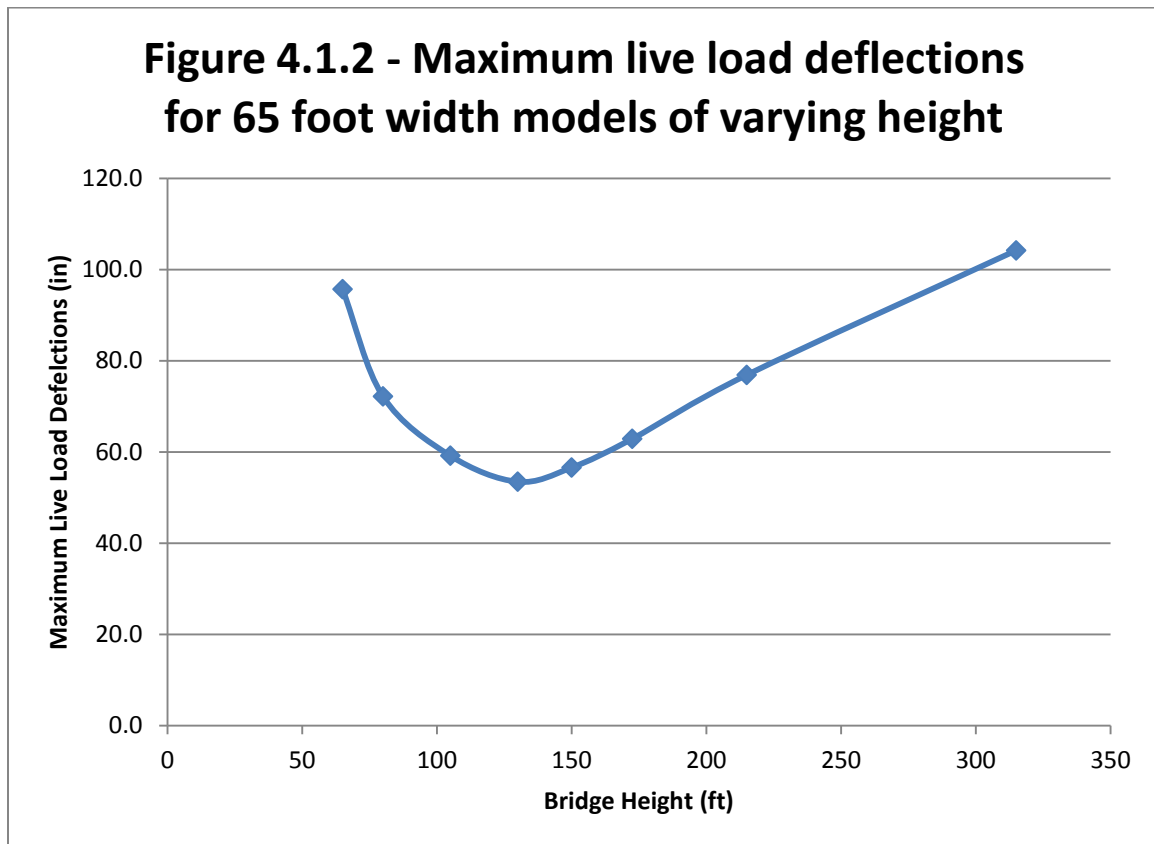
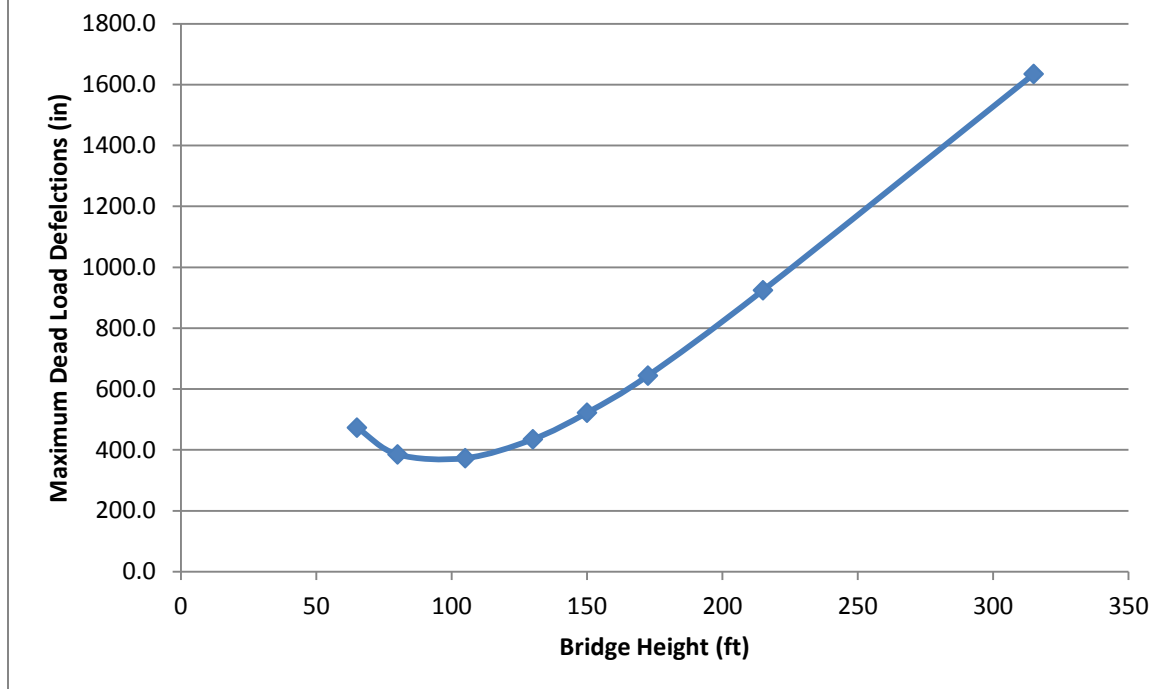


Figure 4.1.3 - Maximum dead load deflections for 65 foot width models of varying height



The graph of the data in the figures makes it very clear as to what the desired radial height of the bridge should be, though there is a large difference between the optimal height to resist live load versus the optimal height to resist the bridge's self-weight. The optimal height for live load deflections is clearly very close to 130 feet (for this particular set of variables), while the optimal height to resist the dead load seems to be very close to 100 feet, which is a fairly large difference. This is due to the fact that as the bridge gets taller, it also gets heavier, and the increase in the self weight of the model outweighs the increase in the strength of the model given by the larger height, and this turning point is right around a 100 foot radius.

The maximum displacement values are important for comparison and also for passing the relevant allowable standards, but looking at the manner in which the bridge is

deflecting can help the analysis progress drastically. This will be done by taking the 65 foot by 130 foot radius model and looking at its deflected shape, which is shown in the figures below and on the following page.

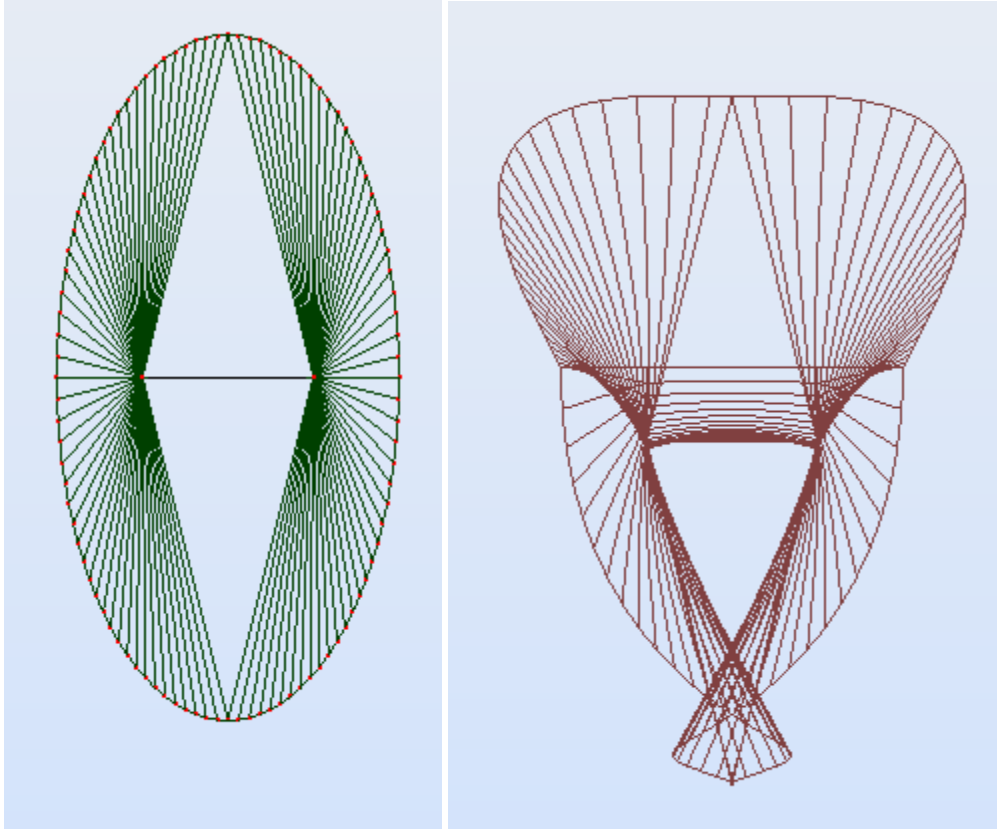


Figure 4.1.4 – The exaggerated deflected dead load shape of the cross-section of the 65 by 130 foot radius model.

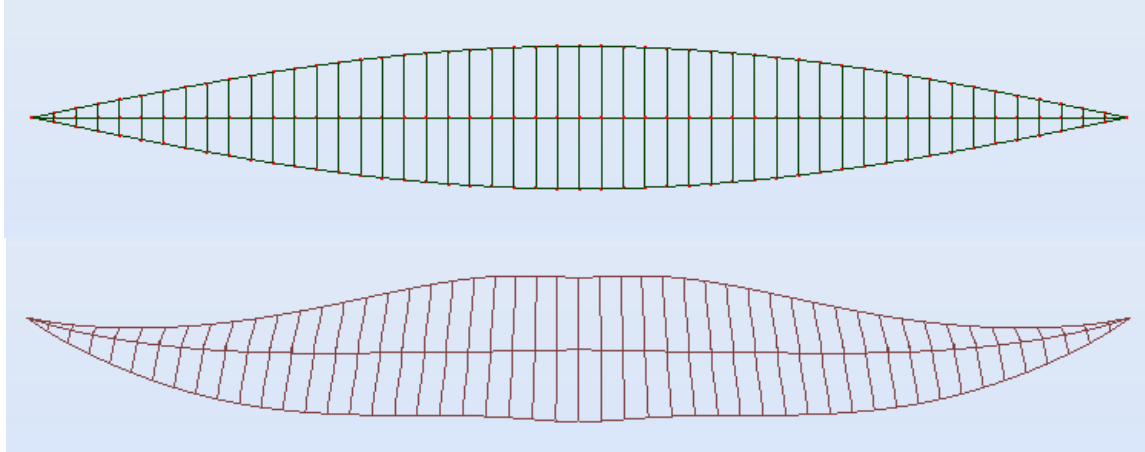


Figure 4.1.5 – The exaggerated deflected dead load shape of the side-view of the 65 by 130 foot radius model.

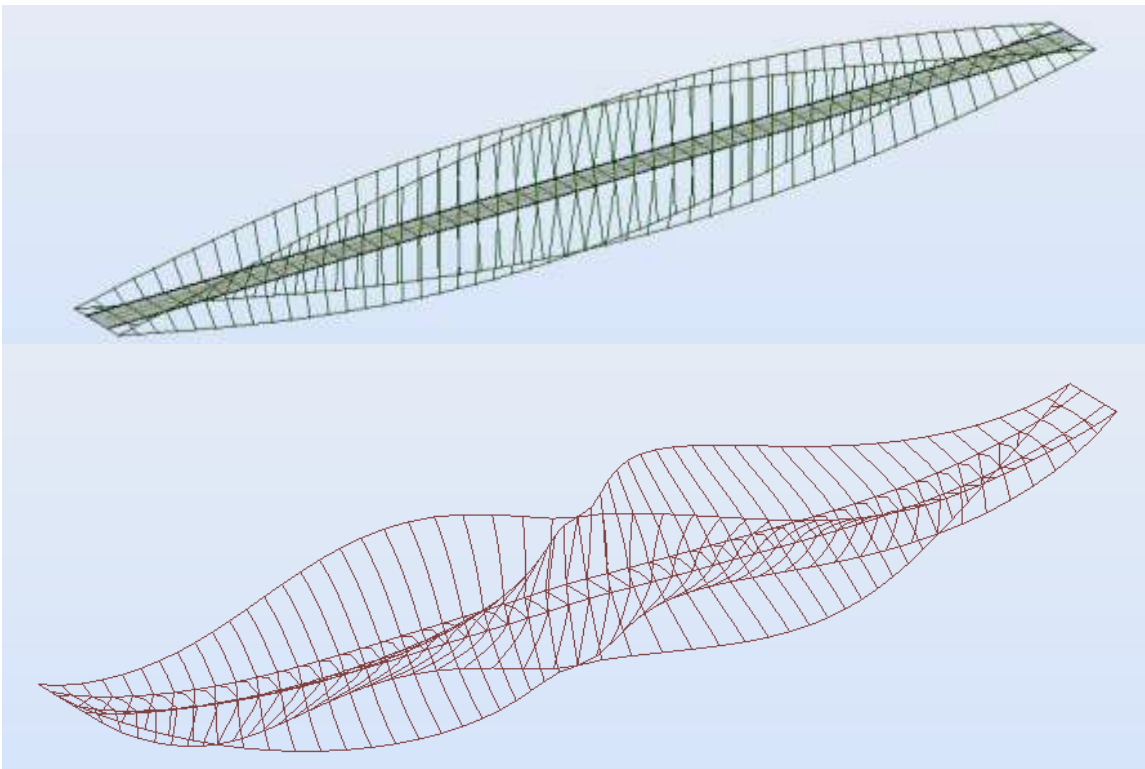


Figure 4.1.6 – The exaggerated deflected dead load shape of the isometric view of the 65 by 130 foot radius model.

The deflected shapes shown in the previous images are extremely exaggerated, but this exaggeration helps make the flaws in this early design easily visible. The main two

problems are glaring in these figures, and they are the shear due to the thinness of the bridge at the ends (as discussed in the previous section) and the lack of support of the helix structure from about the quarter point of the bridge to the end. The outer helical structure is not well supported towards the ends of the bridge, unlike at the middle. The members that connect the helix to the deck towards the center of the bridge are near vertical (in the x-z plane), whereas towards the ends, they approach being completely horizontal. Because the self-weight from the helix is clearly all applied in the negative vertical direction due to gravity, the more horizontal the members are, the weaker they are in resisting the dead load. This causes the upper half of the helix to bow-out, as seen in the figures, whereas the bottom half of the helix simply sinks in towards itself (in the exaggerated deflection, the bottom half of the helix actually overlaps in the image, but this is only due to the excessive exaggeration).

4.2 Deck Thickness Optimization

In order to address the excessive deflections found in the flat deck bridge models in the previous section, the next step in the optimization will be to add a thicker deck, and see the effect it has on the deflections. Just as Robert Maillart first proved with the Zuoz Bridge, the deck can be used as part of the structure to increase the overall strength in resisting loads.

In this section of the analysis, a deck thickness will be added in order to help the bridge resist the shear it is experiencing at its ends. Rather than adding a thick 65 foot wide deck, the models with the deck will have a double deck that is 40 feet wide, which will allow for three 10-foot lanes on each level of the deck. Although the thicker deck will clearly increase the dead load, the deflections due to the dead load will be expected to decrease, as the shear in the ends will be better resisted.

The two models that will be used in the deck thickness analysis will be the 65 by 130 foot cross-section model that was previously established as the strongest model, and the 100 by 100 foot cross-section model. The 100 by 100 foot cross-section was chosen as the perfect circle cross-section, even though the 80 by 80 foot model performed better in the initial testing, because as the deck gets thicker, the members connecting to the helix get shorter, and will actually impede traffic at the center of the bridge. For the 100 foot radius model with a 40 foot deck, the clearance in edge of the right and left lane is 20 feet, which is enough for a tractor trailer. If the height of the bridge was only 80 feet at the middle, the clearance for traffic is only 15 feet at this same point, which is not tall enough for all trucks. This is an example of a compromise that must be made in order to balance aesthetics, usability and structural strength.

The models were each analyzed with 2 decks, one with a thickness of 20 feet, while the next has a thickness of 40 feet. Each deck is 40 feet wide, while the flat deck being compared is still the 65 foot wide one used in the previous sections. The table below shows the results of the analyses in Robot, while the figures on the following pages show the views of the bridge models with the decks.

Table 4.2.1 - Maximum deflections for various deck thicknesses						
	65 x 130 ft models			100 x 100 ft models		
	Flat Deck	20 ft Deck	40 ft Deck	Flat Deck	20 ft Deck	40 ft Deck
Max Live Load Deflection (in)	53.5	39.7	29.9	82.8	43.3	44.0
Max Dead Load Deflection (in)	435.0	223.6	198.0	474.0	342.6	318.4

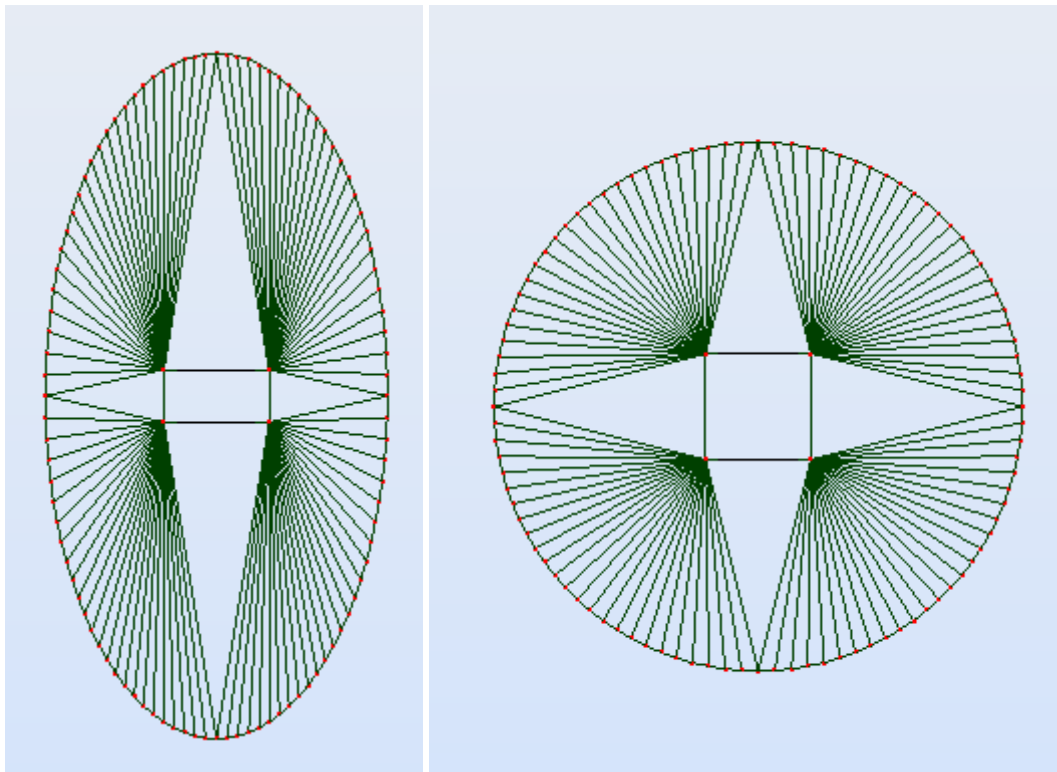


Figure 4.2.1 – Helix bridge model cross-sections with decks. The 65 by 130 foot radius model with a 20 foot tall deck is shown on the left, while the 100 by 100 foot radius model with a 40 foot tall deck is shown on the right.

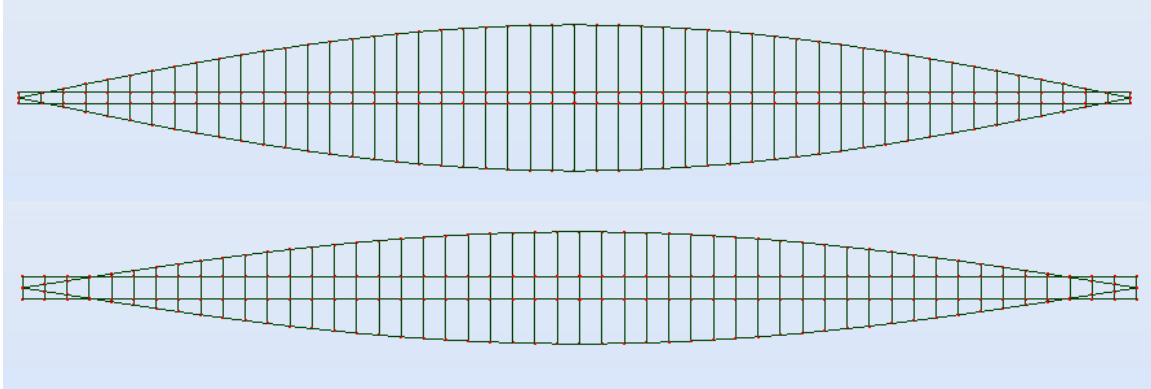


Figure 4.2.1 – Helix bridge model side-views with decks.

The 65 by 130 foot radius model with a 20 foot tall deck is shown on the top, while the 100 by 100 foot radius model with a 40 foot tall deck is shown on the bottom.

The 65 by 130 foot model with the 40 foot deck is clearly the best performer, and for the first time, a model has a maximum live load deflection below the allowable limit of 30 inches. Clearly the deck made a major difference in the shear that was being experienced, as the deflections decrease significantly. An interesting part of the results was that the 20 foot box deck actually produced a lower maximum live load deflection for the 100 by 100 foot radius model. The maximum dead load deflection was significantly lower though, which is the more important parameter now that it is clear that the live load deflections values have been reduced to levels below the allowable maximums. As the bridge is made stronger to decrease the dead load, the live loads will only decrease, so the dead loads will now become the main focus of the analysis.

5.0 Optimizing the Helix Bridge Structure for Dead Load Deflections

As is typical with long span bridges, the deflections due to the live load are clearly not going to be the primary cause of structural concern. In the previous section, a model was created that had a maximum live load deflection of less than the allowable maximum of 30 inches. The 65 by 130 foot radius model with the 40 foot deck had a maximum live load deflection of 29.9 inches. This 2000 foot span model used all 22.5 inch circular cross-section steel members, and the 40 foot thick box deck took a live load of 64 psf over three 10-foot lanes per level. The maximum dead load deflection from the self-weight was found to be 198 inches, which is very high.

Although there are no written standards for the maximum allowable dead load deflection for a bridge, if the deflection is too high, it implies that members are bending, failing, and possibly, buckling. Because of this, the next step in the process will be to make sure every individual member of the bridge passes a certain series of tests. The first of these tests is to make sure that all of the members pass the minimum parameters set forth in ANSI/AISC 360-05. Autodesk Robot can run these calculations on the individual members, and the outputs can be viewed in a table which will give the efficiency ratio of each individual member. The efficiency ratio that is calculated by Robot, is established in ANSI/AISC 360-05 using various properties of the member and it includes safety factors. If a member has an efficiency ratio of greater than 1, the member will come back as an “incorrect section”, as it is not strong enough and must be strengthened in order to pass the tests set forth in ANSI/AISC 360-05. This does not mean the member failed, it can just mean that it is close enough that it does not pass the code standards.

For the 65 by 130 foot radius helix bridge model that passed the live load deflection test, over 50% of the members failed the steel section calculations performed by Robot, including every single member in the top (compression) helix, shown in red in the figures below.

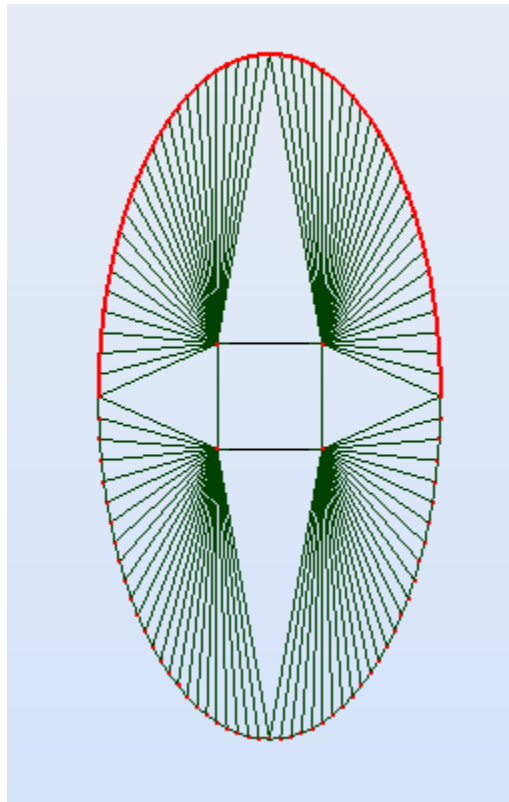


Figure 5.0.1 – Cross-section of the 65 by 130 foot radius model with the compression helix highlighted in red. None of the highlighted members pass code standards.

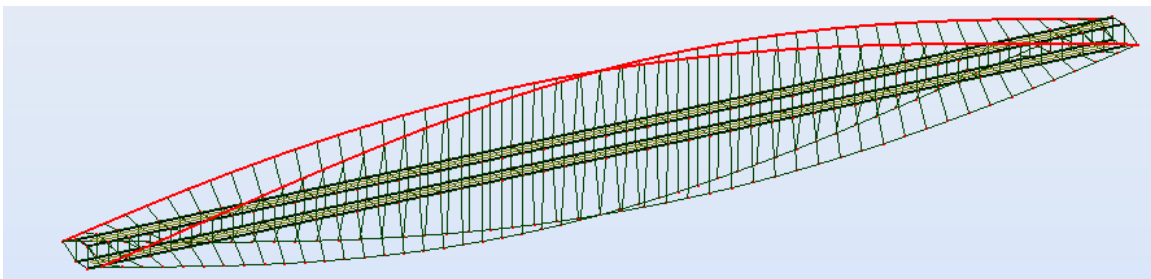


Figure 5.0.2 – Isometric view of the 65 by 130 foot radius model with the compression helix highlighted in red. None of the highlighted members pass code standards.

This simply shows that the bridge is not strong enough, and that the main weakness is in the lack of strength in the top layer of the helix. The top helix is in compression, and that is the area where there is 100% failure. These members must be strengthened and the shape must be improved in order to pass the appropriate tests.

5.1 Deck Diagonal Optimization

The first step in the optimization of the members will be to simply add diagonals to the deck. Adding diagonals helps to distribute the loads from the center of the span to its ends more efficiently. This will add weight to the bridge, but it will also strengthen it, which is what is needed. The table below shows five variations of deck designs, which are all pictured on the next page for reference.

Table 5.1.1 - Maximum deflections for various deck diagonal types					
	Straight	Diagonal (1)	Diagonal (2)	Triangle	Full X
Max Dead Load Deflections (in)	198	223.2	223.2	231.7	248
Max Live Load Deflections (in)	29.9	25.7	25.7	25.5	25.7

Even though the maximum dead load deflections increased significantly due to the added weight, the diagonals are a necessary element to the structure. The live load deflections decreased significantly, which shows that overall, the structure is stronger. Although this addition will not change the fact that the entire compression helix is failing, the diagonal members will be included in all future designs, as it increases the strength of the structure. The chosen design will be the “Diagonal (1)” design. Even though it is tied with “Diagonal (2)” in terms of strength for the flat box deck, when a slope is added to the deck, “Diagonal (1)” will be the better option.

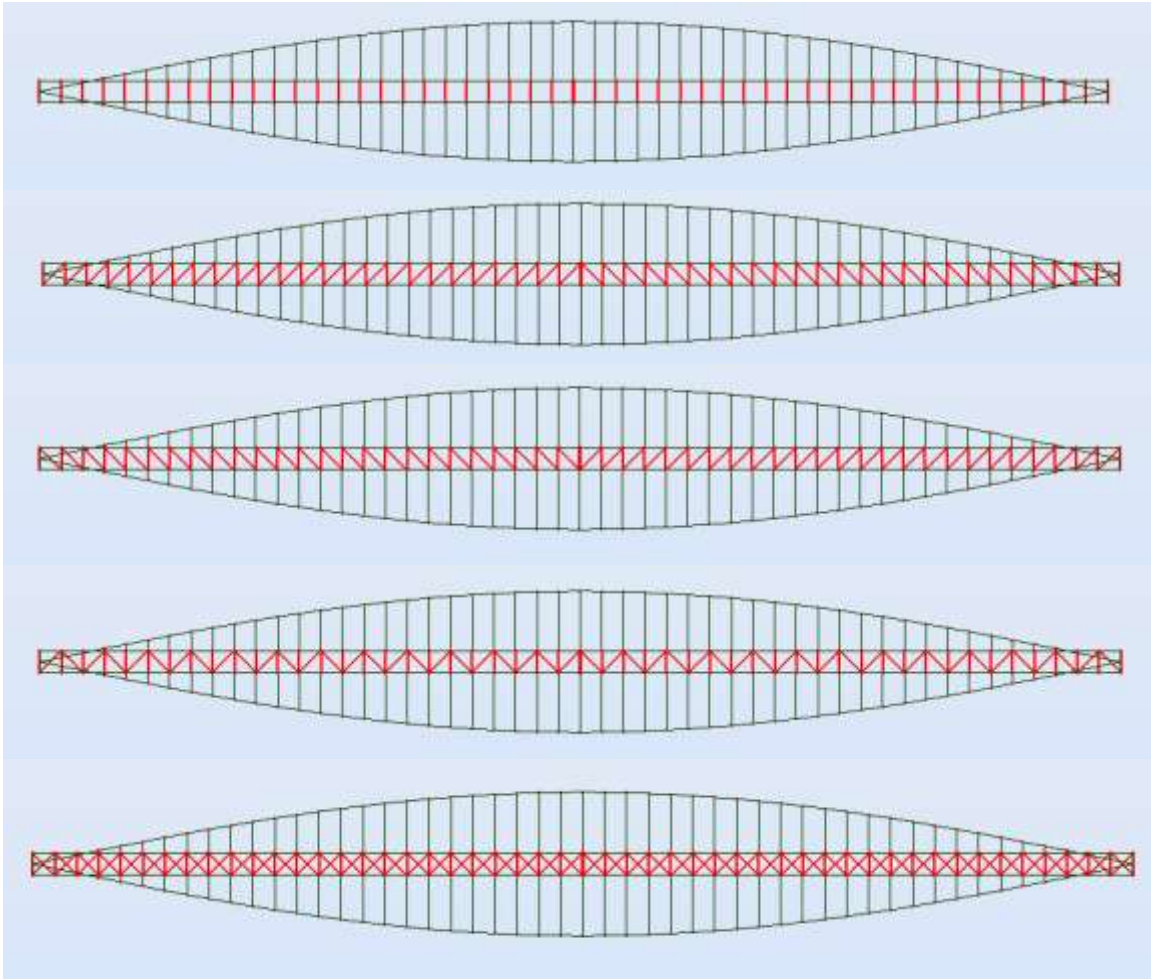


Figure 5.1.1 – Deck diagonal variations listed from top to bottom: Straight, Diagonal (1), Diagonal (2), Triangle and Full X. The deck members are highlighted in red for clarity.

5.2 Layered Helix Optimization

Now that the deck has been strengthened a reasonable amount, the next step in the analysis will be to see the effect of what will be referred to as “layering the helix”. This simply means that there will be an additional (or multiple) supports that follow the same path as the main part of the helix structure, but it lies closer to the deck. The layers of the helix will essentially cut the members that connect the main helix to the deck into sections, and this will add extra members that will take the compressive forces (on top of the bridge) or the tension force (below the bridge). The extra layers take the forces, but they obviously add to the already high self-weight, and that is why various types of layering will be analyzed. Another benefit of the layered helix is that it reduces the length of the members connecting the main helix to the deck. The shorter the members are, the better they will perform in buckling tests, which is important for the second order testing that will be done later in the analysis.

To start, the 65 by 130 foot radius model and the 100 by 100 foot radius cross section model will both be analyzed using multiple types of layering. The “half-cut” layer refers a layer that is added directly in between the outer helix and the deck, cutting all of the connecting members directly in half. The “quarter-cut” refers to the layer that cuts the member between the deck and the “half-cut” layer in half again, while the “three quarter-cut” refers to the layer that cuts the members connecting the “half-cut” layer to the main helix. The “three-eighths cut” and “seven-eighths cut” correspond to layers added three-eighths of the way up the connecting member from the deck, and seven-eighths of the way up the connecting member from the deck to the main helix. The figures on the following pages show the various types of layering that was analyzed.

The aforementioned models being used in this section of the analysis will be the ones that include the 40 foot box deck, as it clearly helped strengthen the bridge the most, and will be included in the final model of the bridge, so all iterations for the rest of the analysis will include the 40 foot box deck. The results of the layered helix analysis are shown in the tables below.

Layers:	None	½ cut	¾ cut	½ & ¾	¼, ½ & ¾	¾ & ⅞	⅞, ¾ & ⅞
Max Dead Load Deflections (in)	304.7	293.2	253.2	261.5	268.2	215.2	224.8
Max Live Load Deflections (in)	38.0	31.2	27.3	24.5	21.8	20.0	18.2

Layers:	None	½ cut	¾ cut	½ & ¾	¼, ½ & ¾	¾ & ⅞	⅞, ¾ & ⅞
Max Dead Load Deflections (in)	223.2	202.5	178.8	176.8	181.5	156.2	160.1
Max Live Load Deflections (in)	25.7	19.8	17.1	14.7	13.4	12.4	11.3

The results shown in the table above represent some very significant reductions in the maximum dead load deflections from the original model with only the outer helix (labeled “none”) in the tables above. Each of the bridge models above uses the 40 foot box deck with the diagonals established in the previous section. All of the members are still 22.5 inch diameter steel circles.

Although there are no clear goals in reducing the maximum dead load deflections to a certain value, it is clear that reducing them will cause fewer members to fail. When the bridge deflects too much, the members bend and compress in ways they cannot handle, so they fail the steel calculation tests that Robot performs. By reducing the dead

load deflections, the bridge members will be more likely to pass the relevant tests, which is the goal in this section of the analysis.

Based on the patterns in the data, it is clear that adding a layer closer to the main (outer) helix increases the strength more than adding one closer to the deck. This is due to the fact that there is a second layer taking compression forces away from the main outer helix structure, and the closer that layer is to the outer helix, the greater the force it can help take away. It is also clear that the models begin to weaken when a third inner helix layer is added, as the self weight of the addition begins to outweigh the strength added by the extra layer.

The figures on the following pages shown what the various layers look like in terms of aesthetics. Anytime members are added to the bridge, it will generally take away from its visual appeal, though it adds to its structural strength. Finding a balance between these two mediums is one of the most important aspects of bridge design.

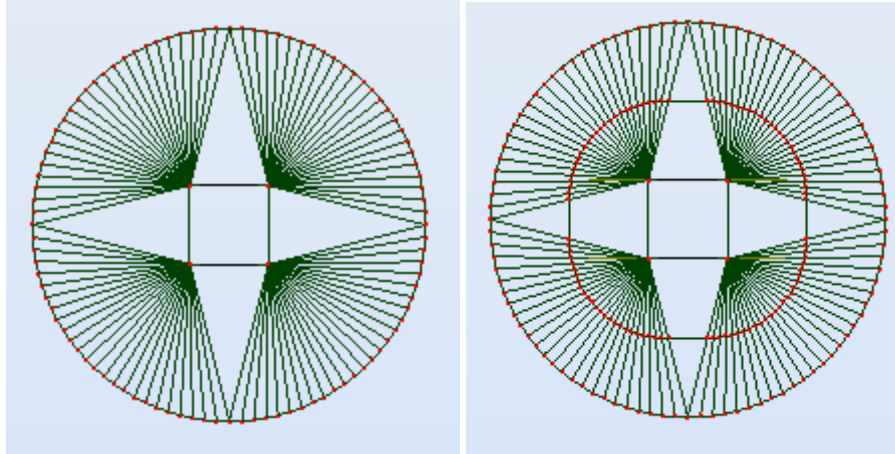


Figure 5.2.1 – Cross-section of the 100 by 100 foot model with no inner helix layers (left) and a $\frac{1}{2}$ inner helix layer (right).

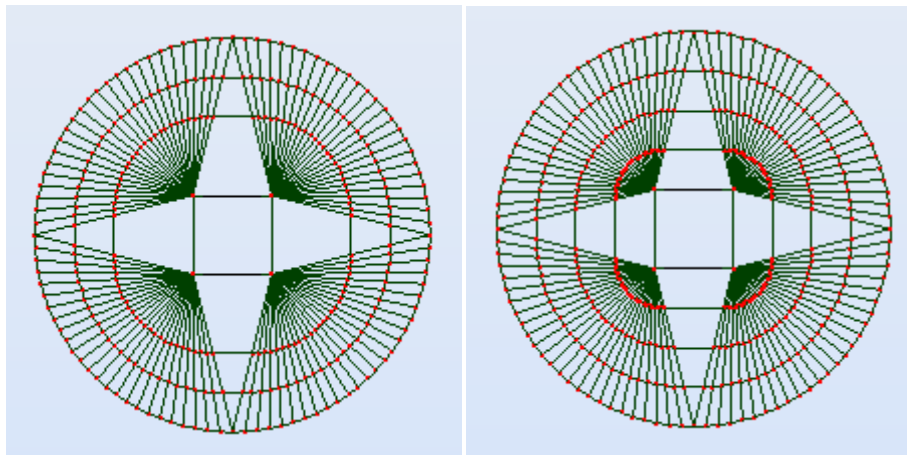


Figure 5.2.2 – Cross-section of the 100 by 100 foot model with $\frac{1}{2}$ & $\frac{3}{4}$ inner helix layers (left) and $\frac{1}{4}$, $\frac{1}{2}$ & $\frac{3}{4}$ inner helix layers (right).

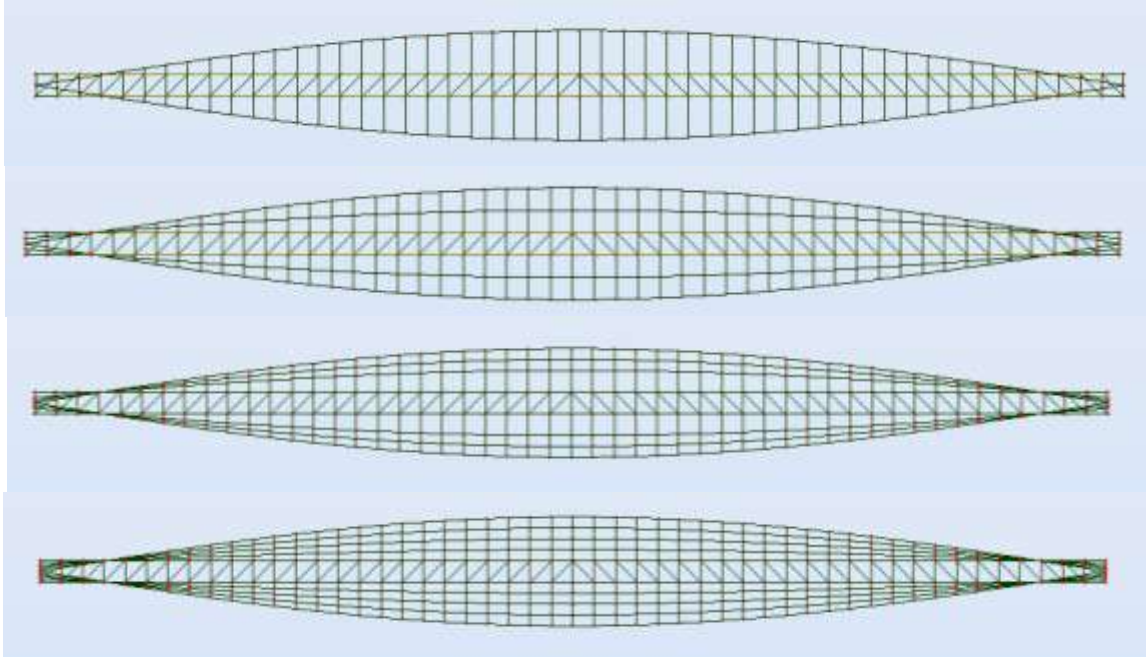


Figure 5.2.5 – Side views of the 100 by 100 foot models, listed from top: No inner helix layer, $\frac{1}{2}$ inner helix layer, $\frac{1}{2}$ & $\frac{3}{4}$ inner helix layers and $\frac{1}{4}$, $\frac{1}{2}$, & $\frac{3}{4}$ inner helix layers.

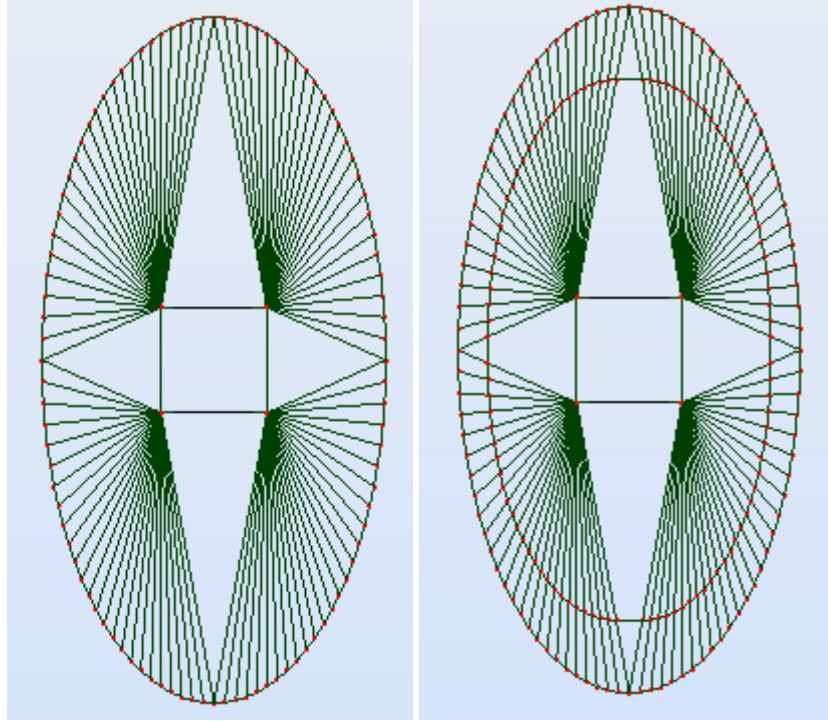


Figure 5.2.4 – Cross-section of the 65 by 130 foot model with no inner helix layers (left) and a $\frac{3}{4}$ inner helix layer (right).

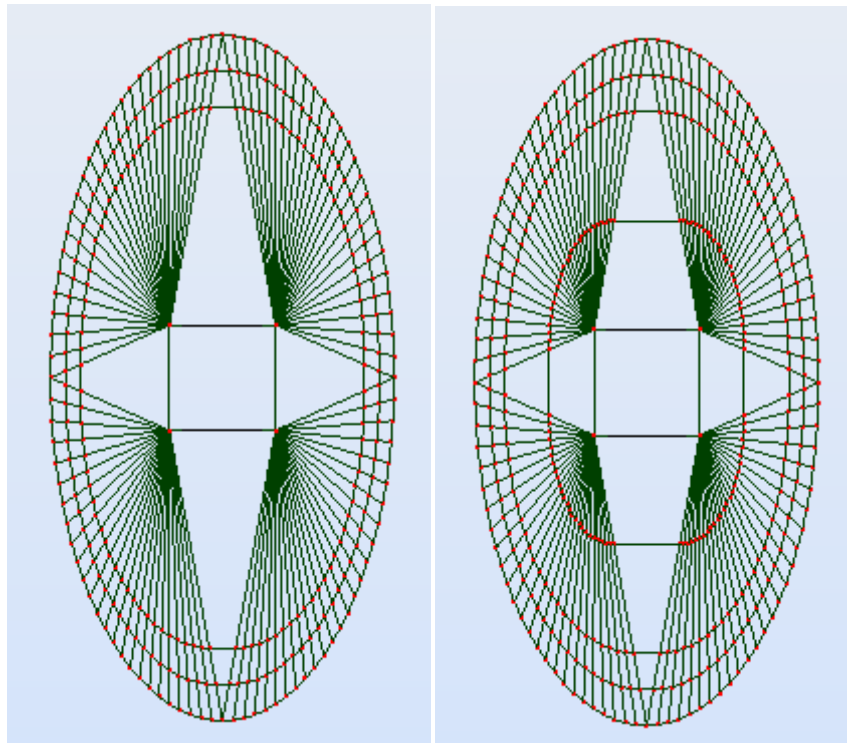


Figure 5.2.5 – Cross-section of the 65 by 130 foot model with $\frac{3}{4}$ & $\frac{7}{8}$ inner helix layers (left) and $\frac{3}{8}$, $\frac{3}{4}$ & $\frac{7}{8}$ inner helix layers (right).

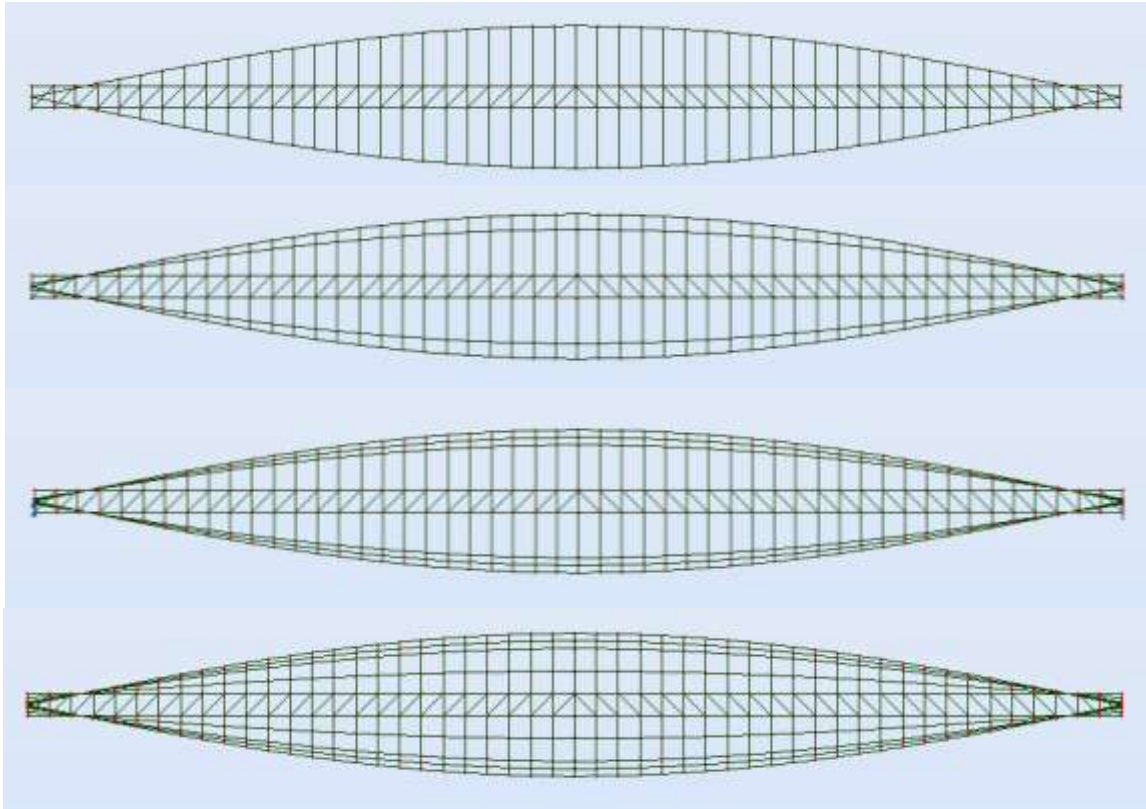


Figure 5.2.6 – Side views of the 65 by 130 foot models, listed from top: No inner helix layer, $\frac{3}{4}$ inner helix layer, $\frac{3}{4}$ & $\frac{7}{8}$ inner helix layers and $\frac{3}{8}$, $\frac{3}{4}$ & $\frac{7}{8}$ inner helix layers.

The strength of adding the inner helix layers lies in the fact that the load is distributed in the layers, rather than all in the one outer helix. To continue the analysis, the best performing bridge in this section will be further analyzed using the member section steel calculations that can be performed in Robot.

The 65 by 130 foot radius model with the $\frac{3}{4}$ and $\frac{7}{8}$ inner helix had the lowest maximum dead load deflection in the previous analysis. Using this model and running the steel design calculations shows that approximately the same percentage of members do not pass the standards set forth in ANSI/AISC 360-05, which was about 50% for the 65 by 130 foot model with no inner helix. The exaggerated deflected shapes are shown in the figures below.

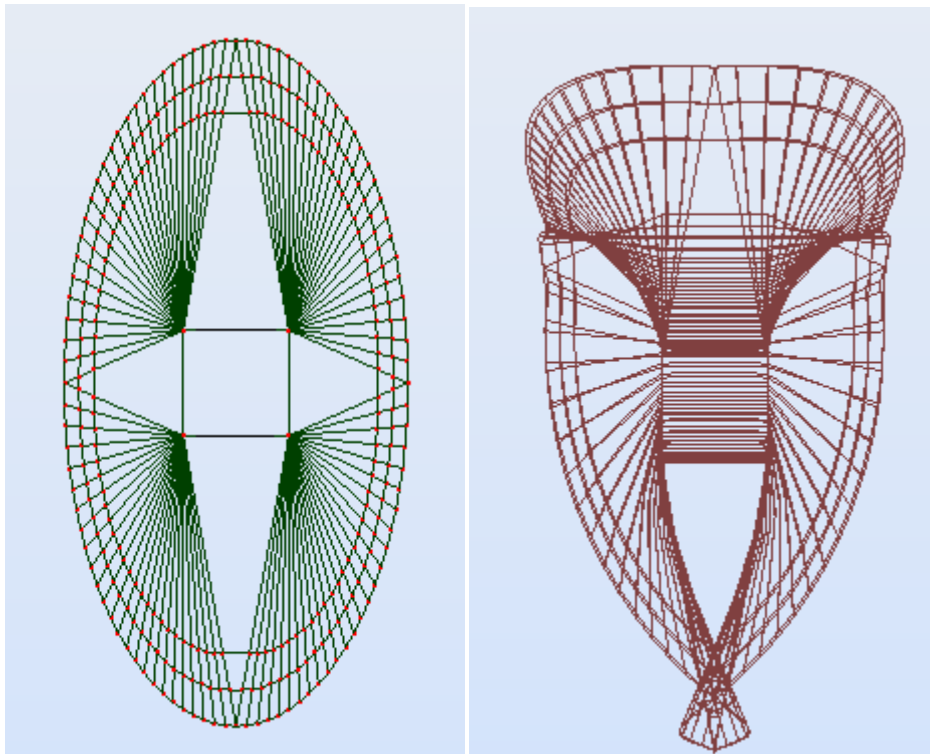


Figure 5.2.7 – Exaggerated deflected cross-section of 65 by 130 foot model with $\frac{3}{4}$ and $\frac{7}{8}$ inner helix layers.

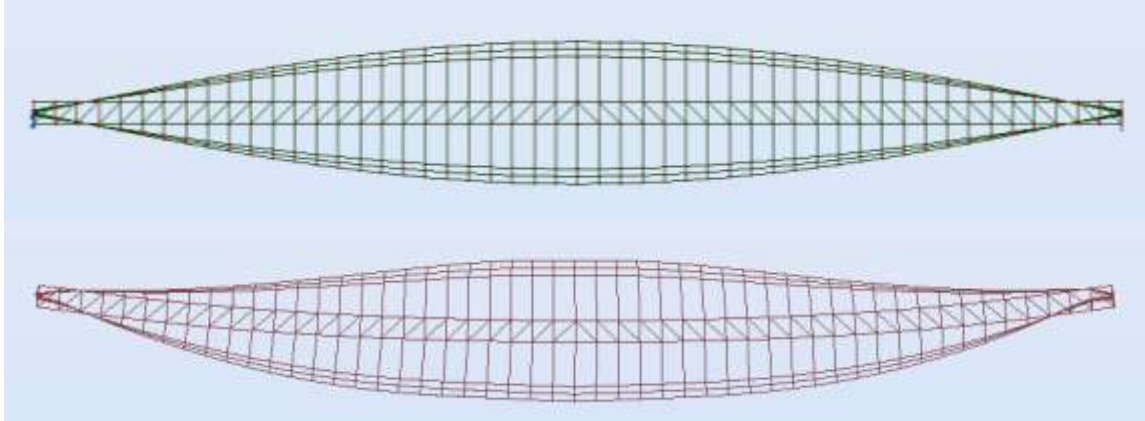


Figure 5.2.8 – Exaggerated deflected side view of the 65 by 130 foot model with $\frac{3}{4}$ and $\frac{7}{8}$ inner helix layers.

It can be seen in the deflected shape figures that the bridge is still deflecting in much the same way it was in the previous analyses. Though the magnitudes of the deflections are certainly lower, the ends are still thin and clearly susceptible to shear. The top helix still bows out and sinks, while the bottom helix sinks inward towards itself due to its own weight. The main problem is still the weakness in the way the deck is connected to the helix, which causes the structure to sag considerable under its own weight. If the helix was supported (connected to the deck) directly from below, it's self-weight would be distributed into that support, but that is not the case with this design, as the model is supported from the sides only, which is the biggest concern that must be addressed moving forward.

5.3 The Use of a Sloped Deck

Another alternative to reduce the load in the upper helix portion of the bridge model is to use the deck to take more of the compressive load. This can be done by arching the bridge deck upwards while leaving the helix in the same location. By arching the deck, it will help take and distribute some of the compressive forces to the ends of the bridge, which should reduce deflections and the stress in the main compressive helix.

The basic 40 foot bridge deck models will be used in this section, along with the best performing layered helix model, which is the $\frac{3}{4}$ & $\frac{7}{8}$ inner layered helix for both the 65 by 130 foot radius model and the 100 by 100 foot radius model. The sloped deck to be used in this section of the analysis will rise 40 feet to the center of the bridge, which gives a grade of 4%, well under the maximum allowable 6% determined for interstate highways by AASHTO. The results of this analysis are shown in the table below.

Table 5.3.1 - Maximum deflections for models with and without sloped decks								
	65 by 130 ft models				100 by 100 ft models			
Sloped Deck	N	Y	N	Y	N	Y	N	Y
Layered Helix	N	N	Y	Y	N	N	Y	Y
Max Dead Load Deflection (in)	223.2	300.0	156.2	219.4	304.7	375.0	215.2	266.4
Max Live Load Deflection (in)	25.7	33.1	12.4	16.2	38.0	43.5	20.0	22.2

As can be seen in the data, the sloped deck actually weakened the bridge, causing larger deflections than had been previously experienced. This could be due to the fact that the slope was a straight line, while the helix is curved, so they did not work together well enough. Using a deck with a curved arch would give better results, but the arch requires a greater slope in the sections near the end of the bridge. The figures on the following pages show the sloped deck bridge models.

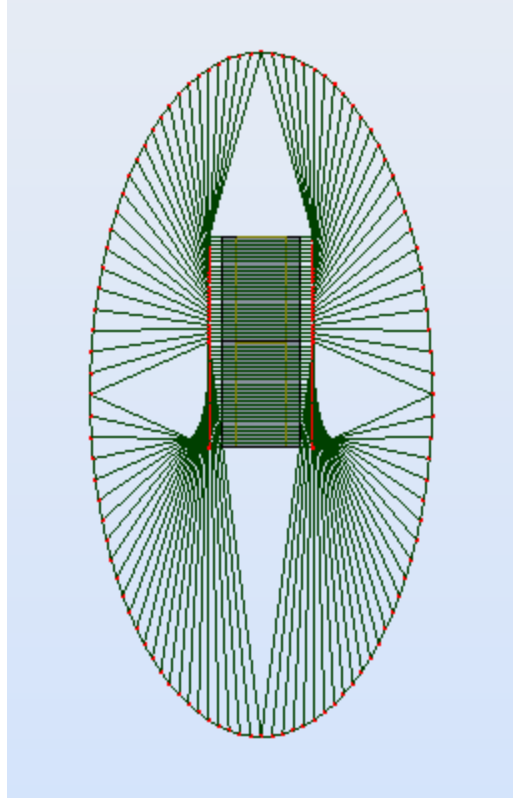


Figure 5.3.1 – Cross-section of the 65 by 130 foot radius model with the sloped deck.

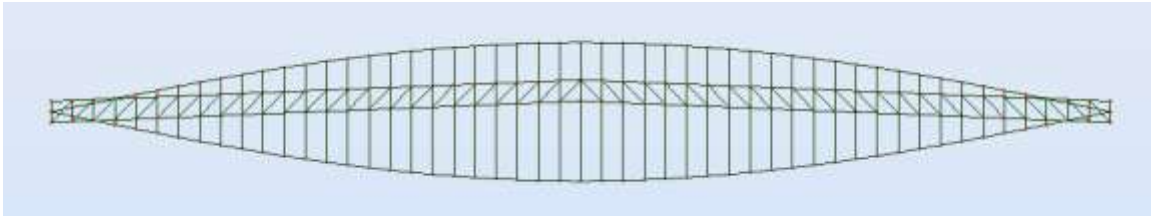


Figure 5.3.2 – Side view of the 65 by 130 foot radius model with the sloped deck.

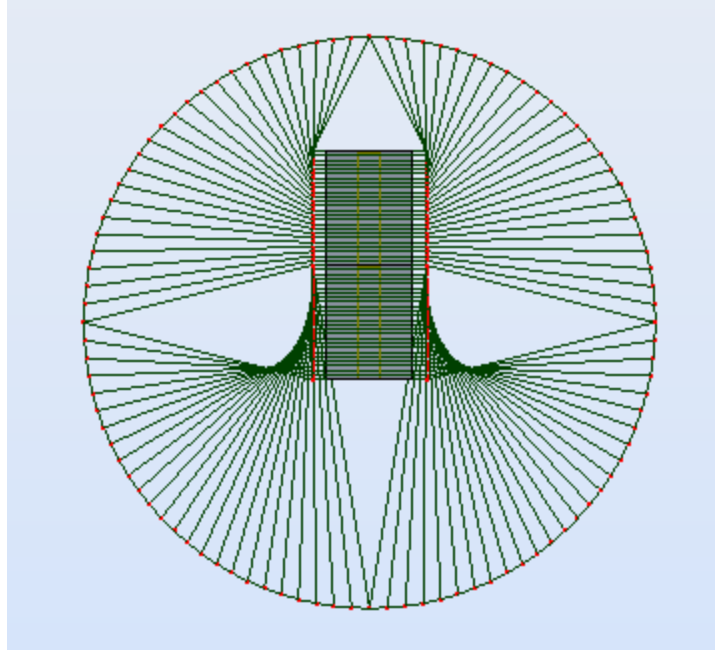


Figure 5.3.3 – Cross-section of the 100 by 100 foot radius model with the sloped deck.

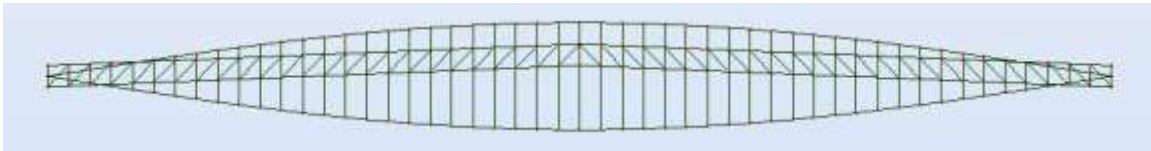


Figure 5.3.4 – Cross-section of the 100 by 100 foot radius model with the sloped deck.

5.4 Bracing the Helix Structure to Reduce Dead Load Deflections

Due to the manner in which every variation of the helix shaped bridge models have deflected, it is clear that the pure helix shape will require some structural modification in order to pass the more stringent tests. The main problem is that the weight of the outer helix structure sags significantly under its own self-weight, because of the way it is connected to the deck, which has proven to be not strong enough to support the structure without significant deflections. This problem is made clear in the figure below, which shows the 40 foot sections numbered 8 through 18 for the 100 by 100 foot radius model.

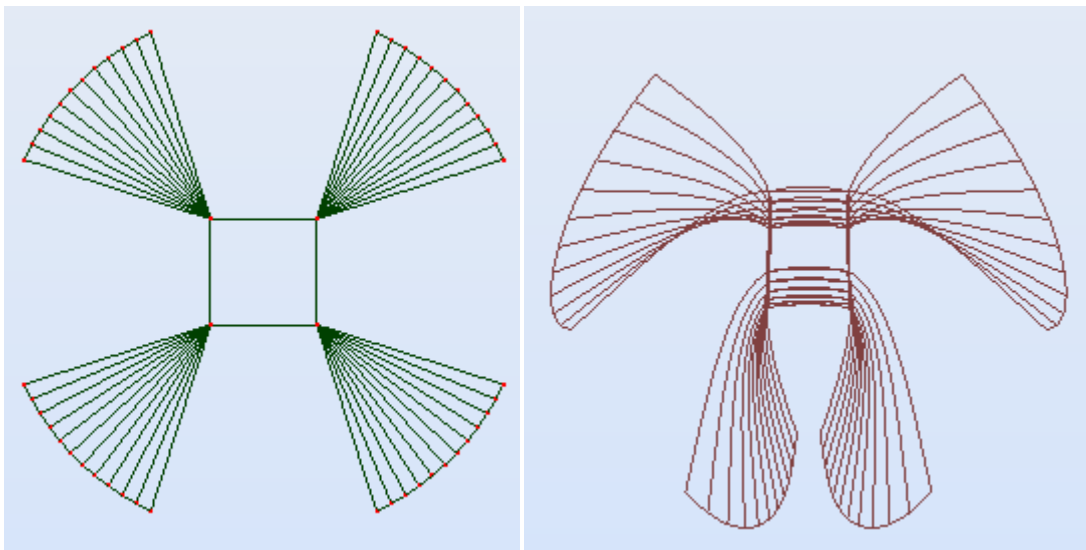


Figure 5.4.1 – Exaggerated deflected shape of sections 8 through 18 of the 100 by 100 foot radius model.

It is extremely clear in the image above that the outer helix structure is sinking severely under its own weight. This must be addressed before the members will begin to pass any of the tests performed in the calculations for ANSI/AISC 360-05, because the bridge is sagging so much under its own weight that the members are taking higher forces than if they were supported and connected in a more efficient manner. The next step is to

determine the type of bracing that is most helpful for the bridge, while not destroying its aesthetic qualities. The table below shows the results of various bracing tests on this abbreviated section of the bridge.

Table 5.3.1 - Maximum deflections for various bracing types for sections 8 through 18					
Bracing:	None	Side	Top & Bottom	Deck (center)	Deck (crossed)
Max Dead Load Deflection (in)*	61.4	78.1	21.9	15.2	16.1

*Please note that the deflection numbers in the models above are only for the abbreviated bridge, which only spans sections 8 through 18, or 440 feet, and that is why the values are so low compared to those in previous sections.

It is clear in the table above that the bracing can cause some significant improvement in the dead load deflections. The abbreviated 440 foot model experiences a maximum dead load deflection of 61.4 inches with no bracing, and it was reduced by approximately 75% by adding bracing that connects to the center of the deck at the sides, and approximately 66% by adding bracing on the top and bottom. Figures of the bracing are shown on the following page.

The side bracing actually makes the deflection worse, due to the fact that this bracing connects the sinking helix on the top of the bridge, directly to the sagging member on the bottom of the bridge, so not support is actually provided. The sinking members are just connected to each other, and the total dead weight is obviously increased, causing a higher deflection. The top and bottom bracing prevents the outward and downward sinking effect by bracing those members together. The outward deflection of the members on the right side of the bridge is canceled out by the outward deflection of the members on the left side of the bridge in this form. The deck connecting bracing examples worked the best, and they counter the vertical force by adding an extra (partially) vertical member, reducing the deflections significantly.

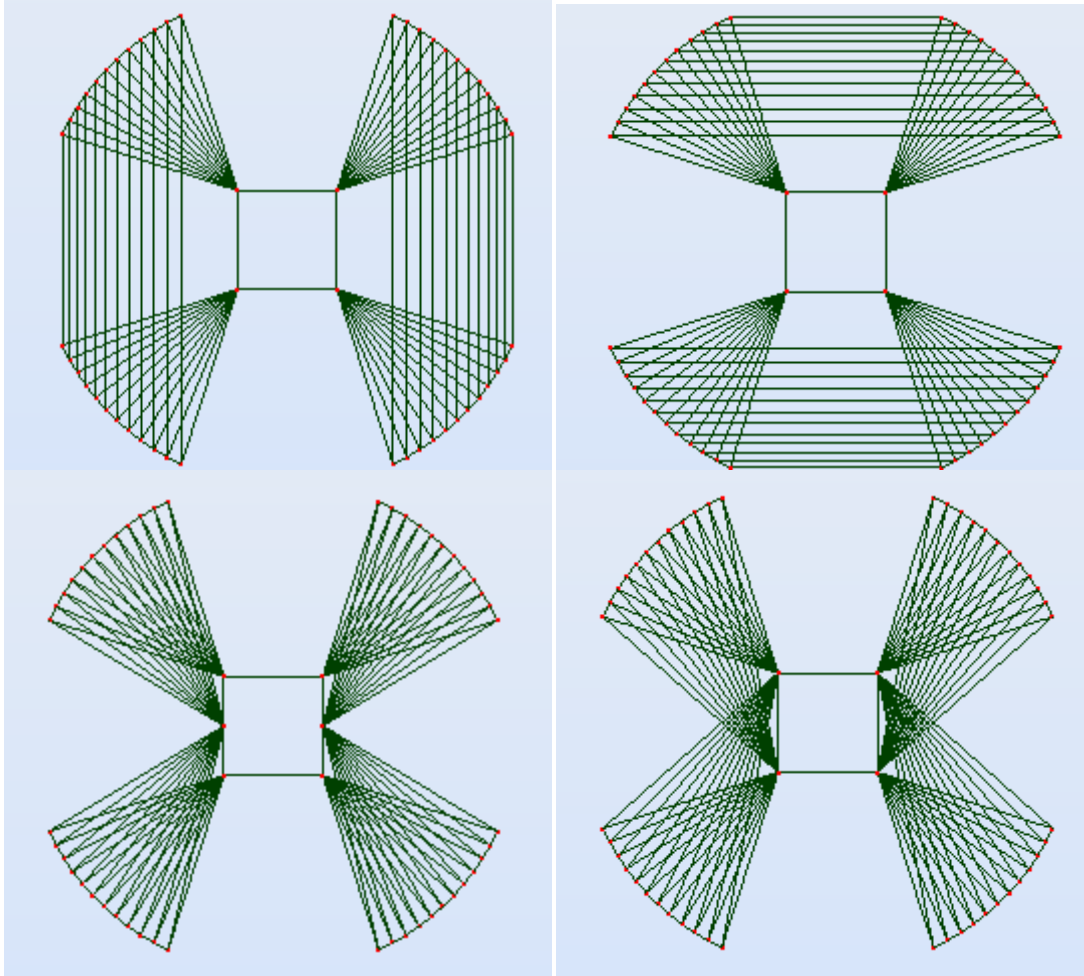


Figure 5.4.2 – Various bracing types, listed from top left to bottom right: Sides, Top & Bottom, Deck (center) and Deck (crossed).

The next step in this section of the analysis is to test the effect of the best bracing techniques on the full size models and measure the effects. The best performing model thus far, the 65 by 130 foot radius with $\frac{3}{4}$ and $\frac{7}{8}$ inner helix layers and a 40 foot box deck with no slope, will be used in this section of the analysis. The results of the two bracing types tested are shown in the table below.

Table 5.4.1 - Maximum deflections for various bracing types						
	65 by 130 ft $\frac{3}{4}$ & $\frac{7}{8}$ inner helix models			100 by 100 ft $\frac{3}{4}$ & $\frac{7}{8}$ inner helix models		
Bracing:	None	Top & Bottom	Deck (center)	None	Top & Bottom	Deck (center)
Max Dead Load Deflection (in)	156.2	123.1	147.0	215.2	223.4	229.4
Max Live Load Deflection (in)	12.4	10.2	10.8	20.0	19.2	17.5

The results shown in the table above are extremely interesting, as the models with top & bottom bracing perform better than the models with the bracing at the center of the deck, unlike what was found with the abbreviated bridge models. This is due to the fact that there is less total weight added by the top and bottom bracing, as there are fewer members added, so the stronger bracing method is seen to perform worse, as its dead weight outweighs its bracing efficiency. Another interesting result of the analysis is that the 100 by 100 ft models all have higher maximum dead load deflections when bracing is added. This shows the overall weakness of that version of the structure, as the added weight does not improve the deflections, when in the more efficient 65 by 130 models, it reduces deflection significantly. The cross-sections of the braced bridges are shown in the figures on the following page, and the negative aesthetic effects are clear.

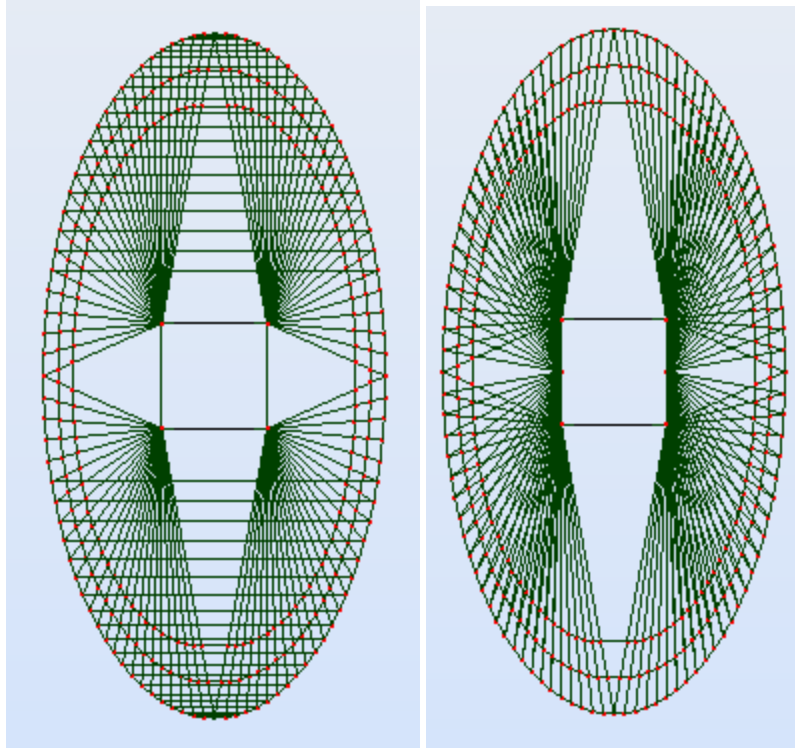


Figure 5.4.3 – Cross-sections of the 65 by 130 foot models with top & bottom bracing (left) and center deck bracing (right).

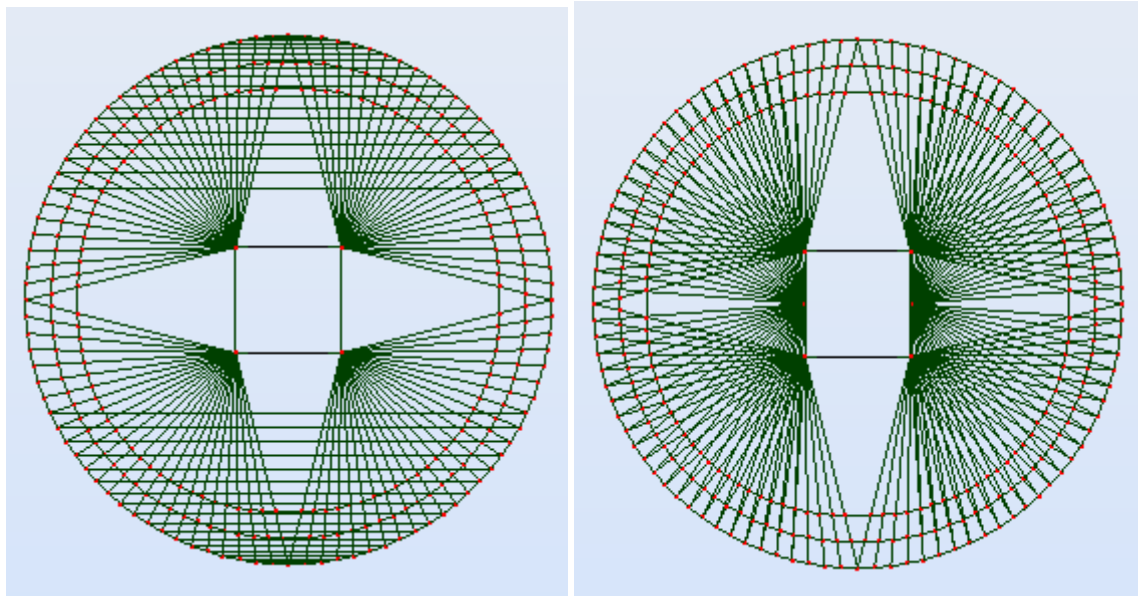


Figure 5.4.4 – Cross-sections of the 100 by 100 foot models with top & bottom bracing (left) and center deck bracing (right).

The top and bottom bracing clearly improved the most efficient model significantly. The best performing model to this point in the analysis now contains the following variables:

- 65 by 130 foot radii
- 22.5 inch diameter circular steel members with a yield strength of 36 ksi
- 40 foot thick box deck with no slope
- $\frac{3}{4}$ and $\frac{7}{8}$ inner helix layers
- Top and bottom bracing

When the steel section calculations are performed on this model, the results show that approximately 45% of the members are still not passing the parameters set forth in ANSI/AISC 360-05. Although the shape has been optimized, there are still significant issues pertaining to the individual members, which means that the next step in the analysis must be to alter the member sections and materials in order to pass the code standards. An isometric view of the bridge listed above can be found on the following page.

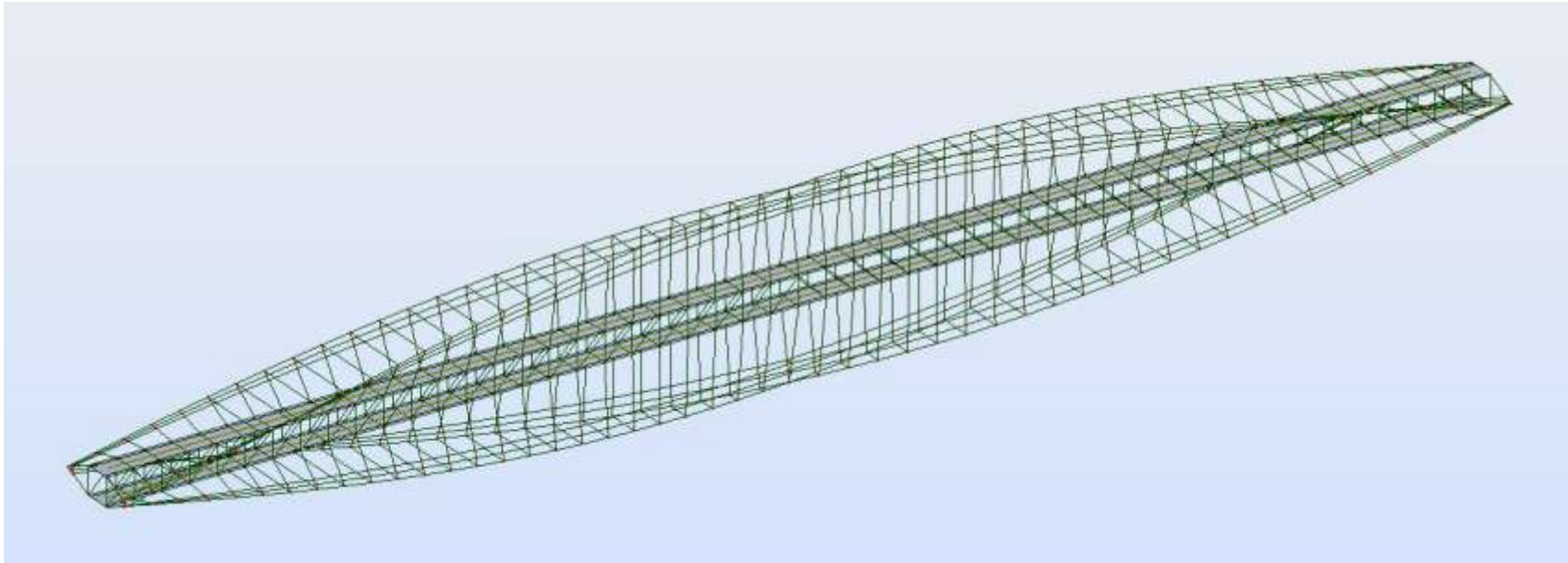


Figure 5.4.5- Isometric view of the most efficient helix bridge shape with bracing.

6.0 Optimizing the Individual Steel Members

The individual steel members for the most efficient helix shaped model are not strong enough to pass the tests performed using the code standards in ANSI/AISC 360-05. Although the dead load deflections have been reduced significantly to manageable levels (10 feet of deflection over a 2000 foot span can be constructed for using pre-cambering techniques), they are still causing enough deflections so that the members are failing. The live load deflections have also been reduced to approximately 10 inches, which is well under the allowable maximum of 30 inches for a 2000 foot span, but the model is still unable to pass the more stringent tests, and a second order analysis has not even been performed to this point.

The first step in improving the strength of the steel is to increase its yield strength. This will not change the live or dead load deflections in any way, but it will improve the performance of the individual members against the steel section code tests calculated by Robot for ANSI/AISC 360-05. This is because the deflections are dependent on the modulus of elasticity of the steel, which is 29×10^6 psi for all steel, as discussed in an earlier section. The individual member strength is dependent on the yield strength of the steel, as each member is individually checked based on its material and size properties.

The previous most efficient model was created using 22.5 inch solid circular members with a yield strength of 36 ksi. Approximately 45% of the members could not pass the standards calculated for in ANSI/AISC 360-05. When the material is changed to a higher strength steel, a vast improvement can be seen. The maximum available yield strength for the materials available in Robot is 105 ksi, which is often used in the cables of long span bridges. When the members are switched to the 105 ksi steel, only about

20% of them fail to pass the ANSI/AISC 360-05 calculations, meaning that 20% of them have an efficiency rating of greater than 1. This is a significant improvement, and the 105 ksi steel will be used as the material for the models for the rest of the analysis. 105 ksi steel is typically only used in high strength cables, but it will be used for the duration of this analysis, though the final models will be rechecked using steel using lower yield strengths. Though the steel strength has been improved, there is still clearly a major issue with the individual member failures against the code calculations, so the next step in the analysis will be to optimize the member section shapes.

6.1 Optimizing the Member Sections

In the previous sections, the shape of the helix bridge was optimized in order to reduce dead load deflections down to a manageable value. The next step is to further reduce the deflections by optimizing the member sections. The member section used until this point in the analysis was a 22.5 inch diameter solid circle in cross-section, but this is clearly not strong enough to pass the next levels of the analysis. Various members sections were tested using the most efficient bridge model to this point in the analysis, and the results are shown in the tables below:

Diameter (in)	22.5	24	24	48	48
Wall Thickness (in)	Solid	Solid	6	Solid	12
Cross-sectional Area (in ²)	397.6	452.4	339.3	1809.6	1357.2
Max Dead Load Deflection (in)	123.1	122.0	120.2	113.5	112.6
Percentage of members failing ANSI/AISC Code tests	20%	20%	10%	0.60%	0.60%

Width & Height (in)	24	24	48	48
Wall Thickness (in)	Solid	6	Solid	12
Cross-sectional Area (in ²)	576.0	432.0	2304.0	1728.0
Max Dead Load Deflection (in)	119.9	118.4	112.4	111.6
Percentage of members failing ANSI/AISC Code tests	10%	6%	0.50%	1.50%

Both circular and square sections were tested, as shown in the tables above. The best overall performance came from the largest square cross-sections, which had the lowest dead load deflections, and the lowest percent of member failures. The first interesting point of note is that increasing the member cross-section size does automatically imply significantly better results. Though the dead load deflections went down when the

diameters and square sides were doubled, they did not decrease very much. This simply shows that a balance between increasing the size and decreasing the self-weight needs to be found. Another observation from the results of these calculations is that the non-solid member performed noticeably better than their solid counterparts. The members listed in the table with a “wall thickness” are pipes or tubes, which have hollow centers. This is a way to find a balance between decreasing the self-weight and designing against buckling. As discussed in an earlier section, a member with a higher of gyration is less likely to buckle. By using a tube cross-section, the member will have a lower self-weight than a solid member of the same outer cross-section dimensions, but a higher radius of gyration than a solid member with the same cross-sectional area. By using this balance, a more efficient member section design can be found.

Using the member section analysis that was just discussed, the next step is to see if all of the members need to be the same section. It is clear that forces distribute differently in members throughout the bridge, as the members making up the main compression helix take a much greater axial load than any other members in the bridge. For example, in the model using a tube cross-section with a square side of 24 inches and a wall thickness of 6 inches, the member with the highest axial force is the member in the main outer helix that connects the first section of the bridge to the pin connection at the end. The axial force in this member is 32,248.75 kips. A member with very little force can be found at the 160 feet from the center of the bridge on top level of the deck, and it experiences an axial force of 0.96 kips. The difference is massive, and this leads into the next part of the optimization. The figures on the next page show the highest and lowest stressed member on the bridge.

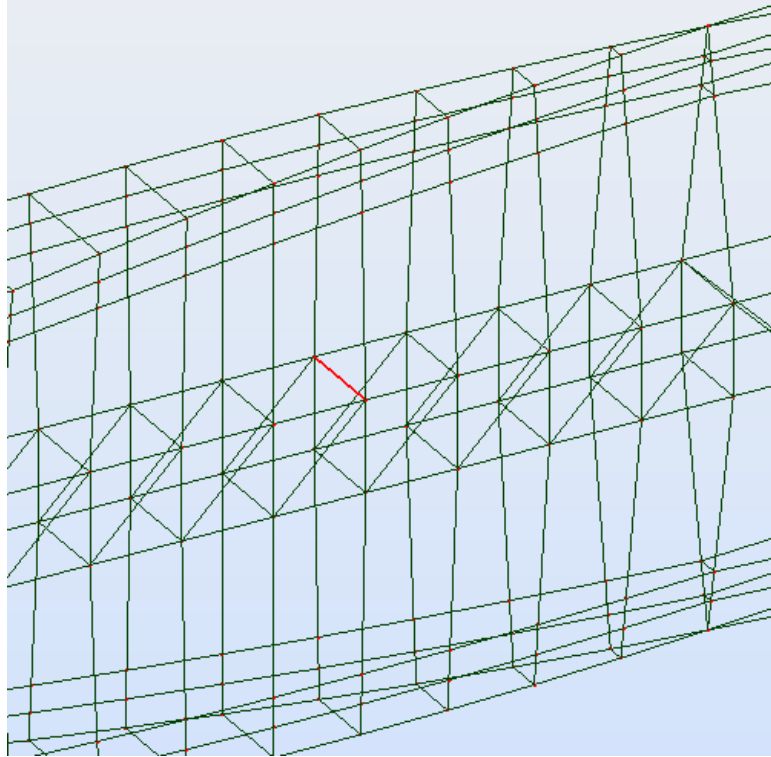


Figure 6.1.1 – The member with the lowest axial force (highlighted in red).

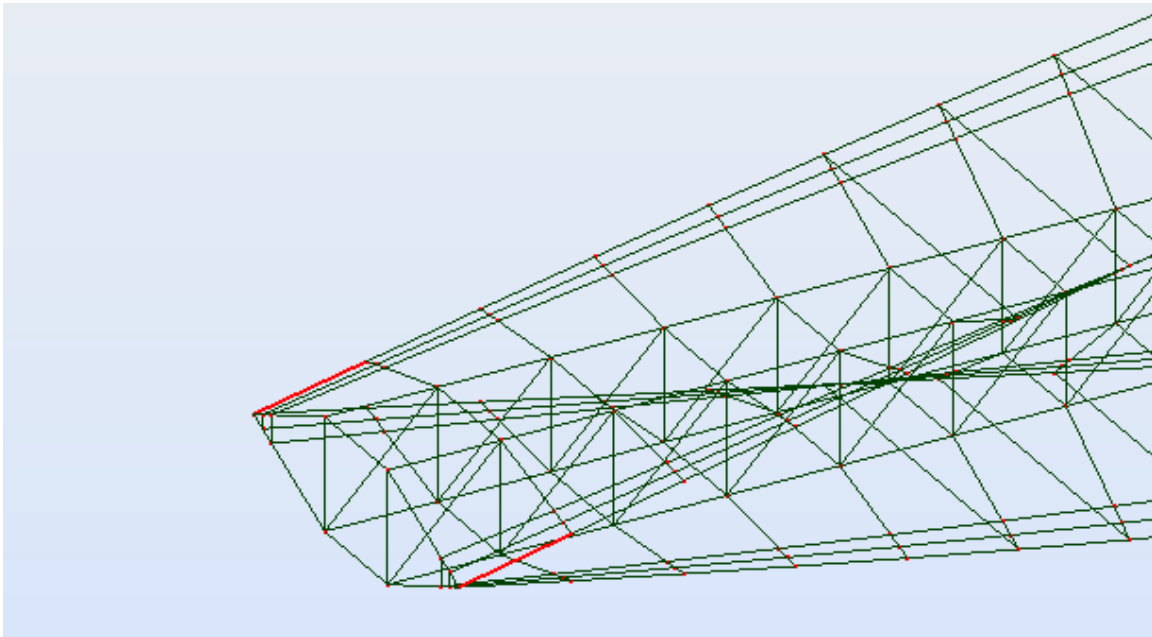


Figure 6.1.2 – The members with the highest axial forces (highlighted in red).

Rather than change the section of each member individually, two of the earlier member sections will be used in one design to test the effect of increasing the sections where the forces are greatest. The outer helix experiences the most force, and therefore is given the 48 inch square tube cross section with a wall thickness of 12 inches, while every other member in the bridge will be the smaller tube cross-section, the 24 inch square with a wall thickness of 6 inches. When the analysis is run with this combination, the change in the results is drastic. The maximum dead load deflection is reduced to 72.1 inches. Out of the 1808 of the members in the bridge, 12 of them have efficiency ratios of greater than 1 in the ANSI/AISC 360-05 steel section calculations, which is still approximately 0.70%, but all of the members that do not pass code are 24 inch tubes, the entire outer helix passes the member tests.

In order to get all of the members to pass the code tests, they are individually found and switched to 48 inch square tube cross-sections. The failing members were the 24 inch cross-sectional tubes that were closest to the supports, where the forces were most concentrated. When these members are switched to 48 inch square tubes, every member in the model passes the ANSI/AISC 360-05 steel section calculations. These calculations only cover the first order dead load case, and the next step is to get the model to pass the second order analysis.

6.2 Failure in the Second Order Analysis

The second order non-linear analysis tests the model by adding the load to the bridge in increments. The standard procedure is to test the bridge in five increments, 20%, 40%, 60%, 80% and 100%, which Robot performs through its non-linear analysis option. This test most importantly tests for major changes in shape that are not recovered from when the design is loaded in separate increments, and a failure of the second order analysis implies that the bridge model is most likely experiencing buckling.

Using the model that passes the first order tests and running a second order analysis shows that the model is not strong enough. The model only makes it through the first two iterations (20 % and 40%) before the analysis begins to show failure. When the analysis is performed by Robot, it loads and unloads in the previously stated increments, if the model passes, the deflection values for the second order analysis will be less than those of the first order analysis. If it fails, it is implied that greater deflections were being experienced. In the analysis itself, a graph is shown, and when each iteration is run, the graph will converge or an error will appear after multiple failures: “No convergence of nonlinear problem”. Because this error appears after only two iterations of five, it is clear that this model is not nearly strong enough to pass the second order tests.

Further optimization of the shape is clearly required, as increasing the member sections infinitely is not a reasonable solution. The exaggerated deflected shape of the model that passes the first order tests is shown on the following page, and a closer look into that shape is vital to the next phase of the optimization.

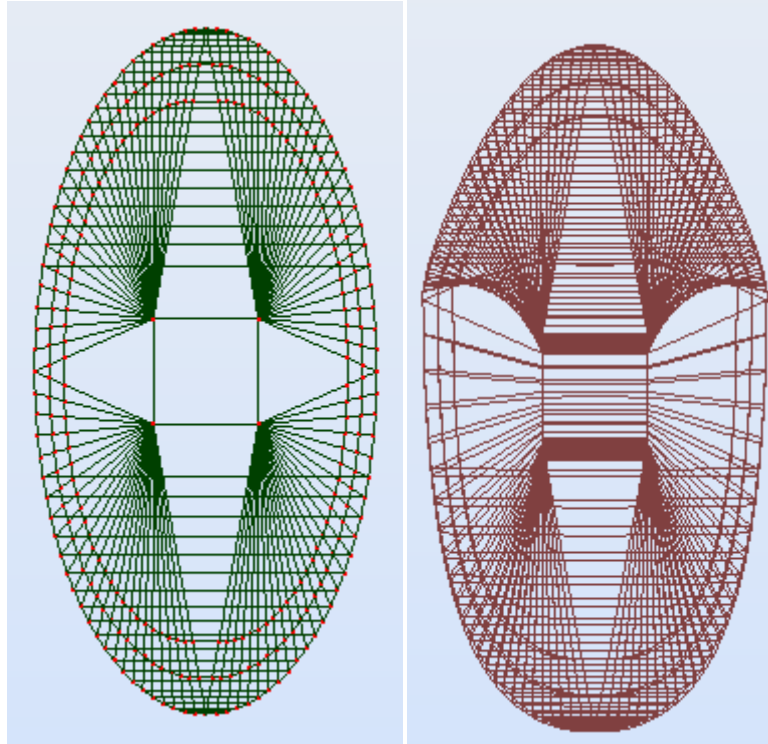


Figure 6.2.1 – Cross-section of the exaggerated deflected shape that passes the first order analysis, but fails the second order analysis.

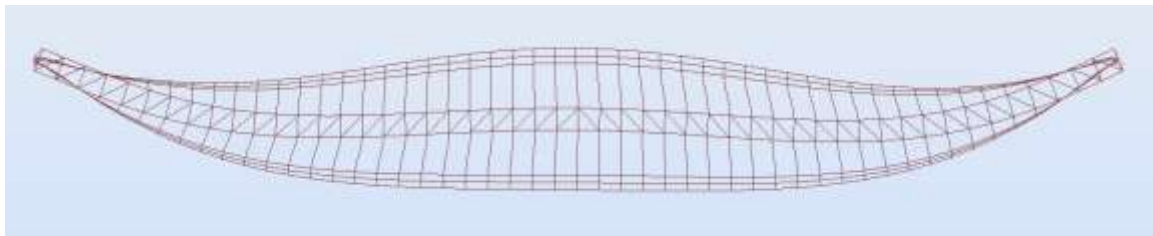


Figure 6.2.2 – Side view of the exaggerated deflected shape that passes the first order analysis, but fails the second order analysis.

It is clear from the figures above that the bridge is deflecting in only one of the two ways that had been experienced in earlier analyses. The sagging or sinking that was being experienced in the outer helix due the dead load has been essentially eliminated by the bracing and the increase in the strength of the outer helix members. The other way in which the bridge is deflecting had not changed, as there is clearly shear being

experienced near the ends of the bridge. This is still due to the excessive thinness of the model towards its ends, a problem that hasn't been addressed to this point. It can be seen in the side-view that the bridge still deflects significantly at the ends, and barely at all towards the strong center. This is still due to the fact that the helix rises at its highest point above the bridge at the center, easily taking the high tension and compression forces, but they are distributed to the ends of the bridge into an area that is very thin and extremely susceptible to shear. The optimization process up to this point maintained the helix shape with only minor bracing, but the helix shape is clearly not strong enough to resist the shear at the ends of the bridge, so further modifications must be made.

7.0 Optimizing Alternative Designs to Pass Second and Third Order Analyses

Though the basic helix structure was able to pass the first order analysis tests, it is unable to pass the second and third order tests that are required for real-world usability. An alternative design will be required in order to pass these more stringent non-linear tests, and it clearly must address the main problem with the basic helix design, which is shear at the ends of the bridge. Another equally important requirement is that the bridge design must maintain the aesthetic integrity of the original helix design. The main purpose of the analysis is to create a bridge that performs to standards structurally, but also utilizes the aesthetic benefits of the curved helix shape, so any alternative design must maintain these ideals.

7.1 Alternative Approaches to Reduce Shear: 2-D Line Models

The main problem to this point in the analysis has been determined to be the shear forces experienced in the bridge models near the supports. The deflections experienced by the bridge as a whole have been seen mostly in the ends of the bridge, with only minor deflections in center sections, where the model is strongest. This is due to the thinness of the bridge, and the lack of strength that goes along with it, at the ends of the bridge near the supports. To further study, and try to negate the shear forces, a series of line models will be analyzed.

The line models look the same as the previous bridges from a side-view in the y-z plane (along the 2000 foot length), but in the x-z plane, they are just a straight line, instead of the earlier full-radius models. These 2-D models obviously aren't capable of carrying traffic, but studying the shape will help with the progression of the analysis. Two variations are used in the following analysis. The first is the use of diagonals in the models, as pictured on the following pages. The other is to use the parabolic moment equation to design the outer structure of the bridge, rather than the helical sine curve. The bridge outer "helix" structure follows the parabolic moment equation discussed earlier, which is the most efficient shape for distributing the load in the y-z plane.

	Helical side-view models				Parabolic side-view models			
	100 foot height		120 foot height		100 foot height		120 foot height	
Diagonals	N	Y	N	Y	N	Y	N	Y
Max Dead Load Deflection (in)	137.0	105.9	132.5	79.5	115.3	94.4	107.2	71.4

As can be seen in the results above, adding diagonals and using the parabolic equation help reduce the dead load deflections drastically. The use of the parabolic equation

strengthens the ends of the bridge near the support, as the outer structure rises quicker towards the middle. For the 100 foot height helix shaped bridge, the first section rises 6.28 feet from the end support to the start of the second section. For the 100 foot parabolic shaped bridge, the first section rises 7.84 feet, which strengthens the ends of the bridge, where the shear is greatest. The table on the following page shows the Z-values of the outer structure for the four line models tested on the previous page. As can be seen in the table, the parabolic shape increases towards its maximum height at the center ($y=1000$ feet) from the edges of the bridge ($y=0$ feet) much quicker for the parabolic shaped models than for the helix shaped models. This increased rise from the edges greatly reduces the deflections, as the helix shaped 100 foot height model has a maximum dead load deflection of 137.0 inches, while the 100 foot height parabolic shaped model has a maximum dead load deflection of 115.3 inches, which is almost 20% less, a major reduction. All of the 2-D models used 48 inch square tubes with 12 inch wall thickness members (in cross-section) for the outermost part of the structure, while the rest of the connecting members are 24 inch square tubes in cross section with 6 inch wall thicknesses.

The next part of the analysis is to look at the effect of the diagonals in the 2-D line models. As can be seen in the results on the previous page, the diagonals drastically reduce the maximum dead load deflections in each model. This is due to the fact that the diagonals help take and distribute the shear forces at the ends of the bridge. This increase in structural strength is readily apparent for the 2-D line models, but it must be noted that diagonals will be troublesome to use in a 3-D model, while the diagonals also take away from the models aesthetically. Images of the 2-D line models can be found on the

following pages. The reduced effect of shear forces is extremely noticeable in the deflected shapes of the models with diagonals. These models are seen to deflect naturally throughout the bridge, rather than excessively near the supports, unlike the other models.

Table 7.1.2 - Bridge outer structure height values for helical and parabolic shapes				
Y-values (ft)	Helix Models		Parabolic Models	
	Z-values for 100 foot height (ft)	Z-values for 120 foot height (ft)	Z-values for 100 foot height (ft)	Z-values for 120 foot height (ft)
0	0.00	0.00	0.00	0.00
40	6.28	7.53	7.84	9.41
80	12.53	15.04	15.36	18.43
120	18.74	22.49	22.56	27.07
160	24.87	29.84	29.44	35.33
200	30.90	37.08	36.00	43.20
240	36.81	44.17	42.24	50.69
280	42.58	51.09	48.16	57.79
320	48.18	57.81	53.76	64.51
360	53.58	64.30	59.04	70.85
400	58.78	70.53	64.00	76.80
440	63.74	76.49	68.64	82.37
480	68.45	82.15	72.96	87.55
520	72.90	87.48	76.96	92.35
560	77.05	92.46	80.64	96.77
600	80.90	97.08	84.00	100.80
640	84.43	101.32	87.04	104.45
680	87.63	105.16	89.76	107.71
720	90.48	108.58	92.16	110.59
760	92.98	111.57	94.24	113.09
800	95.11	114.13	96.00	115.20
840	96.86	116.23	97.44	116.93
880	98.23	117.87	98.56	118.27
920	99.21	119.05	99.36	119.23
960	99.80	119.76	99.84	119.81
1000	100.00	120.00	100.00	120.00

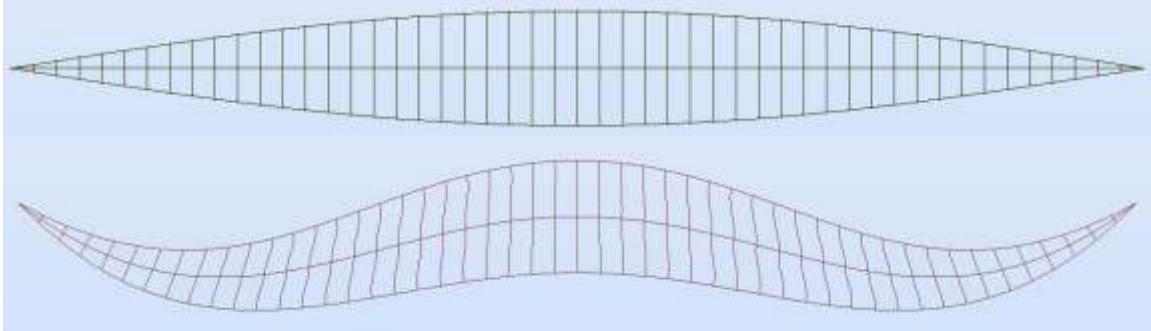


Figure 7.1.2 – Side-view of the 100 foot height helix 2-D model and exaggerated deflected shape. The equation for the outer top (and bottom) members follows the previously discussed sine curve, and severe shear effects are noticeable.

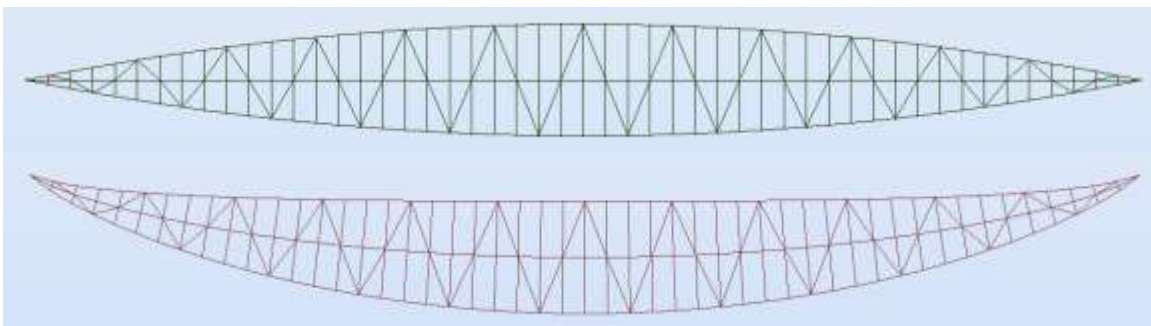


Figure 7.1.3 – Side-view of the 100 foot height parabolic 2-D model with diagonals and exaggerated deflected shape. The equation for the outer top (and bottom) members follows the previously discussed parabolic moment equation, and shear effects are negligible, the bridge sags naturally.

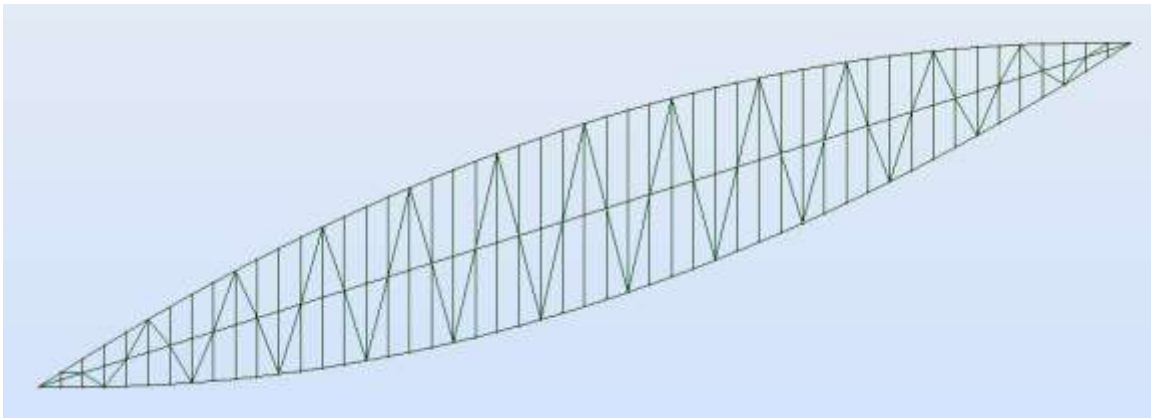


Figure 7.1.3 – Isometric view of the 100 foot height parabolic 2-D model with diagonals

7.2 Alternative Approaches to Reduce Shear: 3-D Models

In the previous section, the effect of using the parabolic moment equation and the effect of diagonals were both studied and seen to reduce the maximum dead load deflections in the 2-D line models drastically. The next step is to apply these theories into 3-D space, which is to essentially abandon the use of the pure helix shape for one that has more structural integrity.

Since the helix shape will not be used for the 3D models created in this section, there is no need to use the sine or cosine equation for the X or Z-values used in the design of the previous bridge models. The bridge models in this section will continue to use the parabolic shape for the Z-values (following the parabolic moment equation in side-view, like the better performing 2-D models), while the X-values will follow the equation of a straight line (which will draw out an “X” when viewed from above). All of the models in this section have a 40 foot deck with no slope and use 48 inch square tubes with 12 inch wall thickness members (in cross-section) for the outermost part of the structure, while the rest of the connecting members are 24 inch square tubes in cross-section with 6 inch wall thicknesses. 3-D models using the parabolic arc in the Y-Z plane and straight line in the X-Y plane were tested with and without diagonals. The models in the table of results on the following page include a 100 foot width by 100 foot height model with and without diagonals and a 65 foot width by 100 foot height model with and without diagonals. The width and height mentioned are just the starting X-value at the ends of the bridge (the distance from the center of the deck to the end support), and the height is the maximum Z- value at the center of the bridge above the center of the deck.

Table 7.2.1 - Maximum deflections for parabolic arc model variations				
	100 ft by 100 ft		65 ft by 130 ft	
Diagonals	N	Y	N	Y
Max Dead Load Deflection (in)	128.5	121.3	81.1	79.8

None of the models in the table above were able to pass a second order analysis, but the reduction in first order dead load deflections is very noticeable. Compared to the 65 by 130 foot helix model with a 40 foot deck and no bracing, the parabolic 65 by 130 foot model performs substantially better. The aforementioned helix model had a maximum dead load deflection of 104.4 inches, while the parabolic model has a maximum dead load deflection of 81.1, a significant improvement.

Although there is not a major difference aesthetically between the 2 models, it is very clear that the helix model is significantly weaker. This further proves the inefficiencies that were being experienced with the models created earlier in the analysis. The images on the following pages show various views of the models using the parabolic equation shown in the data above.

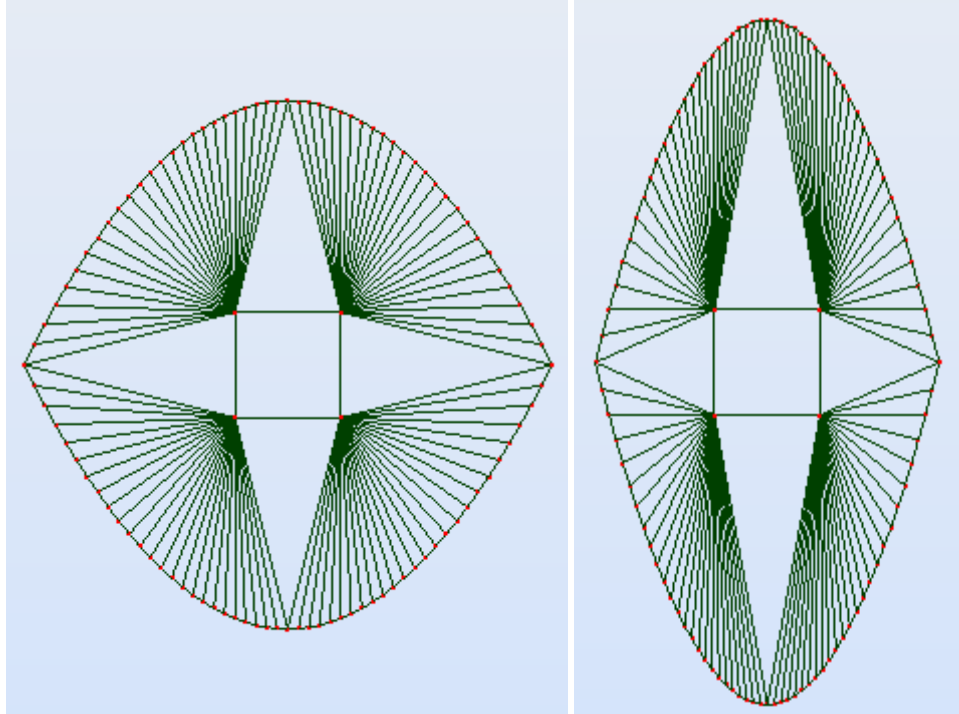


Figure 7.2.1 – Cross-sections of the 100 foot width by 100 foot height (left) and 65 foot width by 130 foot height (right) models that follow the parabolic moment equation.

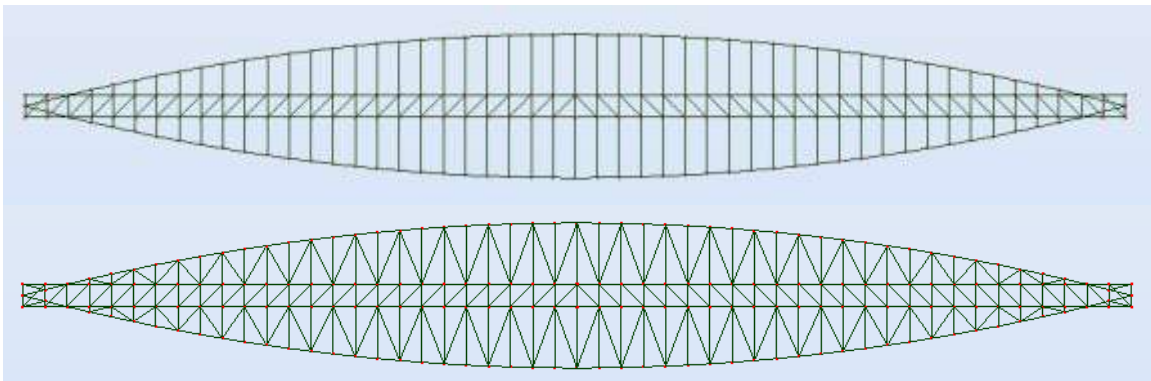


Figure 7.2.2 – Side-views of the 65 foot width by 100 foot height parabolic models with and without diagonals. The outer curve follows the parabolic moment equation.

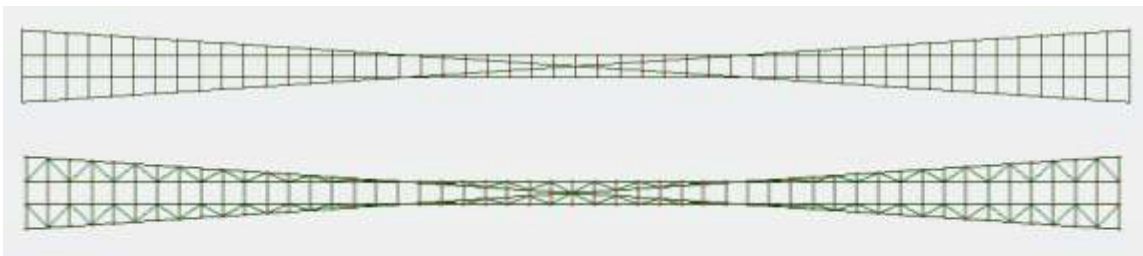


Figure 7.2.3 – Top views of the 65 foot width by 100 foot height parabolic models with and without diagonals. The outer curves follow a straight line path from above.

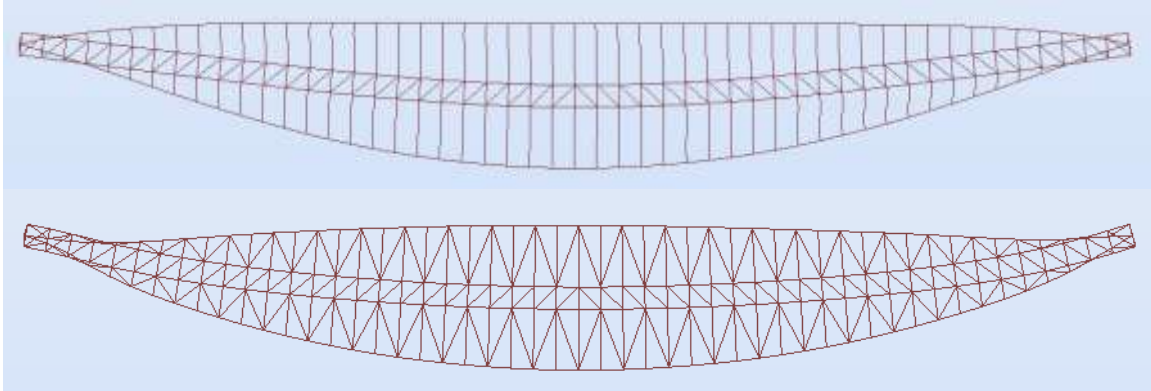


Figure 7.2.4 – Side-views of the exaggerated deflected shapes of the 65 foot width by 100 foot height parabolic models with and without diagonals. As can be seen, the model with the diagonals deflects more naturally due to gravity as the shear forces at the ends are better resisted

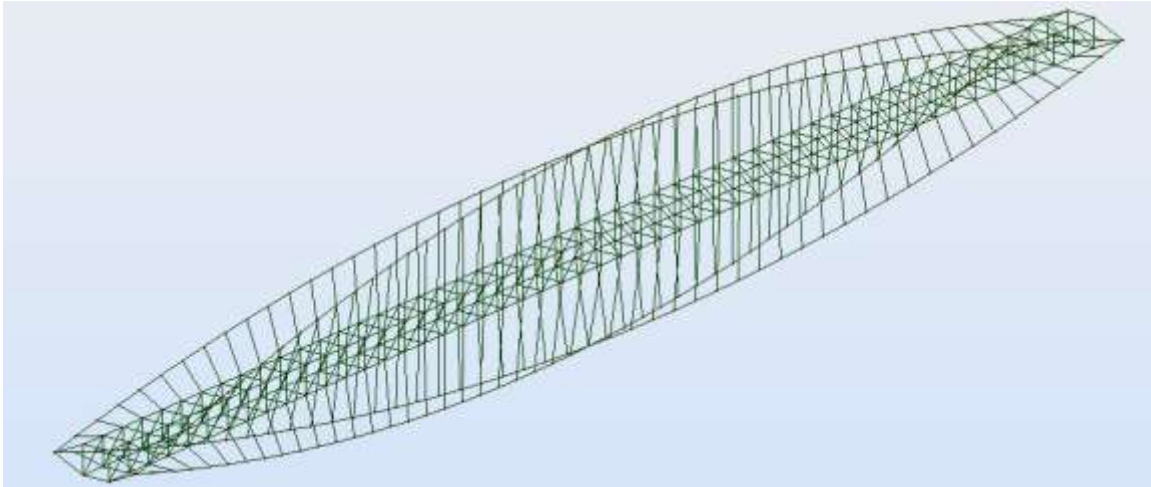


Figure 7.2.5 – Isometric view of the 65 foot width by 100 foot height parabolic model without diagonals.

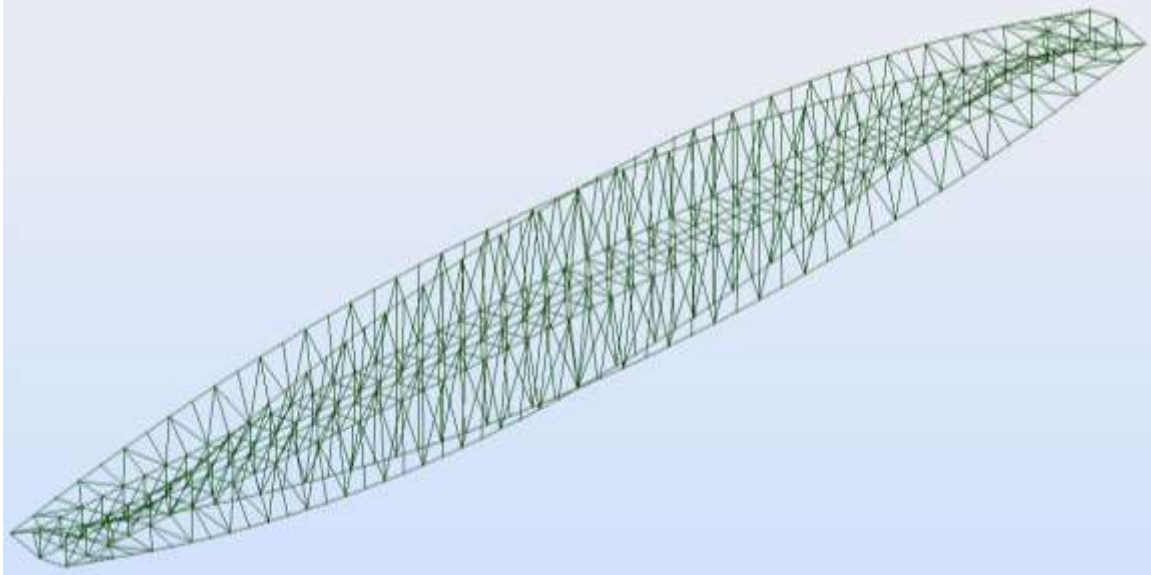


Figure 7.2.6 - Isometric view of the 65 foot width by 100 foot height parabolic model with diagonals.

As can be seen in the figures, the cross-section no longer makes the shape of the aesthetically desired circle or ellipse. It is also clear that the diagonals severely impact the aesthetics of the bridge design, giving them an almost cluttered feel.

To show the differences between the helix shaped models and the parabolic shaped models that follow straight line paths from above, a series of images will be used to display the differences. In general, they have the same overall dimensions and can fit into the same envelope, but the parabolic model (65 by 130 with no diagonals) has a maximum dead load deflection of 81.1 inches, while the 65 foot by 130 foot helix model with no bracing or layering deflects a maximum of 104.4 inches, or about 25% more.

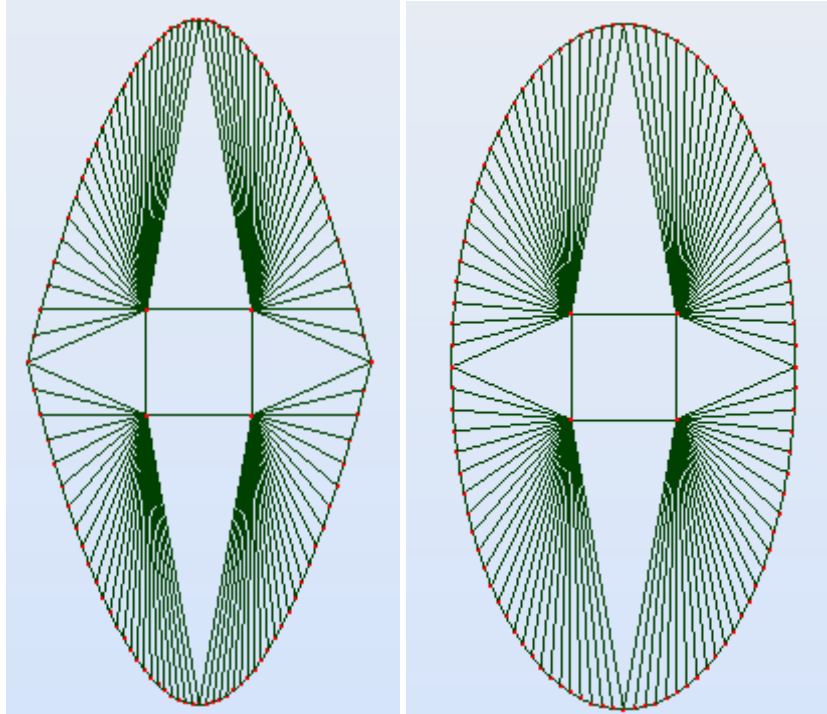


Figure 7.2.7 – Cross-sections of the parabolic (left) and helical (right) shaped models.

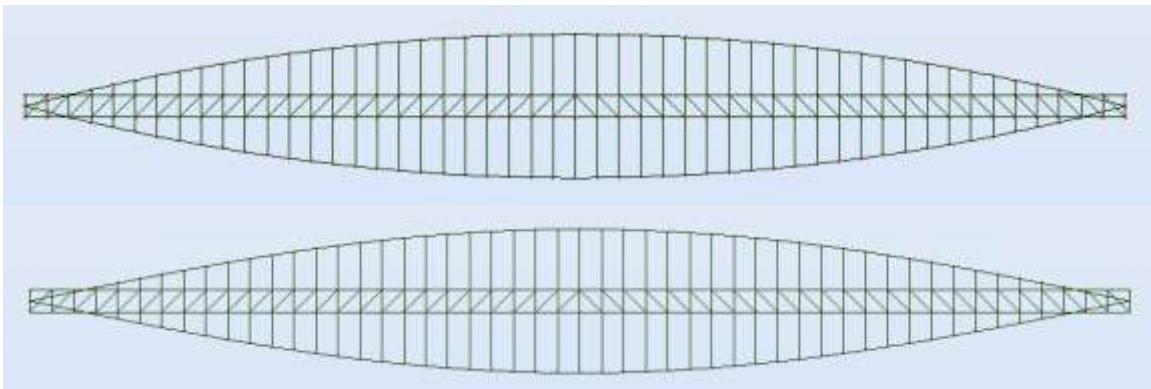


Figure 7.2.8 – Side-views of the parabolic (top) and helix (bottom) shaped models.

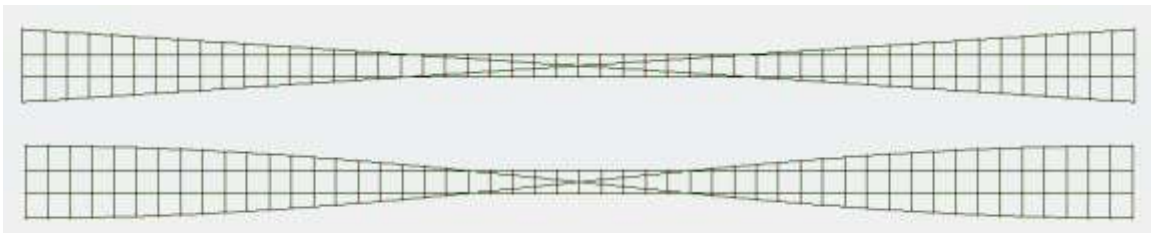


Figure 7.2.9 – Top-views of the parabolic (top) and helix (bottom) shaped models.

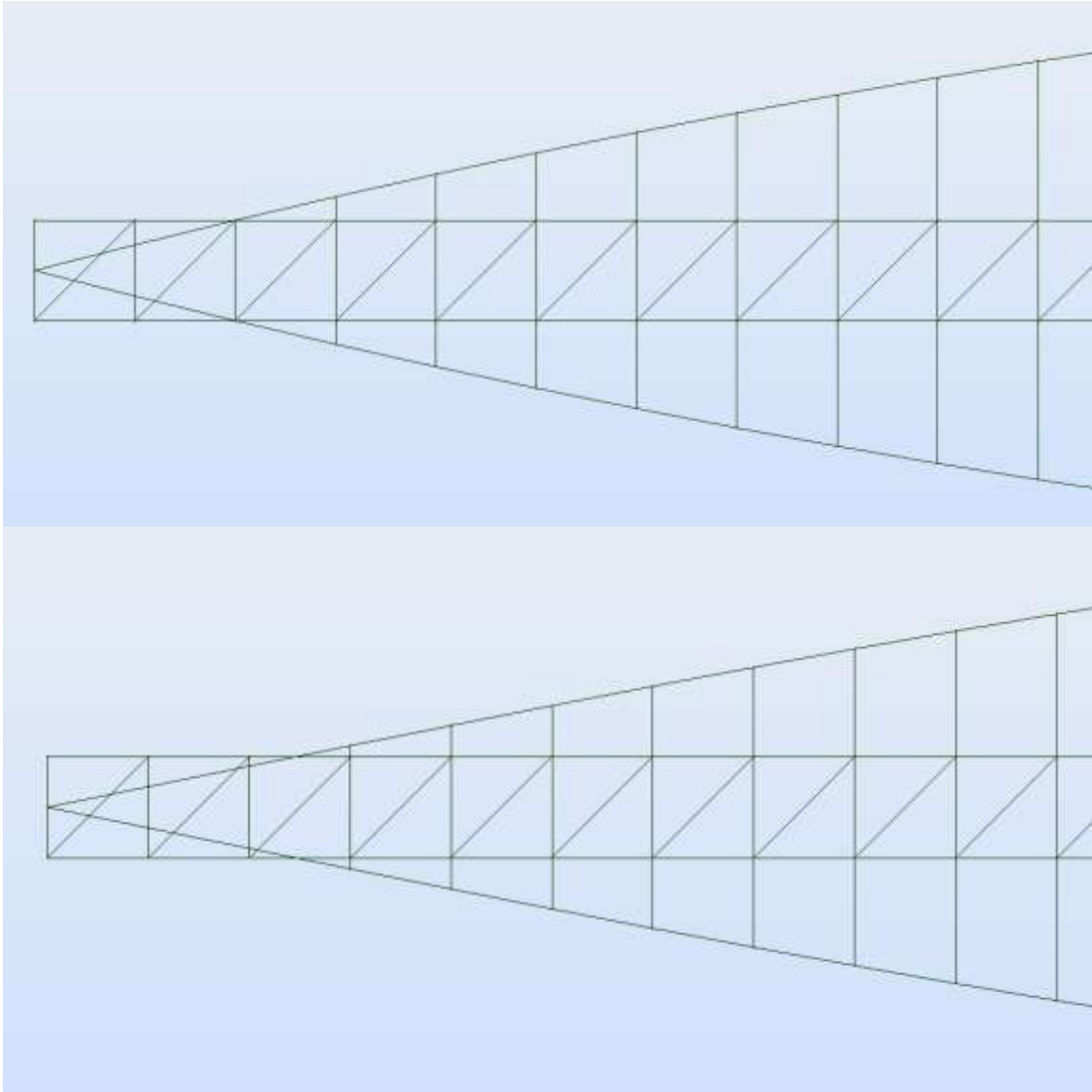


Figure 7.2.10 – Enlarged side-views of the first sections of the parabolic (top) and helix (bottom) shaped models. As can be seen, the height of the outer curve in the parabolic model increases quicker from the end supports towards the middle, and this makes the ends more resistant to shear.

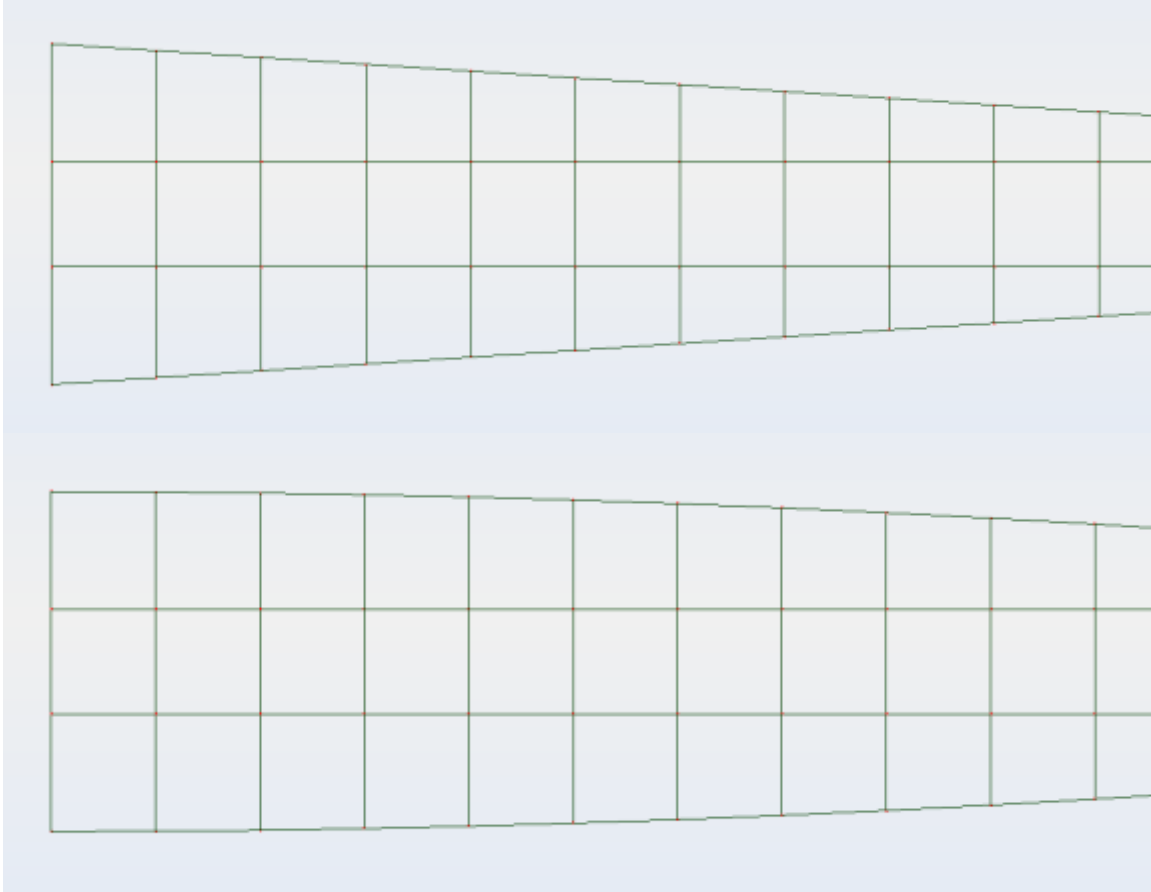


Figure 7.2.11 – Enlarged top-views of the first sections of the parabolic (top) and helix (bottom) shaped models. As can be seen, the straight line model takes a direct path to the supports, while the helix is perpendicular to the supports at the ends. This curve causes the helix to “bow-out”, as discussed in earlier sections, causing significant deflections.

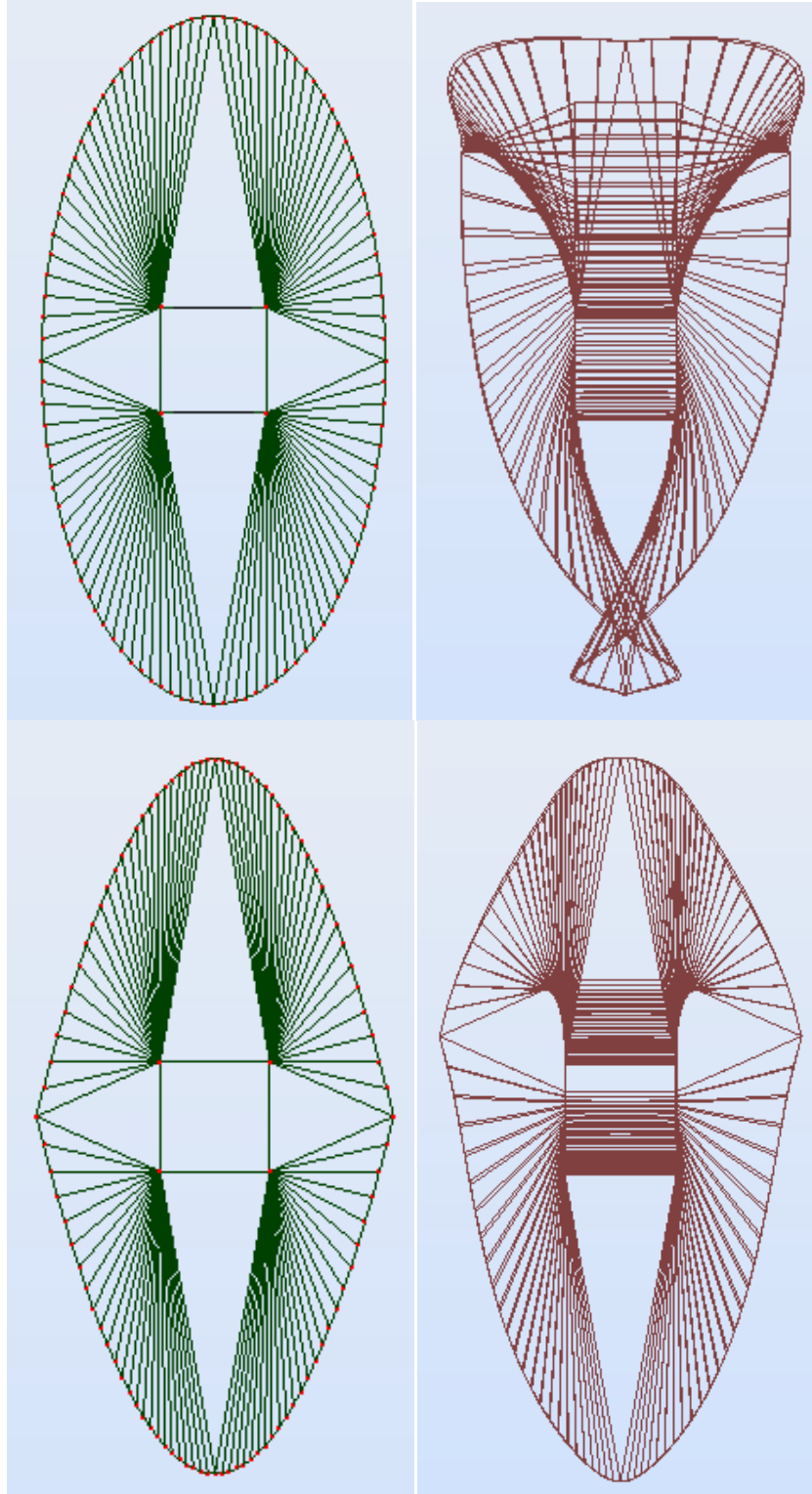


Figure 7.2.12 – Cross-sections of the deflected shapes of the helix (top) and parabolic (bottom) shaped models. The effects of the outward pushing and sagging are clearly visible in the helix model (top), while they are not seen in the parabolic model below.

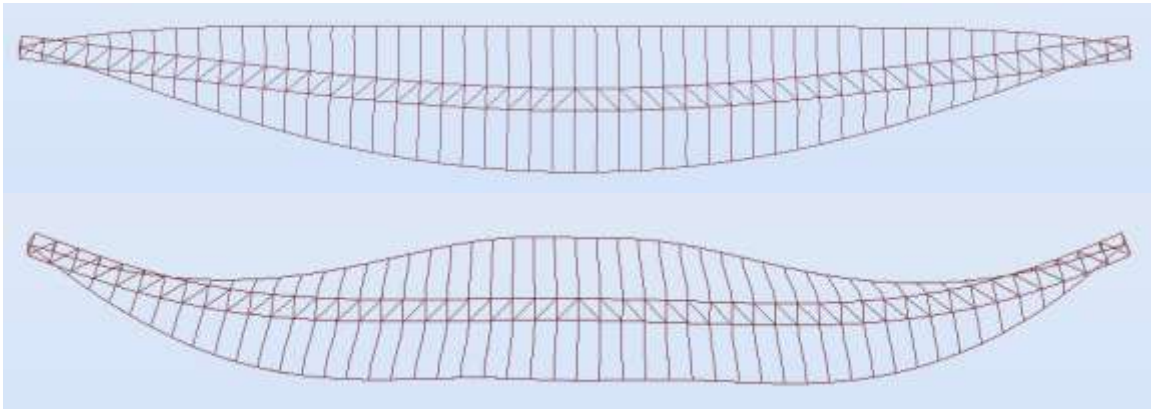


Figure 7.2.13 – Side-views of the exaggerated deflected shapes of the parabolic (top) and helix (bottom) models. The effects of shear and the excessive deflection of the outer helix are extremely noticeable in the helix model (bottom), but are clearly mitigated in the parabolic model (top).

The major differences between the parabolic and helix shaped models are very clear in the images shown on the previous pages. The parabolic shaped models are stronger for two primary reasons. The first is the fact that the parabolic shape is better at taking the shear forces at the ends of the bridge. The shear force is better distributed because the bridge rises higher from the ends, causing the bridge to deflect less due to shear and have a more natural deflected shape. The force at the supports is an upward one, so the internal shear force near the ends of the bridge is better distributed when the bridge is taller near the ends. The other major difference between the two models is the fact that the parabolic model also takes a straight line path from support to support when viewed from above (the change of the X -values of the points on the outer parabolic structure is constant and equal across the entire span, creating a straight line). The curve in the helix model causes the compressive force to push the helix both upwards and outwards, rather than the compressive force in the straight line model, which only creates an upward push in the top outer support structure. The outward push in the curved helix

model further exaggerates the sagging of the helix shaped models, as the outward push combined with gravity causes the sagging. In the parabolic shaped straight line model, the upward push caused from the compression counteracts the sagging effect, which reduces the effects of the shear forces and the defections.

The parabolic shaped models with straight lines connecting the supports across the bridge still do not pass the second order analysis tests. This is still due to the fact that there is excessive bending and buckling of the members near the end due to the fact the models are too thin near the supports. The next strategy is to add a third arch to the bridge, down the center, to further support the bridge near the supports. This triple parabolic arch model (with full diagonals in each arch and bracing to support the center arch) is created first without a deck or roadway of any kind, in order to first study the visual effects and the structural strength improvements, before creating a full model. The connecting members simply meet along a straight line in the center of the model, as shown in the images on the following pages.

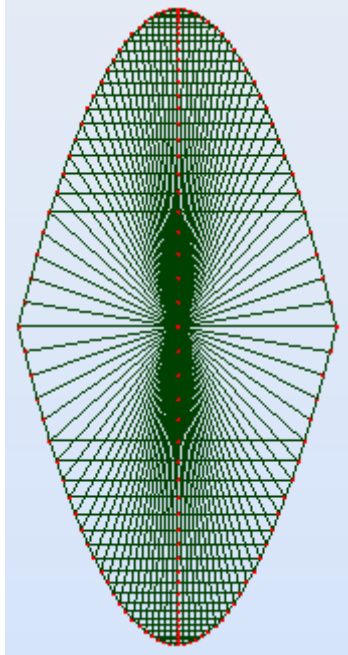


Figure 7.2.14 – Cross-section of the triple parabolic arch model.

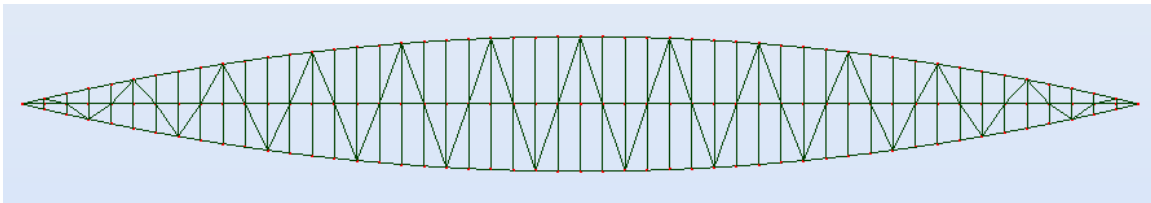


Figure 7.2.15 – Side-view of the triple parabolic arch model.



Figure 7.2.16 – Top-view of the triple parabolic arch model.

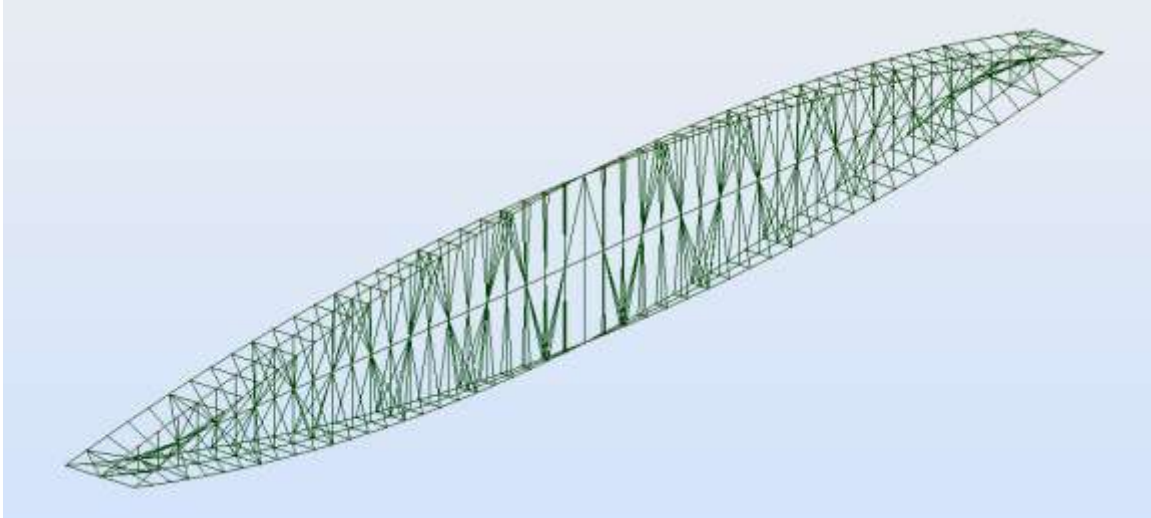


Figure 7.2.16 – Top-view of the triple parabolic arch model.

This model passes the second order analysis performed by Robot. Although this is an overall step forward in the analysis process, as can be seen in the images, the model has an extremely cluttered visual feel to it, which is not aesthetically desirable. The third arch would also require major modifications to the deck system, as a median would need to be built at the center of the bridge for traffic flow purposes. This would require a wider deck, and new way to distribute the lanes (the current 3 lanes in each direction model would not work because of the median). Due to these factors, this model will not be pursued any further, and a new alternative will be studied in the next section.

7.3 Alternative Designs: Arching the Deck

The problem to this point in the analysis has been determined to be the weakness in the in the upper portion of the helix (or parabola) near the ends of the deck. These members are bending excessively and/or buckling, and this is causing the models to fail the second order analyses being performed by Robot. The most simply way to fix this issue is to add additional support to the compressive (upper) part of the structure, and one way to do this is to use the deck to take some of the compressive force end distribute it to the ends. This is a similar idea to the triple parabolic arch model from the last section, but an arched deck is now used in lieu of the third parabolic arch.

Because of AASHTO standards, a road cannot have a maximum grade of more than 6%, which is what the deck must be designed for [21]. The ideal scenario for the deck would be for it stay within the AASHTO standards, while also following the parabolic moment equation shape, which has proven to be the strongest arch shape throughout the analysis. Two different designs will be tested, both of which use an arched deck to take a compressive force on the top of the bridge.

The first model has a deck which follows the parabolic shape, and the deck sits entirely above the parabolic support system. Because the slope of a parabolic deck is at a maximum in the first section from the support, this is the only section that will be at the maximum 6% grade. The rest of the sections will follow the shape of the arch, leading to a maximum height at the center of 31.25 feet. The 40 foot deck is added to this value, giving a maximum height at the center of 71.25 feet above the supports. Because the ideal total height of the bridge has been proven to be at least 200 feet, the lower tension supports will reach a maximum depth of 129.75 feet below the supports. This will also

require a middle layer connecting the lower tension structure to the upper compression structure, as the members would have to be too long if they connected directly from the lower level to the upper.

The second model has a partially straight-sloped, partially parabolic-sloped deck, which is infused with the upper parabolic compression structure. The height of the bridge is 100 feet at the center, while it also has a depth of 100 feet, giving it the same total height of 200 feet. To allow for the top layer of the deck to reach a maximum height of 100 feet, while also staying within AASHTO standards, the deck will increase at the maximum 6% grade until it is even with the upper parabolic structure, and then it will follow the same parabolic arch as the upper structure, fusing the two together. This will give the deck a desirable height, while also keeping it aesthetically within the parabolic model shape.

Both deck bridges use 48 inch square tubes with 12 inch wall thicknesses in the outer compression and tension parabolic arches, as well as in the top most layer of the deck, while all other members are of the smaller square tube variety. Images of both of the bridges are found on the following pages.

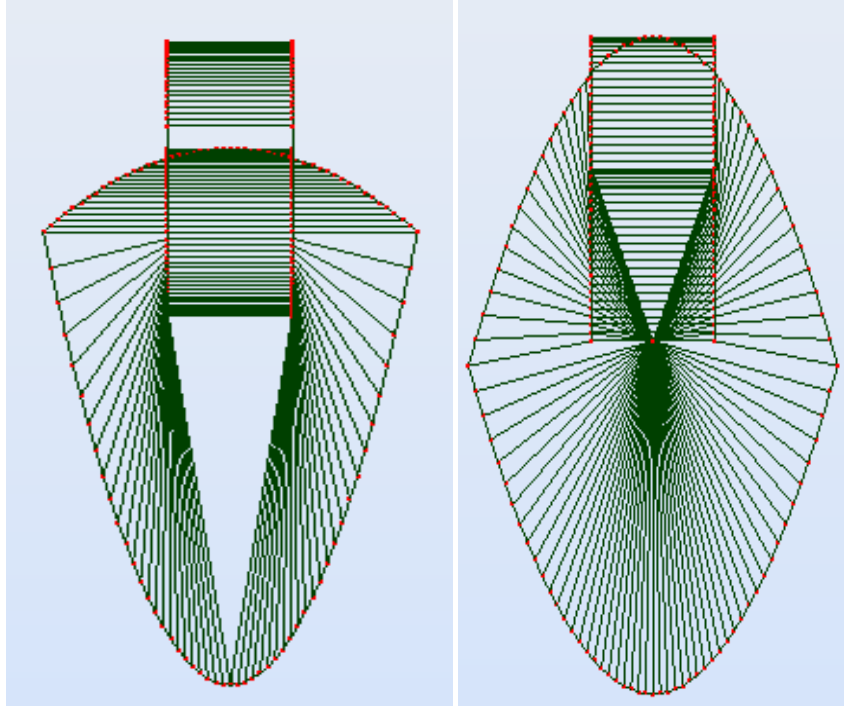


Figure 7.3.1 – Cross-sections of the deck above the arch (left) and the deck infused with the arch (right) models. Both models have 40 foot wide decks and 60 foot horizontal radii (or 120 foot total widths).

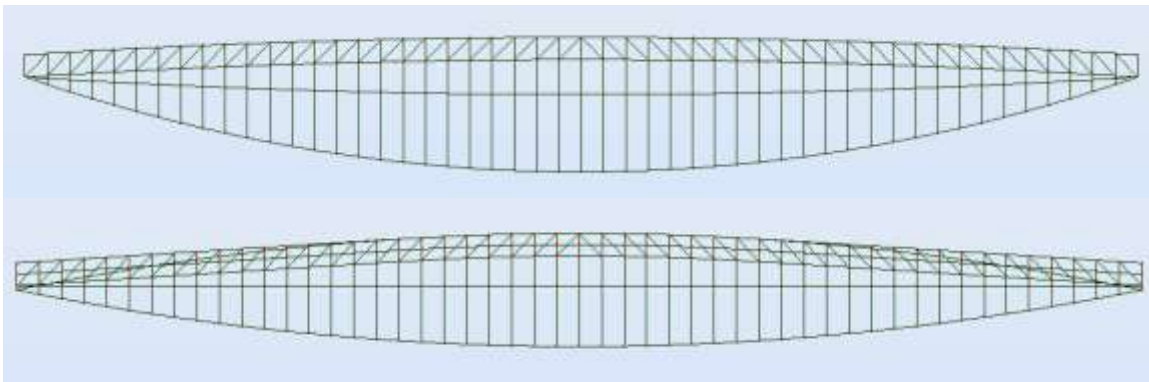


Figure 7.3.2 – Side-views of the deck above the arch (top) and the deck infused with the arch (bottom) models.

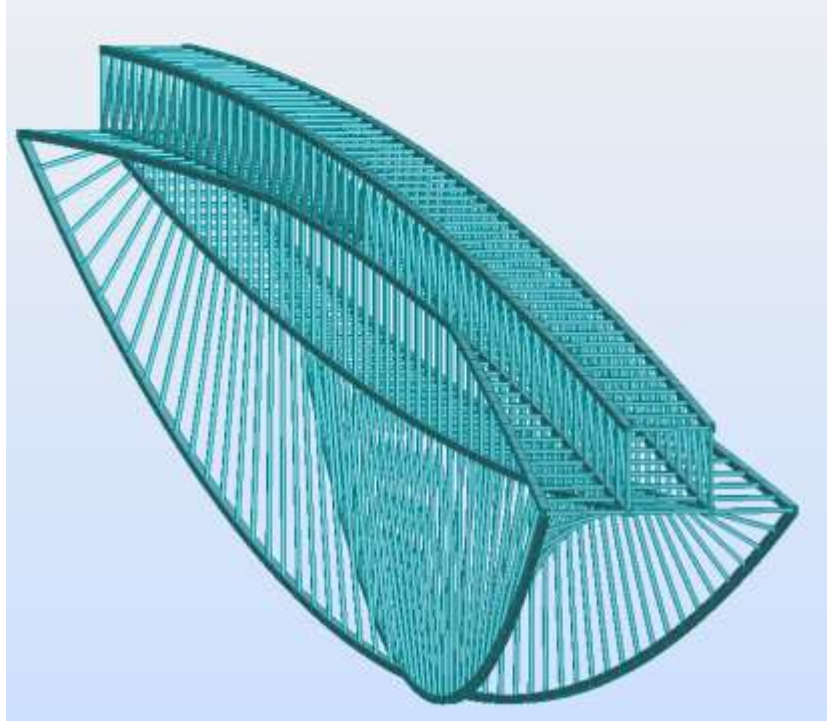


Figure 7.3.3 – Isometric view of the deck above the arch model with member sections turned on.

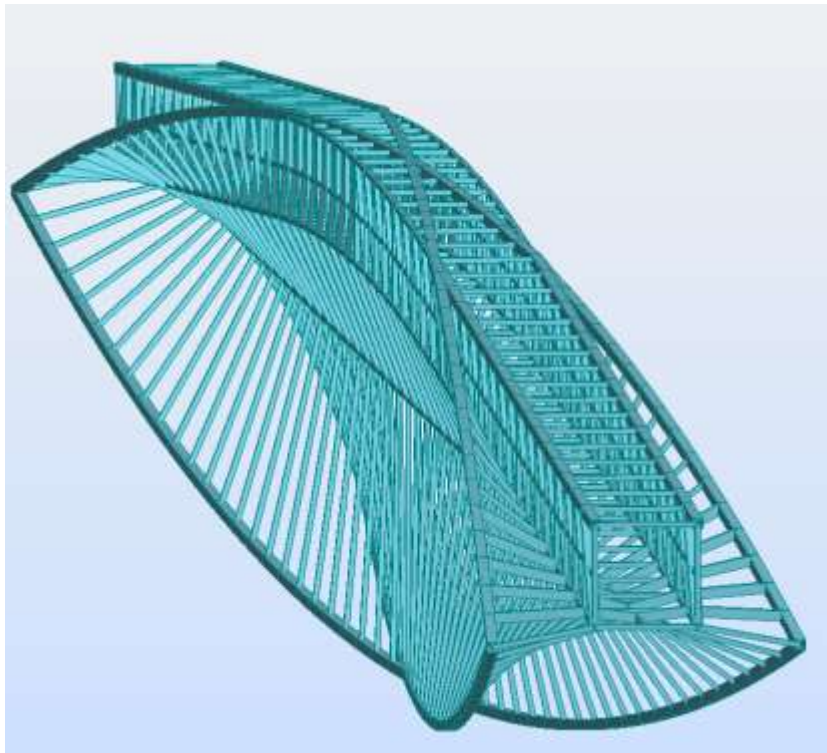


Figure 7.3.4 – Isometric view of the deck infused with the arch model with member sections turned on.

As can be seen on the figures on the previous pages, the decks are used with the crossing parabolic arches to give additional support in compression. This allows for both of these models to pass the second order analyses performed by Robot, as shown in the table below.

Table 7.3.1 - Maximum deflections for the arched deck models		
	Deck above the arches	Deck infused with the arches
Max 1 st order deflection (in)	124.7	128.3
Max 2 nd order deflection (in)	120.9	123.9
Max 3 rd order deflection (in)	120.4	Failure

It is clear that the added strength due to the arched deck allows for the models to be strong enough to pass the tests, although they have ventured extremely far from the original helix idea (in an aesthetic sense). These models show that a steel bridge can be built to cross a 2000 foot span, but they do not use any elements of the aesthetically desirable helix shape, so a final alternative design will be explored in the next section.

7.4 Alternative Design: The Double Helix

The designs that have been used to this point in the analysis have used the helix shape so that it starts at one end of the bridge and does a half turn across the span to connect at the other side. This “half-helix” shape is used 4 times, and the helix structure that has been used throughout the analysis is created. It is necessary to use the helix that only does a half turn over the span because any greater amount of turn would cause the bridge to have a point of zero height which occurs somewhere along the span besides at the ends, which will cause immediate structural failure. The highest point of the span must be at the center, where the strength is needed the most. The problem with the “half-helix” shape is that its height does not increase quickly enough from the ends of the bridge as it spans towards the center, which causes the ends to be thin, weak and susceptible to buckling. One way to improve this is to increase how quickly the height of the outer structure rises from the ends, towards the center. This was in fact performed earlier in the analysis, as increasing the overall height of the helix structure causes the helix to rise quicker from the ends. It was also seen that increasing the height after a certain point will not help, as the added self-weight eventually causes the structure to experience greater deflections. A different shape could be used that would increase the slope of the outer structure as it spans from the ends towards the center, but using a different arc or parabolic equation would leave the helical design, which is not desired

In order to maintain the helix shape and decrease the shear at the ends of the bridge, an alternate helix shape will be combined with the existing one. The current “half-helix” makes one half turn across the span of the bridge, and reaches a maximum height at the center. The proposed alternative will combine this helix with a “full-helix”

or a helical shape that starts at the same zero point, but makes a full turn around the bridge over the span. It reaches a maximum height at the quarter point of the span, and has a height of zero at the center. If used without the “half-helix” for support at the center, failure would be inevitable; as the bridge would have no strength at the point it is most needed.

The initial combination of the half and full helix uses the following variables:

- 100 foot by 100 foot radius in cross section for both helixes
- 40 foot box deck with no slope and a middle level
- 48 inch square tube with a 12 inch wall thickness for all of the outer helix members, and the members that connect the three peaks
- 24 inch square tube with a 6 inch wall thickness for all other members
- No inner helix layers
- Both helixes are connected to the closest corner of the deck every at 40 foot section, and are also connected to each other by a member from the ends of the span until they intersect 1/3 of the way across the span from the nearest end. The three highest points are connected directly to each other by a members divided into 40 foot sections.

Using these parameters, the double helix combination passes the first three iterations of the second order test before non-convergence of the non-linear analysis is found. The first order maximum dead load deflection is found to be 194.3 inches. The figures on the following pages show various images of the double helix combination alternative design.

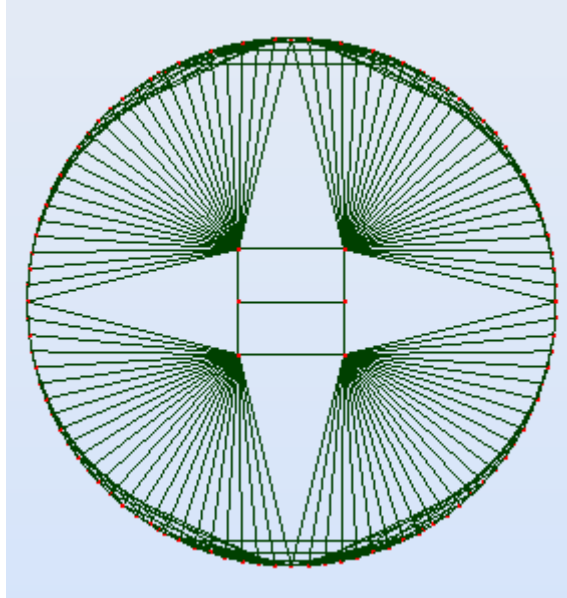


Figure 7.1.1 – Cross-section of the 100 by 100 foot radius double helix model

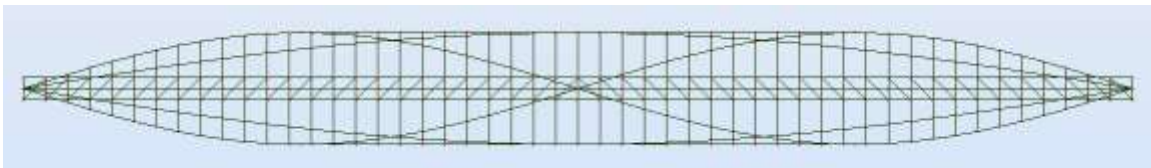


Figure 7.1.2 – Side view of the 100 by 100 foot radius double helix model

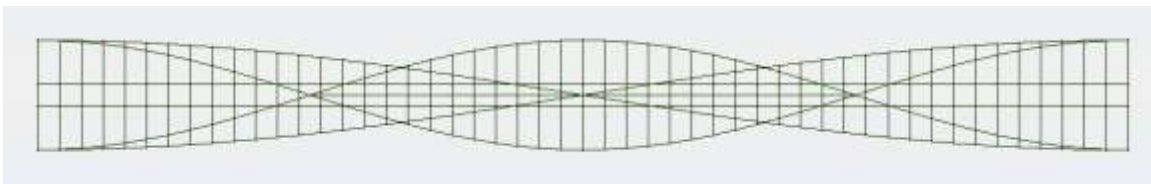


Figure 7.1.3 – Top view of the 100 by 100 foot radius double helix model

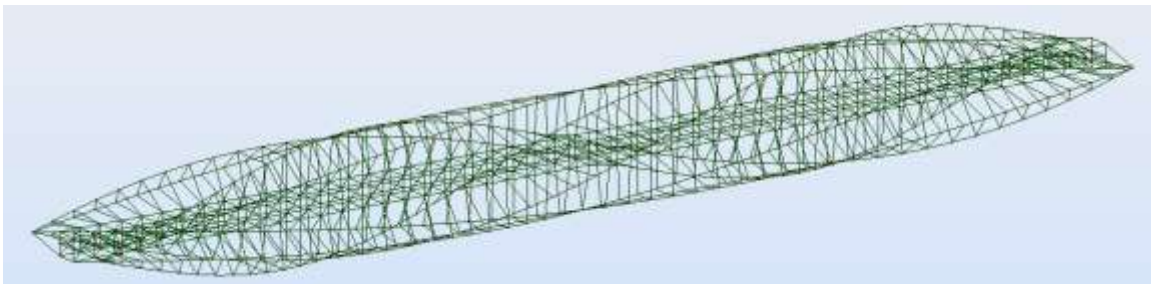


Figure 7.1.4 – Isometric view of the 100 by 100 foot radius double helix model

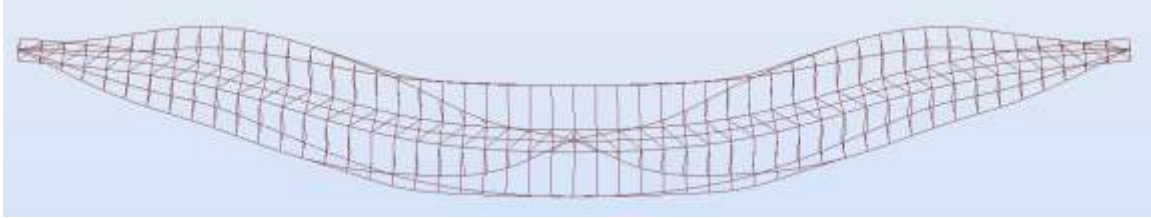


Figure 7.1.5 – Side view of the exaggerated deflected shape of the 100 by 100 foot radius double helix model

The improvement in this design is instantly recognizable in the figures. The “full-helix” shape rises from the end of the bridge to its maximum height 500 feet into the span from both ends. This has a major positive effect on the way the bridge deflects, as can be seen in the deflected shape figure above. Rather than deflecting quickly at the ends and then barely at all in the center, as was the problem with every previous design, this design deflects evenly throughout the span, which shows that shear at the ends is no longer the primary concern.

Even though this bridge model performs the best out of any previous model in terms of deformation due to shear, it still needs to be modified to pass the second and third order tests. The modification must reduce the weight of the bridge without affecting its structural integrity, and it is clear that removing members that do not take much force is the primary goal. As previously discussed, the “full-helix” does not take load at the center of the bridge because it reaches zero height, so it is just adding dead weight to the structure. When the “full-helix” shape is removed in between the points where it intersects the “half-helix” (the middle third of the bridge), the self-weight of the bridge is reduced significantly, but the structure is equally strong. This modification allows for the bridge to pass both the second and third order analyses. The figures on the following pages show the modified double helix bridge.

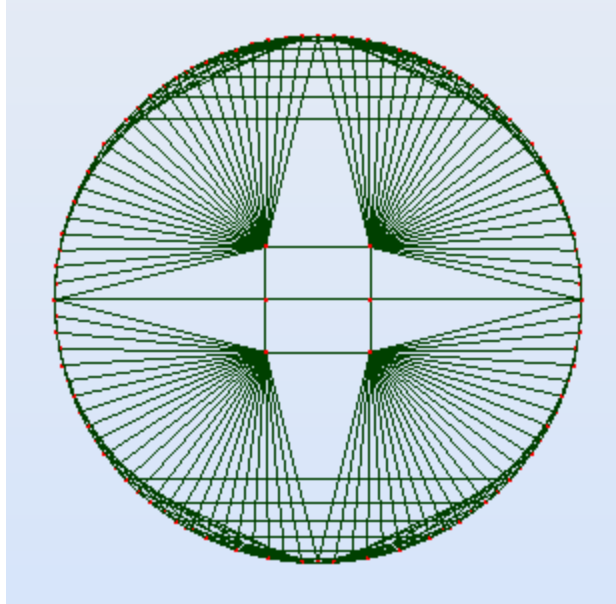


Figure 7.1.6 – Cross-section of the modified 100 by 100 foot radius double helix model

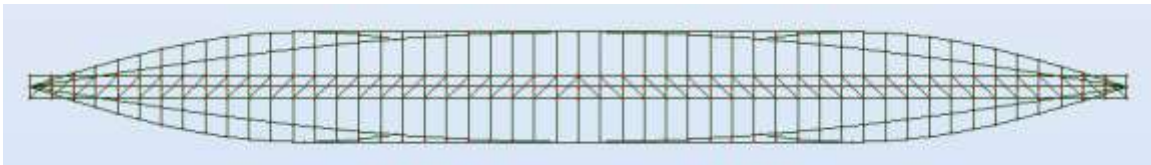


Figure 7.1.7 – Side view of the modified 100 by 100 foot radius double helix model

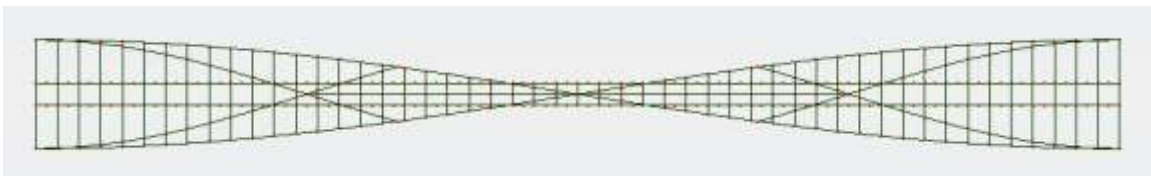


Figure 7.1.8 – Top view of the modified 100 by 100 foot radius double helix model

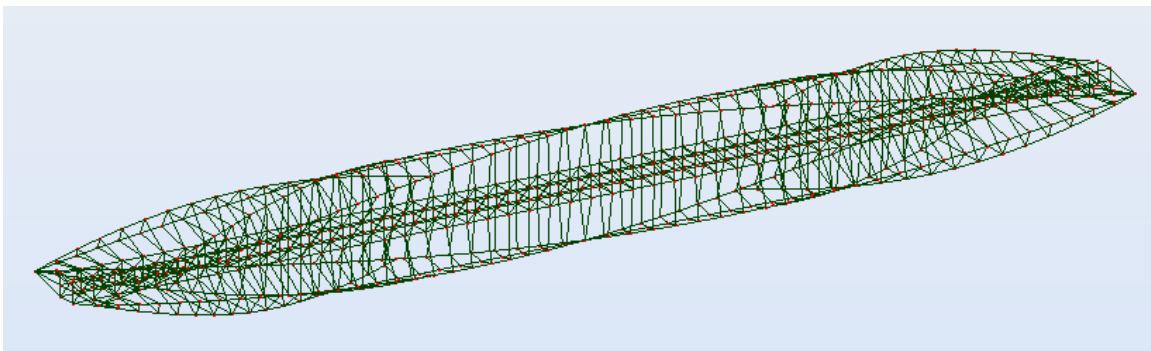


Figure 7.1.9 – Isometric view of the modified 100 by 100 foot radius double helix model

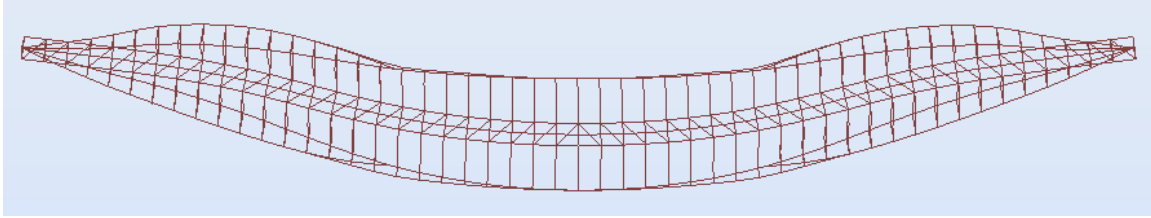


Figure 7.1.10 – Side view of the exaggerated deflected shape of the modified 100 by 100 foot radius double helix model

This modified double helix structure passes the second and third order tests performed by Robot. Even though this design passes all of the appropriate tests, there must be seen if a more efficient design can be found. The 100 by 100 foot radius was chosen early on in the optimization process as the most efficient perfect circle cross-section, but this must be retested. The results are shown in the table below.

Table 7.1.1 - Maximum deflections for modified circular cross-section double helix variations				
	90 foot radius	100 foot radius	110 foot radius	120 foot radius
Max 1 st order deflection (in)	170	150.2	132.8	117
Max 2 nd order deflection (in)	Failure	149.8	Failure	Failure
Max 3 rd order deflection (in)	Failure	150	Failure	Failure

As can be seen in the data table above, the optimal radius is 100 feet for the perfect circle cross-section. The 90 foot radius does not have a high enough maximum height to resist its own self-weight, whereas the higher radius models have longer members, which are more prone to buckling.

To further continue the optimization process, bridge models with varying radii were tested again with the modified double helix shape. The results of this analysis is shown in the table on the following page.

Table 7.1.2 - Maximum deflections for modified oval cross-section double helix variations				
	50 by 100 foot radii	60 by 120 foot radii	70 by 140 foot radii	80 by 160 foot radii
Max 1 st order deflection (in)	137.3	110.10	90.19	75.5
Max 2 nd order deflection (in)	Failure	109.9	89.9	Failure
Max 3 rd order deflection (in)	Failure	110.07	90.16	Failure

The results of this optimization show that the oval cross-section models perform better than the circular cross-section models, as expected. The 70 by 140 foot radius model has a maximum live load deflection of 6.5 inches when all three decks are loaded with vehicular traffic, the equivalent of 9 traffic lanes, which is 50% more than the 6 traffic lanes that were initially being analyzed for.

8. Conclusions and Recommendations

The initial purpose of this study was to explore the use of the helix shape in steel bridge design. The starting point of the analysis was chosen to be a helix with a flat deck and a 65 foot radius which was to provide the support over the 2000 foot span. The maximum live load deflection was 95.7 inches, well over the allowable 30 inches, while the maximum deflection due to the dead load was an unreasonable 473.2 inches. These values were reduced significantly, and through the optimization and modification process, a perfect circle cross-section double helix bridge was found to pass all of the relevant code standards, including the second and third order analyses for its self-weight.

In conclusion, it is clear that the pure helix shape (half helix) is not strong enough to be the only major structural element for a 2000 foot span steel bridge. This purer form of the bridge could be used in scenarios where the span is shorter, as its shortcomings will not be so exaggerated. The double helix modification was a necessary step to preserve the aesthetics of the helix bridge, while also making it structurally sound.

It has been proven that the modified “double helix” shape can perform very well, and the final recommended design is the 60 foot by 120 foot double helix variation. It was chosen over the better performing 70 by 140 foot variation because it is slightly smaller, and therefore would cost less. It also allows for more clearance underneath the bridge, which could be extremely important in a real world scenario.

The helix is clearly not the most efficient structural design shape, but it can be made strong enough, which makes it practical. The fusion of powerful aesthetics and structural strength come together with the recommended design, and that was clearly always the desired effect.

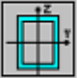
Appendices

CODE: *ANSI/AISC 360-05 An American National Standard, March 9,2005*
ANALYSIS TYPE: *Member Verification*

CODE GROUP:
MEMBER: *2885 Simple bar_2885* POINT: *2* COORDINATE: *x = 0.50 L = 20.09 ft*



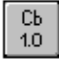
LOADS:
Governing Load Case: 1 DL1

MATERIAL:
STEEL F1554-105 $F_y = 105.00$ ksi $F_u = 125.00$ ksi $E = 29000.00$ ksi

 SECTION PARAMETERS: **Rect 48,12**

d=48.00 in	$A_y=288.000$ in ²	$A_z=288.000$ in ²	$A_x=1728.000$ in ²
b=48.00 in	$I_y=414720.000$ in ⁴	$I_z=414720.000$ in ⁴	$J=699631.418$ in ⁴
tw=12.00 in	$S_y=17280.000$ in ³	$S_z=17280.000$ in ³	
tf=12.00 in	$Z_y=24192.000$ in ³	$Z_z=24192.000$ in ³	

MEMBER PARAMETERS:

 $L_y = 40.18$ ft $K_y = 1.00$ $KL_y/r_y = 31.12$	 $L_z = 40.18$ ft $K_z = 1.00$ $KL_z/r_z = 31.12$	 $L_b = 40.18$ ft $C_b = 1.00$
---	---	---

INTERNAL FORCES:

$T_r = -475.43$ kip*ft	
$P_r = 58816.88$ kip	
$M_{ry} = 3293.51$ kip*ft	$V_y = 31.01$ kip
$M_{rz} = 7.35$ kip*ft	$V_z = 22.87$ kip

NOMINAL STRENGTHS:

$F_i T * T_n = 115427.14$ kip*ft
$F_{ic} * P_n = 140726.47$ kip
$F_{ib} * M_{ny} = 190512.00$ kip*ft $F_{iv} * V_{ny} = 16329.60$ kip
$F_{ib} * M_{nz} = 190512.00$ kip*ft $F_{iv} * V_{nz} = 16329.60$ kip

SAFETY FACTORS

$F_{ib} = 0.90$	$F_{ic} = 0.90$	$F_{iv} = 0.90$
-----------------	-----------------	-----------------

SECTION ELEMENTS:
UNS = Compact STI = Compact

VERIFICATION FORMULAS:
 $P_r / (F_{ic} * P_n) + 8/9 * (M_{ry} / (F_{ib} * M_{ny}) + M_{rz} / (F_{ib} * M_{nz})) = 0.43 < 1.00$ LRFD (H1-1a) Verified
 $V_{ry} / (F_{iv} * V_{ny}) = 0.00 < 1.00$ LRFD (G2-1) Verified
 $V_{rz} / (F_{iv} * V_{nz}) = 0.00 < 1.00$ LRFD (G2-1) Verified
 $K_y * L_y / r_y = 31.12 < (K * L / r)_{max} = 200.00$ $K_z * L_z / r_z = 31.12 < (K * L / r)_{max} = 200.00$ STABLE

Section OK !!!

Figure A.1 – Sample steel section calculation output by Robot. This member is highlighted in red in figure A.3.

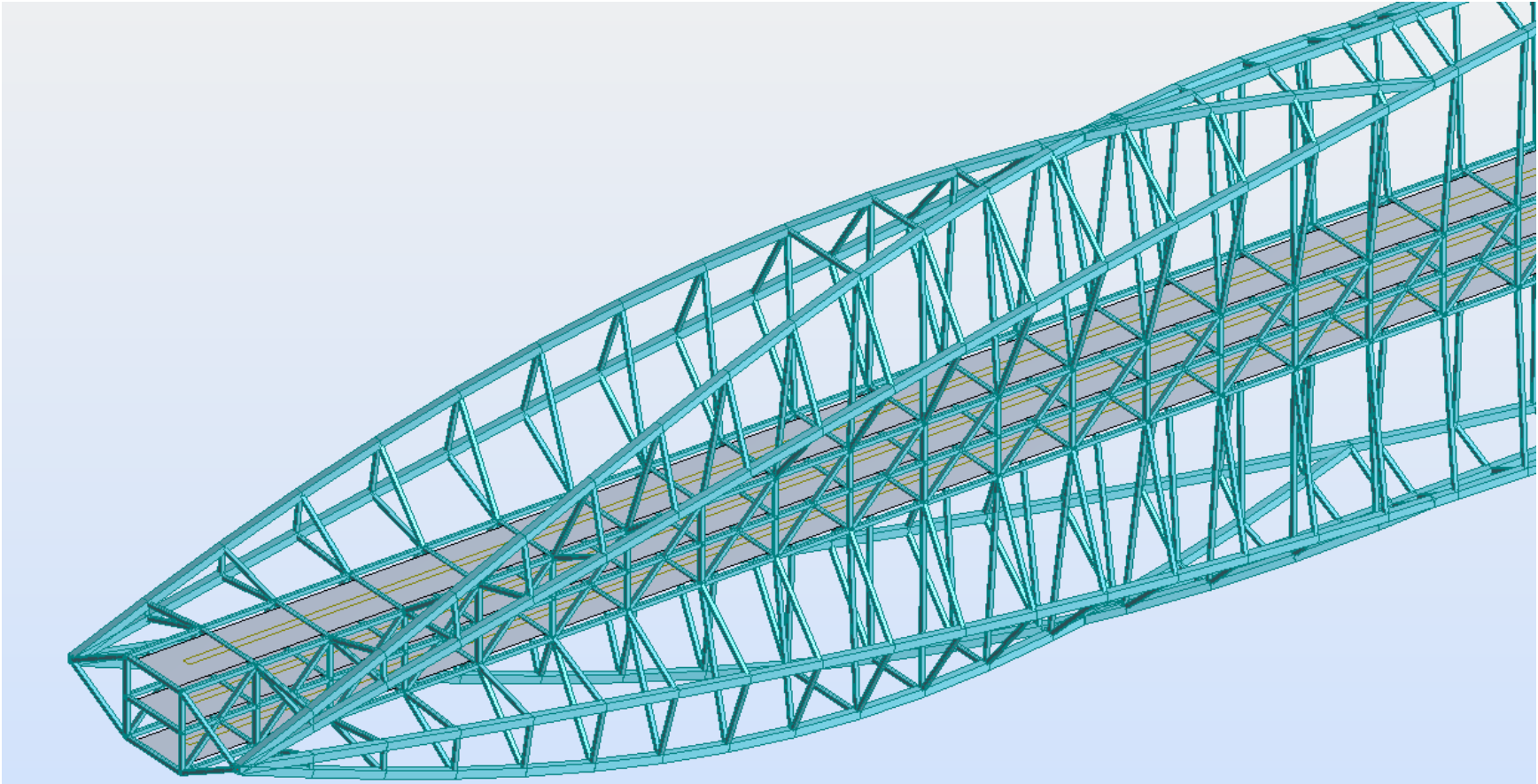


Figure A.2 – Isometric view of the 60 by 120 double helix bridge showing member sections.

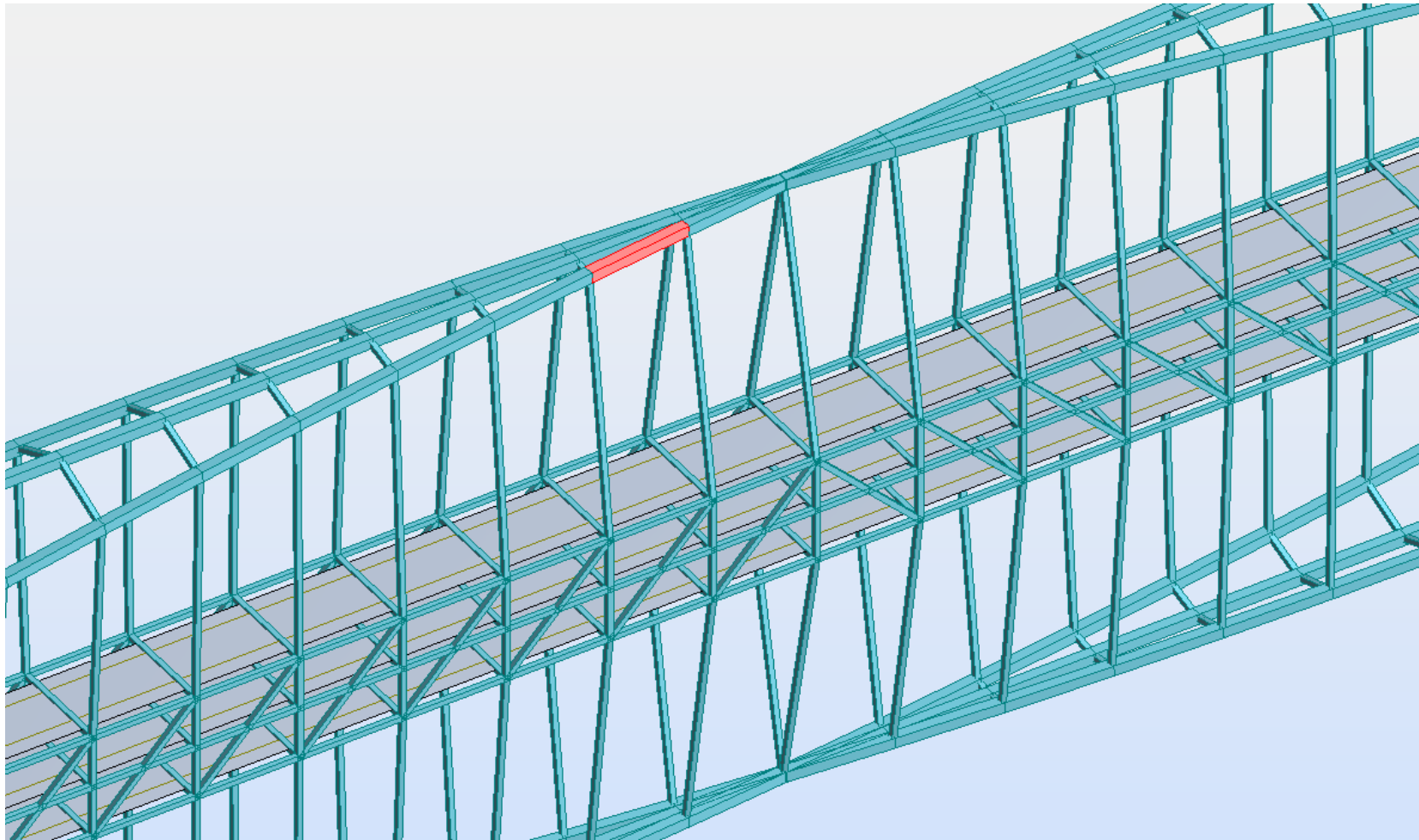


Figure A.3 – Isometric view of the 60 by 120 double helix bridge showing the member sections (2).
The member highlighted in red is used in the sample calculations in figure A.1

Bibliography

- [1] Billington, David. *Robert Maillart*. 1st ed. Cambridge: Cambridge University Press, 1997. Print.
- [2] Nicolas Janberg. *ZuoZ Bridge*. 2009. Photograph. StructuraeWeb. 13 Feb 2012. <<http://en.structurae.de/photos/index.cfm?JS=152333>>.
- [3] *Salginatobel Bridge*. Photograph. Great Buildings <http://www.greatbuildings.com/gbc/images/cid_aj2192_b.jpg>
- [4] Tzonis, Alexander, and Rebeca Donadei. *Santiago Calatrava The Bridges*. 1st ed. New York: Universe Publishing, 2005. Print.
- [5] *Bach de Roda Bridge*. Photograph <http://1.bp.blogspot.com/_MCYBcy9WcNg/TLoGjBbNSnI/AAAAAAAAAEXc/9R4Pdy2TUc/s1600/ponte_felipeII.jpg>
- [6] *Oudry-Mesly Footbridge*. Photograph <<http://up.iranblog.com/Files0/9851f7c6ba2b4f828add.jpg>>.
- [7] *Alamillo Bridge*. Photograph. <http://www.mimoa.eu/images/3802_1.jpg>.
- [8] *Trinity Footbridge*. Photograph <http://www.architravel.com/files/buldingsImages/bulding791/trinity%20bridge_main.jpg>.
- [9] "The Helix." *Arup*. Arup, 2011. Web. 22 Apr 2012. <http://www.arup.com/Projects/Helix_bridge.aspx>.
- [10] Prinzler, Sven. "Akashi Kaikyo Bridge." *Structurae*. Wilhelm Ernst & Sohn, 2010. Web. 22 Apr 2012. <<http://en.structurae.de/structures/data/index.cfm?ID=s0000001>>.
- [11] Virola, Juhani. "World's Longest Bridge Spans." . N.p., 20 Feb 2012. Web. 22 Apr 2012. <<http://bridge.aalto.fi/en/longspan.html>>.
- [12] Wang, Fu-Min. "The Chaotianmen Bridge." . Chongqing Communications Research and Design Institute, 2009. Web. 22 Apr 2012. <<http://bscw-app1.ethz.ch/pub/bscw.cgi/d376909/18-F.M. Wang.pdf>>.
- [13] *Chaotianmen Bridge*. Photograph <http://cache.atlas.sina.com.cn/nd/citylifehouse/citylife/4e/2c/20090517_11460_1.jpg>.

- [14] "The Lupu Bridge." . N.p., n.d. Web. 22 Apr 2012.
<<http://www.lupubridge.com/index.php/en>>.
- [15] *The Lupu Bridge*. Photograph
<http://upload.wikimedia.org/wikipedia/commons/6/65/Lupu_Bridge_Shanghai_at_World_Expo_2010_-_Seen_from_Pudong-edit.jpg>.
- [16] Holth, Nathan, and McOmber Rick. "Pont de Québec." *Historic Bridges*. N.p., 14 Apr 2011. Web. 22 Apr 2012.
<<http://www.historicbridges.org/bridges/browser/?bridgebrowser=quebec/quebec/>>.
- [17] *Pont de Quebec*. Photograph
<<http://www.dimensionsguide.com/wp-content/uploads/2009/12/Longest-Truss-Bridge.jpg>>.
- [18] "Beam Formulas with shear and Moment Diagrams." *American Wood Council*. American Forest & Paper Association, 2007. Web. 12 Apr 2012.
<<http://www.awc.org/pdf/DA6-BeamFormulas.pdf>>.
- [19] "Bending." *Structuralpedia*. 2009. Web. 13 Apr 2012.
<<http://structuralpedia.com/index.php?title=Bending>>.
- [20] Beer, Ferdinand, Russell Johnston, John Dewolf, and David Mazurek. *Mechanics of Materials*. 6th ed. New York: McGraw Hill, 2012. Print.
- [21] Tonia, Demetrios, and Jim Zhao. *Bridge Engineering*. 2nd ed. New York: McGraw Hill, 2007. Print.
- [22] Delvin, Keith. "The Double Helix." *Mathematical Association of America*. (2003): n. page. Web. 13 Apr. 2012. <http://www.maa.org/devlin/devlin_04_03.html>.
- [23] "Autodesk Robot Structural Analysis Professional 2012 User's Guide." *Autodesk*. 2012. Web. 13 Apr 2012.
<<http://docs.autodesk.com/RSA/2012/ENU/landing.html>>.

Unreferenced sources:

Autodesk Robot Structural Analysis Professional 2012

Professor Cosmas Tzavelis